



**UNIVERSIDAD NACIONAL AUTÓNOMA
DE MÉXICO**

FACULTAD DE FILOSOFÍA Y LETRAS

**UN MODELO DE RIESGO DE INCENDIO
EN MICHOACÁN, MÉXICO**

T E S I S

QUE PARA OBTENER EL GRADO DE
MAESTRA EN GEOGRAFÍA
(ORIENTACIÓN DE GEOGRAFÍA AMBIENTAL)
"MANEJO INTEGRADO DEL PAISAJE"

PRESENTA:
SONIA MARÍA JUÁREZ OROZCO

DIRECTOR DE TESIS:
Dr. JEAN FRANÇOIS MAS CAUSSEL



MÉXICO, D.F.,

200



Universidad Nacional
Autónoma de México



UNAM – Dirección General de Bibliotecas
Tesis Digitales
Restricciones de uso

DERECHOS RESERVADOS ©
PROHIBIDA SU REPRODUCCIÓN TOTAL O PARCIAL

Todo el material contenido en esta tesis esta protegido por la Ley Federal del Derecho de Autor (LFDA) de los Estados Unidos Mexicanos (México).

El uso de imágenes, fragmentos de videos, y demás material que sea objeto de protección de los derechos de autor, será exclusivamente para fines educativos e informativos y deberá citar la fuente donde la obtuvo mencionando el autor o autores. Cualquier uso distinto como el lucro, reproducción, edición o modificación, será perseguido y sancionado por el respectivo titular de los Derechos de Autor.

A mi abuelita María Inés Liévanos Pérez

Agradecimientos

Agradezco al Centro de Investigaciones en Geografía Ambiental de la Universidad Nacional Autónoma de México y al ITC (International Institute of Geoinformation Science and Earth Observation) por brindarme todas las facilidades para llevar a cabo el estudio de la Maestría en Geografía con orientación al Manejo Integrado del Paisaje. Asimismo agradezco al ITC y a la Dirección General de Posgrado (UNAM) por las becas que me otorgaron para el desarrollo de mis estudios de maestría.

Agradezco profundamente a todas las personas que me ayudaron a crecer personal y académicamente acompañándome en el desarrollo de mi maestría. Ustedes representaron una luz en el sinuoso camino que conduce al conocimiento.

Mi más profundo agradecimiento a mis supervisores de tesis, cuyos consejos, cariño, apoyo y guía me impulsaron a desarrollar ésta tesis. Agradezco profundamente al Dr. Jean Mas por su apoyo, comprensión y confianza en mi, por todos sus comentarios constructivos que ayudaron a mejorar sustantivamente el trabajo y por su compromiso como tutor de ésta tesis. También quiero expresar mi gratitud al Dr. Alejandro Velásquez por sus valiosos comentarios a la tesis y porque gracias a su esfuerzo se hizo posible mi estancia en el ITC. Al Dr. Yousif Hussin, mi supervisor del ITC le agradezco su guía y apoyo en la realización de la tesis. Al Dr. Michael Weir, le brindo mi más sincero agradecimiento por su apoyo moral y sus valiosos comentarios y correcciones durante el desarrollo del manuscrito. Agradezco al Dr. Victor Jetten, presidente del comité de Tesis en el ITC, por sus valiosos comentarios y apoyo durante el desarrollo de la tesis. A mis sinodales: Dra. Lilia Manzo, Dr. Diego Pérez, Dr. Jean Mas, Dr. Yousif Hussin y Mtro. Antonio Navarrete por sus valiosos comentarios que mejoraron el contenido de esta tesis. Finalmente agradezco a todas aquellas personas que colaboraron con datos, información e ideas para desarrollar esta tesis, entre las cuales se encuentran la Dra. Isabel Cruz y el Prof. Ignacio Galindo.

Quiero expresar mi gratitud al Dr. Zoltan Verkedy por su generoso apoyo y gentileza en los momentos más difíciles. Asimismo, le agradezco al Dr. Abbas Farshad por su apoyo durante el desarrollo de la tesis y al Dr. Mike McCall por el cariño y apoyo que me brindó durante mi estancia en Enschede, Holanda. Al Mtro. Antonio Navarrete amigo y sinodal de esta tesis por sus invaluable consejos y comentarios para mejorar el modelo, en especial por su ayuda en el procesamiento de la imagen ASTER y el procesamiento de mapas básicos para el desarrollo de los submodelos de Combustible, Ignición y Detección.

Le agradezco y dedico ésta tesis a mi familia por todo su cariño y paciencia. A mi mamá, mi papá, Susi, Tito, Migue, Santi, Efra, Dis, Chela, Laura, Jorge. A mi madrina Blanca por todo su cariño. A mi mamá y a mi abuelita por ser un ejemplo de vida. A Erick y a mi mamá por su apoyo incondicional. Erick: *Elen silen lumen omeltielmo*.

Finalmente, quiero agradecer a todos mis amigos. A mis amigos internacionales: Daniel, David, Mutumwa, Ram and Rubeta. A Mariela, Rafa, Daniel y Toño por su amistad y los grandes momentos compartidos. A mis amigos de la Maestría en Morelia: Ale, Carlos, Daniel, Jacky Mathews, Jacky Mena, Nacho, Nubia, Rodolfo y Yuri. A mis amigos incondicionales, Ceci, Laura, Yanet, Yazmin y Taz! A todos mis amigos que no se encuentran mencionados en este corto agradecimiento.

Tabla de Contenidos

| | |
|--|-----------|
| A MI ABUELITA MARÍA INÉS LIÉVANOS PÉREZ | 3 |
| AGRADECIMIENTOS | 4 |
| RESUMEN EJECUTIVO | 11 |
| 1 INTRODUCCIÓN | 11 |
| 2 MÉTODO | 11 |
| 2.1 FASE EXPLORATORIA | 11 |
| 2.2 FASE DE MODELAJE | 11 |
| 2.2.1 SUBMODELO COMBUSTIBLE | 12 |
| 2.2.2 SUBMODELO IGNICIÓN | 12 |
| 2.2.3 SUBMODELO DETECCIÓN | 13 |
| 2.2.4 SUBMODELO RESPUESTA | 13 |
| 2.2.5 MODELO ESTÁTICO DE RIESGO DE INCENDIO | 13 |
| 2.2.6 MODELO MULTI-TEMPORAL DE RIESGO DE INCENDIO (SUBMODELO CLIMA) | 13 |
| 2.3 VALIDACIÓN | 14 |
| 3 RESULTADOS | 14 |
| 3.1 FASE I. EXPLORATORIA | 15 |
| 3.1.1 FACTORES BIOFÍSICOS QUE AFECTAN LA INCIDENCIA Y COMPORTAMIENTO DE INCENDIOS FORESTALES | 15 |
| 3.2 FASE II. MODELAJE | 16 |
| 3.2.1 SUBMODELO COMBUSTIBLE | 16 |
| 3.2.2 SUBMODELO IGNICIÓN | 16 |
| 3.2.3 SUBMODELO DETECCIÓN | 17 |
| 3.2.4 SUBMODELO RESPUESTA | 17 |
| 3.2.5 MODELO ESTÁTICO DE RIESGO DE INCENDIO | 17 |
| 3.2.6 MODELO MULTI-TEMPORAL DE RIESGO DE INCENDIO (SUBMODELO CLIMA) | 18 |
| 3.3 FASE III. VALIDACIÓN | 18 |
| 4 CONCLUSIONES | 19 |

1. INTRODUCTION **23**

| | |
|--|-----------|
| 1.1 BACKGROUND | 23 |
| 1.1.1 FOREST FIRES AND INFLUENCING FACTORS | 23 |
| 1.1.2 CLASSIFICATION OF FOREST FIRE | 24 |
| 1.1.3 FOREST FIRES: EFFECTS AND CONSEQUENCES | 25 |
| 1.1.4 FIRE HAZARD, RISK AND DANGER DEFINITIONS | 25 |
| 1.1.5 THE ROLE OF REMOTE SENSING AND GIS IN FIRE MODELLING | 26 |
| 1.1.5.1 Active fires | 27 |
| 1.1.5.2 Burnt scars | 27 |
| 1.1.5.3 Forest fires modelling | 28 |
| 1.1.6 FOREST FIRES IN MEXICO | 29 |
| 1.1.1. ACTUAL FIRE COMBATING AND PREVENTION IN MEXICO | 30 |
| 1.2 RESEARCH PROBLEM | 31 |
| 1.3 RATIONALE | 32 |
| 1.4 RESEARCH OBJECTIVES AND QUESTIONS | 33 |

2 STUDY AREA **34**

| | |
|-----------------------|-----------|
| 2.1 LOCATION | 34 |
| 2.2 CLIMATE | 34 |
| 2.3 VEGETATION | 36 |
| 2.4 LAND USE | 39 |
| 2.5 POPULATION | 40 |

3 METHOD **41**

| | |
|---|-----------|
| 3.1 EXPLORATORY PHASE | 41 |
| 3.1.1 LITERATURE REVIEW AND SELECTING FACTORS INFLUENCING FOREST FIRE | 41 |
| 3.1.2 DATA PROCESSING | 41 |
| 1. STUDY AREA DEMARCATION | 42 |
| 3.1.3 VEGETATION TYPE MAP IMPROVEMENT | 44 |
| 3.1.4 BURNT AREA MAPPING | 44 |
| 3.1.5 ANALYSIS OF FACTORS INFLUENCING FOREST FIRES | 44 |
| 3.2 MODELING PHASE | 45 |
| 3.2.1 FUEL RISK SUB-MODEL | 46 |
| 3.2.1.1 Land cover index | 47 |
| 3.2.1.2 Slope index | 50 |
| 3.2.1.3 Elevation index | 50 |
| 3.2.1.4 Aspect index | 51 |

| | | |
|------------|---|-----------|
| 3.2.2 | IGNITION RISK SUB-MODEL | 51 |
| 3.2.3 | FIRE DETECTION RISK SUB-MODEL. | 52 |
| 3.2.4 | RESPONSE RISK SUB-MODEL | 53 |
| 3.2.4.1 | On-road response | 54 |
| 3.2.4.2 | Off-road response | 55 |
| 3.2.5 | STATIC FIRE RISK MODEL | 56 |
| 3.2.6 | WEATHER RISK SUB-MODEL. | 57 |
| 3.3 | VALIDATION PHASE | 62 |
| 3.4 | MATERIALS | 63 |
| 3.4.1 | CARTOGRAPHIC DATA AND IMAGERY | 63 |
| 3.4.1.2 | IMAGES | 63 |
| A) | MODIS IMAGES | 63 |
| B) | ASTER IMAGES | 64 |
| 3.4.2 | GROUND RECORDS | 65 |
| C) | COFOM RECORDS | 65 |
| 4 | RESULTS AND DISCUSSION | 66 |
| 4.1 | EXPLORATORY PHASE | 66 |
| 4.1.1 | BURNT AREA MAP | 66 |
| 4.1.2 | ANALYSIS OF BIOPHYSICAL FACTORS INFLUENCING FOREST FIRE | 67 |
| 4.1.2.1 | Vegetation type | 67 |
| 4.1.2.2 | Elevation | 68 |
| 4.1.2.3 | Slope | 69 |
| 4.1.2.4 | Aspect | 70 |
| 4.1.2.5 | Ignition factors | 70 |
| 4.1.2.6 | Weather | 71 |
| 4.2 | MODELLING PHASE | 72 |
| 4.2.1 | FUEL RISK SUB-MODEL | 72 |
| 4.2.2 | IGNITION RISK SUB-MODEL | 73 |
| 4.2.3 | WEATHER RISK SUB-MODELS | 73 |
| 4.2.4 | DETECTION RISK SUB-MODEL | 74 |
| 4.2.5 | RESPONSE RISK SUB-MODEL | 75 |
| 4.2.6 | STATIC FIRE RISK MODEL | 75 |
| 4.3 | VALIDATION | 79 |
| 4.4 | RELEVANCE OF THE OBTAINED RESULTS | 81 |
| 5 | CONCLUSIONS AND RECOMMENDATIONS | 83 |
| 5.1 | CONCLUSION | 83 |
| 5.2 | RECOMMENDATIONS | 84 |
| | REFERENCES | 86 |

| | |
|--|-----------|
| APPENDICES | 93 |
| <hr/> | |
| A. LAND COVER MAP | 93 |
| B. VEGETATION TYPES | 93 |
| C. WEATHER SUB-MODELS | 95 |
| D. STUDY CASE: GIS FOREST FIRE RISK MODEL (IN SPANISH) | 99 |
| | |
| MODELO DE RIESGO DE INCENDIO | 99 |
| <hr/> | |
| | |
| UN ESTUDIO DE CASO EN | 99 |
| <hr/> | |

List of figures

| | |
|--|----|
| FIGURE 1-1. MAIN CAUSES OF FOREST FIRES IN 1998, MEXICO..... | 29 |
| FIGURE 2-1 STUDY AREA LOCALIZATION IN AN ASTER IMAGE OF MICHOACÁN, MEXICO..... | 35 |
| FIGURE 2-2. CLIMATOGRAPHS FROM (A) LOS REYES STATION (SUBTROPICAL) AND (B) CARAPAN STATION (TEMPERATE) IN MICHOACÁN, MEXICO | 36 |
| FIGURE 3-1. MICHOACÁN’S MUNICIPALITIES WITH HIGHEST PERCENTAGE OF FOREST FIRES IN FOUR YEARS..... | 43 |
| FIGURE 3-2 FACTOR ANALYSIS..... | 45 |
| FIGURE 3-3. FUEL RISK SUB-MODEL..... | 46 |
| FIGURE 3-4. SCHEMATIC OF A FIRE ON A SLOPE. | 50 |
| FIGURE 3-5. IGNITION RISK SUBMODEL..... | 52 |
| FIGURE 3-6 DETECTION RISK SUB-MODEL..... | 53 |
| FIGURE 3-7 RESPONSE RISK SUB-MODEL | 54 |
| FIGURE 3-8. A COMPARISON OF WALKING MODEL | 55 |
| FIGURE 3-9. WEATHER RISK SUB-MODEL..... | 57 |
| FIGURE 3-10. LINEAR REGRESSION BETWEEN ELEVATION AND TEMPERATURE FOR THE MONTHS JANUARY TO JUNE | 60 |
| FIGURE 3-11. LINEAR REGRESSION BETWEEN ELEVATION AND TEMPERATURE FOR THE MONTHS JULY TO DECEMBER | 61 |
| FIGURE 4-1. TWO EXAMPLES OF A DIGITALIZED BURNT AREA. SETTLEMENTS SHOWN IN THIS PICTURE: 1) SANTA CLARA DE VALLADARES, 2) LOS LIMONES, 3) ETUCUARO, 4) VALLE DE GUADALUPE, 5) GÓMEZ FARIAS 6) CHILCHOTA..... | 66 |
| FIGURE 4-2 STUDY AREA BURNT AREA MAP..... | 67 |
| FIGURE 4-3. ALTITUDINAL DISTRIBUTION OF LAND COVER CLASSES | 68 |
| FIGURE 4-4. ALTITUDINAL DISTRIBUTION OF BURNT AREAS..... | 69 |
| FIGURE 4-5. BURNT SCAR DISTRIBUTION PER SLOPE CLASS..... | 69 |
| FIGURE 4-6 BURNT SCAR DISTRIBUTION PER ASPECT CLASS. | 70 |
| FIGURE 4-7. BURNT SCAR DISTRIBUTION ACCORDING TO DISTANCE TO (A) AGRICULTURE FIELDS, (B) GRASSLANDS, (C) SETTLEMENTS, (D) ROADS | 71 |
| FIGURE 4-8. FIRE FREQUENCY IN THE DRY SEASON FROM 2003 TO 2006..... | 72 |
| FIGURE 4-9. FIRE FREQUENCY AND TEMPERATURE (°C), TEMPERATURE OF THE FIRST SIX MONTHS OF THE YEAR.. | 72 |
| FIGURE 4-10 FIRE FREQUENCY OF THE FIRST SIX MONTHS OF THE YEAR. PP = MEAN PRECIPITATION (MM) AND E= EVAPORATION | 72 |
| FIGURE 4-11. PERCENTAGE OF BURNT AREA BY FIRE RISK CLASS USING EQUATIONS 1, 2 AND 3..... | 76 |
| FIGURE 4-12. FUEL RISK MAP | 77 |
| FIGURE 4-13. IGNITION RISK MAP | 77 |
| FIGURE 4-14. DETECTION MAP | 77 |
| FIGURE 4-15. RESPONSE RISK MAP | 77 |
| FIGURE 4-16. STATIC FIRE RISK | 78 |
| FIGURE 4-17. AUGUST FIRE RISK | 78 |
| FIGURE 4-18. APRIL FIRE RISK | 78 |
| FIGURE 4-19. DISTRIBUTION OF THE BURNT SCARS IN THE FIRE RISK CATEGORIES OF THE STATIC RISK MODEL | 80 |
| FIGURE 4-20. ROC CURVE. LINES OA CORRESPOND TO A PERFECT MODEL, OM TO A NULL MODEL AND OBM TO THE STATIC RISK MODEL. | 80 |

List of tables

| | |
|---|----|
| TABLE 3-1 COMPARISON BETWEEN COFOM REPORTS AND MODIS HOT SPOT | 43 |
| TABLE 3-2. CHARACTERISTICS OF LAND COVER TYPES AND LAND COVER INDEX RATING. | 49 |
| TABLE 3-3. SLOPE INDEX..... | 50 |
| TABLE 3-4. ELEVATION INDEX..... | 50 |
| TABLE 3-5. ASPECT INDEX..... | 51 |
| TABLE 3-6 DISTANCE TO ROADS, AGRICULTURE FIELDS AND GRASSLANDS INDICES | 52 |
| TABLE 3-7. DETECTION RISK INDEX..... | 53 |
| TABLE 3-8 ON-ROAD RESPONSE INDEX | 54 |
| TABLE 3-9. SLOPE FRICTION INDEX..... | 55 |
| TABLE 3-10. ELEVATION FRICTION INDEX | 55 |
| TABLE 3-11 LAND COVER FRICTION INDEX..... | 56 |
| TABLE 3-12 TEMPERATURE INDEX | 59 |
| TABLE 3-13 PRECIPITATION INDEX | 59 |
| TABLE 3-14. CARTOGRAPHY AND IMAGERY USED IN THE STUDY | 63 |
| TABLE 3-15 EOS MOD_14, AND MOD_40 SATELLITE IMAGE’S CHARACTERISTICS [113]..... | 63 |
| TABLE 4-1. BURNT SCARS PER VEGETATION TYPES | 68 |
| TABLE 4-2. BURNT SCARS PER SLOPE CLASS..... | 69 |
| TABLE 4-3. AREA (%) PER RISK CATEGORY OF FUEL RISK SUB-MODEL..... | 72 |
| TABLE 4-4. AREA (%) PER RISK CATEGORY OF THE IGNITION RISK SUB-MODEL..... | 73 |
| TABLE 4-5, AREA (%) PER RISK CATEGORY OF APRIL SUB-MODEL | 74 |
| TABLE 4-6. AREA (%) PER RISK CATEGORY OF AUGUST SUB-MODEL..... | 74 |
| TABLE 4-7. AREA (%) PER RISK CATEGORY OF THE DETECTION SUB-MODEL..... | 74 |
| TABLE 4-8. AREA (%) PER RESPONSE CATEGORY OF THE RESPONSE SUB-MODEL..... | 75 |
| TABLE 4-9. AREA (%) PER RISK CATEGORY OF STATIC FIRE RISK SUB-MODEL | 76 |
| TABLE 4-10. BURNT AREA (%) PER FIRE RISK CATEGORY FOR THE FUEL SUB-MODEL | 81 |
| TABLE 4-11. BURNT AREA (%) PER FIRE RISK CATEGORY FOR THE DETECTION SUB-MODEL | 81 |
| TABLE 4-12. BURNT AREA (%) PER FIRE RISK CATEGORY FOR THE IGNITION SUB-MODEL | 81 |
| TABLE 4-13. BURNT AREA (%) PER FIRE RISK CATEGORY FOR THE RESPONSE SUB-MODEL | 81 |
| TABLE 4-14. BURNT AREA (%) PER FIRE RISK CATEGORIES FOR THE STATIC SUB-MODEL..... | 81 |
| TABLE 4-15. BURNT AREA (%) PER FIRE RISK CATEGORY FOR THE MONTH OF APRIL | 81 |
| TABLE 4-16. BURNT AREA (%) PER FIRE RISK CATEGORY FOR THE MONTH OF AUGUST..... | 81 |
| TABLE 0-1. BURNT AREA (%) PER FIRE RISK CATEGORY FOR THE MONTH OF JANUARY | 98 |
| TABLE 0-2. BURNT AREA (%) PER FIRE RISK CATEGORY FOR THE MONTH OF FEBRUARY..... | 98 |
| TABLE 0-3. BURNT AREA (%) PER FIRE RISK CATEGORY FOR THE MONTH OF MARCH..... | 98 |
| TABLE 0-4. BURNT AREA (%) PER FIRE RISK CATEGORY FOR THE MONTH OF MAY | 98 |
| TABLE 0-5. BURNT AREA (%) PER FIRE RISK CATEGORY FOR THE MONTH OF JUNE..... | 98 |
| TABLE 0-6. BURNT AREA (%) PER FIRE RISK CATEGORY FOR THE MONTH OF JULY | 98 |
| TABLE 0-7. BURNT AREA (%) PER FIRE RISK CATEGORY FOR THE MONTH OF SEPTEMBER | 98 |
| TABLE 0-8. BURNT AREA (%) PER FIRE RISK CATEGORY FOR THE MONTH OF OCTOBER | 98 |
| TABLE 0-9. BURNT AREA (%) PER RISK CATEGORY FOR THE MONTH OF NOVEMBER | 98 |
| TABLE 0-10. BURNT AREA (%) PER FIRE RISK CATEGORY FOR THE MONTH OF DECEMBER | 98 |

Resumen ejecutivo

1 INTRODUCCIÓN

La presencia de incendios se ha incrementado significativamente en tamaño, frecuencia e intensidad alrededor del mundo. México, un país megadiverso, presenta fuegos recurrentes especialmente en los años afectados por el fenómeno meteorológico de El Niño. Sin embargo, los esfuerzos del gobierno para la prevención de incendios aún son insuficientes para reducir su frecuencia e intensidad. Aunado a esto, la generación de mapas de riesgo de incendio forestal a escala media es aún escasa para la mayor parte del país. Para evitar la pérdida de bosques y desastres naturales relacionados con los incendios, México necesita desarrollar con alta eficiencia estrategias de prevención de incendios. Los incendios modifican su entorno provocando importantes cambios bióticos y abióticos en los ecosistemas. Dado que, no todos los ecosistemas se encuentran adaptados al creciente número de incendios forestales, éstos no solo llegan a causar daños a la biodiversidad sino también graves pérdidas socio-económicas. En México, Michoacán se encuentra entre los estados con mayor número de incendios al año. La principal causa de incendios en este estado son tanto la quema de pastizales como el descuido de fogatas. El objetivo general de este estudio es modelar el riesgo de incendios para una zona crítica del estado de Michoacán, México. Para ello el método se dividió en tres fases: Exploratoria, Modelización y Validación. El presente estudio integra las variables biofísicas y humanas dentro del modelo de riesgo de incendios. Se consideraron cuatro factores principales: 1) Combustible, 2) Ambiente físico, 3) Factores detonantes y 4) Prevención y supresión. De estos factores, el combustible es el más importante ya que es elemento indispensable para la ignición y la expansión del fuego.

2 MÉTODO

2.1 FASE EXPLORATORIA

La primera fase se enfocó en la realización de un mapa de áreas quemadas y en el análisis de factores biofísicos y sociales relacionados con los incendios. Para el mapeo de áreas quemadas se utilizó una imagen ASTER del año 2007 utilizando una combinación de bandas 3, 2, 1 en rojo, verde y azul. Dado que la imagen pertenece al final de la temporada de secas las áreas quemadas fueron fácilmente identificadas, del resto de coberturas, por su coloración negruzca. La digitalización de dichas áreas se llevó a cabo mediante la interpretación visual de la imagen. Las áreas quemadas identificadas en la imagen se cruzaron con los mapas de pendiente, orientación de ladera, altitud, tipo de vegetación y mapas de distancia a áreas agrícolas, pastizales, áreas urbanas y caminos. Dicho cruce permitió un análisis estadístico para determinar diferencias significativas en relación a los factores y la presencia de áreas quemadas. Las pruebas aplicadas fueron ANOVA para muestras normales y de varianzas homogéneas y Kruskal-Wallis para varianzas heterogéneas.

2.2 FASE DE MODELADO

En la segunda fase se modeló el riesgo de incendio forestal. El modelo se dividió en cinco submodelos elaborados con los factores analizados en la fase previa y el cálculo de detección y respuesta por parte de las autoridades. Los submodelos fueron nombrados según el factor principal en el que se

enfocaron, siendo éstos: 1) Combustible, 2) Ignición, 3) Detección, 4) Respuesta y 5) Clima. Su construcción se basó en índices lógicos basados en una exhaustiva revisión bibliográfica y conocimiento experto. La suma de los primeros cuatro submodelos conforma un modelo estático de riesgo de incendio. Finalmente, el modelo se vuelve multi-temporal al sumar el modelo estático con el submodelo de clima, ya que éste considera los cambios de riesgo para cada mes del año. A continuación se describen brevemente los submodelos.

2.2.1 Submodelo Combustible

El combustible es una de las principales variables que determina la ocurrencia y expansión de un incendio forestal. Es uno de los tres componentes indispensables para la combustión y en su ausencia el desarrollo de un incendio es imposible. Para construir éste submodelo se utilizaron mapas de pendiente, orientación de ladera, altitud y cobertura de suelo. Este último incluye el tipo de vegetación. Para construir el submodelo, la información de los factores mencionados se reclasificó de acuerdo a índices de riesgo. De ésta manera la suma de los mapas de riesgo constituye el mapa final de riesgo de combustible. Para generar el índice de riesgo de incendio basado en la cobertura de suelo se tomaron en cuenta los resultados de el taller nacional de consulta y validación de la información dentro del marco del programa "Los incendios en México: un diagnóstico de su efecto en la diversidad biológica", organizado por la CONABIO en 1998 donde un grupo de 21 expertos discutió la susceptibilidad de diferentes tipos de vegetación a un incendio. Asimismo se utilizó información bibliográfica acerca de la densidad de árboles y biomasa por tipo de vegetación. De ésta forma, se consideró al Bosque Tropical Caducifolio como el tipo de vegetación con mayor riesgo, seguido del Bosque de Pino. Los índices de riesgo basados en los factores topográficos de pendiente, orientación de ladera y altitud se construyeron a partir de tres conceptos. El primero de ellos es que el grado de inclinación tiene una relación directa con la exposición del combustible al fuego. Por lo tanto a mayor inclinación de la pendiente mayor contacto de la flama con el combustible y mayor riesgo. El segundo, toma en cuenta el efecto ladera que se presenta en el hemisferio norte de la Tierra, dónde debido a la exposición solar, las laderas sur son más secas y calientes que las laderas norte. El material seco y caliente de dichas laderas tiene por lo tanto mayor probabilidad de incendiarse. Por ultimo se consideró la altitud pues en zonas alejadas de grandes cuerpos de agua, a medida que ésta se incrementa la precipitación aumenta y la temperatura disminuye por lo que el riesgo de incendio es menor en altitudes mayores.

2.2.2 Submodelo Ignición

El ser humano es el responsable de más del 90% de incendios en México. En Michoacán la quema de pastizales y el descuido de fogatas son las principales causas. De Enero a Mayo se presenta la temporada seca, la cual coincide con las prácticas de quema agrícolas de la región. La expansión del fuego de los terrenos agrícolas al bosque suele ser un fenómeno común. La cercanía a carreteras y poblados es un factor que también puede promover la presencia de incendios. Se ha comprobado que existe un efecto de borde en la vegetación que rodea a las carreteras. En particular, el incremento de la temperatura de la superficie cercana a las carreteras con respecto a las áreas más alejadas es uno de los principales factores que pueden favorecer a los incendios. Asimismo, no es raro encontrar vegetación exótica o invasiva típica de sitios perturbados junto a caminos. Entre éstas especies frecuentemente se encuentran especies pirófilas, como algunas especies de pastos. Tomando ésta

información en consideración los índices desarrollados en éste submodelo se basan en que a mayor cercanía a campos agrícolas, pastizales, poblados y caminos, el riesgo de incendio se incrementa. La suma final de los mapas de índice de riesgo de distancia constituye, finalmente, el mapa de riesgo de ignición.

2.2.3 Submodelo Detección

En la realización de éste submodelo se calculó la visibilidad que existe desde torres forestales, ciudades y carreteras. Dicho cálculo se basó en el modelo digital de elevación del área y la localización de los puntos de observación. El producto resultante fue un mapa de visibilidad. Las áreas no visibles en el mapa se clasificaron como de mayor riesgo. Las áreas visibles por otro lado tienen menor riesgo ya que los incendios pueden ser detectados y apagados con mayor rapidez.

2.2.4 Submodelo Respuesta

El submodelo de respuesta considera el tiempo potencial que ocurre entre la ignición y la llegada del personal de la brigada contra incendios forestales (CONAFOR y COFOM). El cálculo del tiempo de respuesta fue simple y directo, pues, está en función de la velocidad de reacción dividida entre la distancia al incendio (cualquier punto). Para su cálculo, el submodelo consideró el recorrido dentro y fuera de las vialidades. Dado que la primera aproximación a un incendio se lleva a cabo por automóvil, los caminos y carreteras juegan un papel primordial para las brigadas anti-incendio. Por ello, en este estudio, se clasificaron los caminos dependiendo de su capacidad de carga, considerándose que, entre menor es la capacidad de carga de un camino, el tiempo de respuesta disminuye. Cuando no es posible arribar a un incendio por medio de un automóvil, la aproximación se hace a pie. Para considerar este tipo de aproximación, se utilizó un mapa de fricción calculado a partir del modelo digital de elevación e información de cobertura de suelo del área de estudio. Una vez que la fricción es calculada, se genera el mapa de respuesta. Para ello se generó un mapa de distancia desde los centros de brigada ponderado con los valores de fricción. Finalmente, dicho mapa se reclasificó en intervalos homogéneos de 3 km, considerándose que a mayor distancia entre el centro de brigada y el incendio, existe menor capacidad de respuesta.

2.2.5 Modelo estático de riesgo de incendio

El modelo estático de riesgo de incendio se compone de la suma de los submodelos de combustible, ignición, detección y respuesta. Para determinar el peso que se le daría a cada submodelo se compararon tres ecuaciones. La ecuación uno se definió por la suma no ponderada de submodelos. La ecuación dos, dio mayor peso al submodelo de combustible. Finalmente, la ecuación tres dio mayor peso al combustible, y en segundo lugar a la fuente de ignición, puesto que el hombre es el causante principal de incendios en Michoacán.

2.2.6 Modelo multi-temporal de riesgo de incendio (Submodelo Clima)

La probabilidad de que se produzca un incendio aumenta cuando el combustible se encuentra seco. Por lo tanto, las condiciones climáticas ideales para que se desarrolle un incendio son baja humedad y altas temperaturas. Asimismo, los vientos favorecen su propagación. Las variables consideradas para

la construcción de este submodelo fueron temperatura y precipitación. De ésta forma, el submodelo de clima dará una idea indirecta acerca de la humedad del combustible muerto (hojarasca, troncos y ramas depositados en el suelo). Sin embargo, para obtener resultados más precisos, se recomienda para estudios posteriores incluir otras variables como humedad relativa y velocidad y dirección del viento.

Este submodelo fue calculado para los doce meses del año, por lo que incluye los cambios promedio en temperatura y precipitación a lo largo del año. Para ello se utilizó información de 32 estaciones meteorológicas recolectada entre los años 1977 y 2000. Para el cálculo de riesgo de incendio climatológico se generaron mapas indicadores de riesgo de incendio para la temperatura y la precipitación utilizando una lógica simple: a mayor sequedad y temperatura en el ambiente, mayor riesgo de que se produzca un incendio. Finalmente, el submodelo Clima se calculó por mes sumando y reclasificando homogéneamente los mapas indicadores de riesgo de incendio para temperatura y precipitación con el mapa estático de riesgo de incendio.

2.3 Validación

En la tercera fase se validaron los submodelos y el modelo estático utilizando el mapa de áreas quemadas del sitio de estudio. Para ello se compararon las áreas quemadas contra las áreas clasificadas como de alto, medio y bajo riesgo en los submodelos. Se consideró que entre mayor sea la coincidencia de las áreas quemadas con las áreas de alto riesgo mejor funcionamiento del modelo. Asimismo, se aplicó un análisis estadístico complementario ROC (Receiving Operating Characteristic analysis) para validar el modelo, ya que predice la ubicación de un incendio al comparar el mapa de probabilidad de ocurrencia de incendio y la presencia o ausencia de áreas quemadas.

3 RESULTADOS

Los productos finales de este estudio fueron un mapa estático de riesgo de incendio y doce modelos climáticos de riesgo de incendio. El conocimiento de las áreas de riesgo permitirán hacer futuras recomendaciones para planes de prevención de incendio forestal.

El presente estudio mostró que los factores de los submodelos de Combustible e Ignición juegan un papel fundamental para determinar el riesgo de incendio. En este caso, los tipos de vegetación con mayor superficie forestal quemada fueron: Bosque de encino, matorral y bosque de pino. La distribución de áreas quemadas además mostró una tendencia a incrementarse en cierto tipo de elevación, pendiente y orientación de ladera, distribuyéndose principalmente en altitudes medias orientadas al sur y en laderas de pendiente pronunciada. Los resultados también mostraron que áreas cercanas a campos de cultivo, pastizales o caminos existe mayor superficie quemada, pero a medida que la distancia aumenta la superficie quemada disminuye. Por otro lado, el submodelo de Detección reveló que existe gran parte del área de estudio es visible desde ciudades, carreteras y torres forestales. Sin embargo, es importante considerar para la planificación forestal aquellas áreas que permanecieron como no visibles desde estos puntos. De acuerdo al submodelo de Respuesta el 36.3% del área de estudio tiene una respuesta de alta a máxima, el 42.3% de media moderada y el 5.6% de baja a mínima. El resultado global de la suma de dichos modelos en su versión estática muestra que el 91% de la superficie forestal se encuentra dentro del riesgo medio alto a alto.

3.1 FASE I. EXPLORATORIA

3.1.1 Factores biofísicos que afectan la incidencia y comportamiento de incendios forestales

- **Tipo de vegetación.** El combustible es indispensable para generar un incendio. Por lo tanto, las características del tipo de vegetación tienen gran influencia en el desarrollo de incendios forestales. El tipo de vegetación predominante en el área de estudio es el bosque de pino con una superficie total de 84 250 ha, seguido por el matorral secundario (57902 ha), el bosque de encino (23665 ha), el bosque de pino-encino (23521 ha), y el bosque tropical caducifolio (1009 ha). Siendo los tipos de vegetación con mayor superficie quemada: el bosque de encino (4388 ha), el matorral secundario (4316 ha), y el bosque de pino (4185 ha). La superficie quemada entre tipos de vegetación es similar, y debe ser considerada como un signo importante de degradación forestal en esta área. Sin embargo, es importante considerar que la proporción de la superficie quemada de bosque de pino es de 4%, mientras que para el bosque de encino y el bosque tropical caducifolio asciende a 19% y 17%, respectivamente. Por lo tanto, proporcionalmente a su área el bosque de encino fue significativamente más afectado que otro tipo de vegetación ($H = 21.84, P = 0.0002$).
 - **Altitud.** Dependiendo de ciertas características de la vegetación tales como la composición de especies y su densidad algunos tipos de vegetación son más propensos a sufrir incendios. Por lo tanto, la distribución altitudinal de la vegetación tiene una estrecha relación con la distribución de la superficie quemada. Las áreas quemadas se encontraron principalmente entre los 2000 y 2800 m s.n.m., siendo los tipos de vegetación predominantes entre estas altitudes son el Bosque de Encino y de Pino. A mayor altitud generalmente, el fuego se extingue ya sea porque la cobertura de la vegetación disminuye o a que los cambios en temperatura y humedad que existen a altitudes mayores pueden inhibir el esparcimiento de los incendios. Por otro lado, dado que nuestro interés se centra únicamente en incendios forestales, en este análisis se excluyeron las áreas no forestales tales como pastizales y campos agrícolas, ubicados principalmente en altitudes menores a 2000 m s.n.m. No obstante, es común que los incendios provenientes de estas áreas se extiendan a elevaciones mayores debido al efecto de la pendiente y el viento en el esparcimiento del fuego.
 - **Pendiente.** La presencia de áreas quemadas fue mayor en pendientes pronunciadas que en áreas con poca pendiente, con excepción de la clase de pendientes muy inclinadas, cuya área es la más pequeña e inaccesible de todas ($H = 139.2, P = 0.0001$).
 - **Orientación.** La distribución de la superficie quemada fue significativamente diferente entre los diferentes tipos de orientación de ladera ($F_{(7,1671)} = 2.79, P = 0.0069$). De acuerdo con la prueba de Tukey, no hubo diferencias significativas entre las áreas quemadas expuestas al sur, pero sí entre las expuestas al Oeste, Noroeste y Noreste. La distribución de las áreas quemadas predominó en laderas con orientación sur, ya que al recibir más horas de sol al día, estas laderas presentan mayor sequedad y temperaturas más altas que las laderas norte.
 - **Factores de ignición.** La principal causa de incendios en México son las actividades humanas. En el estado de Michoacán la quema de pastizales y de campos agrícolas son las principales actividades generadoras de incendios. Ambas actividades se llevan a cabo durante la temporada de secas que va de enero a mayo. El análisis realizado en este estudio encontró que existe una clara relación entre la distancia a pastizales y campos agrícolas y el aumento de
-

la superficie quemada. A medida que el bosque se encuentra más cerca de campos de cultivo o pastizales, hay más fragmentos quemados y el área quemada es mayor, y a medida que se aleja, el área quemada es menor. La distancia a caminos y ciudades también ejerce un efecto. El efecto borde presente alrededor de caminos y carreteras también podría estar influenciando la distribución del área quemada. Además, es importante considerar que los caminos proporcionan acceso al humano hacia áreas forestales o remotas. Al igual que en los casos anteriores el área quemada aumenta a medida que la distancia a caminos y ciudades disminuye. Sin embargo, cabe la pena mencionar que la distancia a asentamientos humanos tiene un efecto menor con relación a la superficie quemada.

- **Clima.** La temporada de incendios ocurre durante la primera mitad del año. Abril y mayo son los meses donde ocurren la mayor incidencia de incendios. La temperatura y la baja precipitación ocurrida en estos meses permite que el combustible vegetal se seque favoreciendo, así, a los incendios forestales. Asimismo, los incendios provocados por humanos tienen mayor influencia cuando las condiciones naturales, tales como, altas temperaturas y baja humedad son propicias para los incendios.

3.2 FASE II. MODELAJE

3.2.1 Submodelo Combustible

El combustible y los factores relacionados con su distribución tales como la elevación, la pendiente y la orientación de ladera tienen un gran efecto en la distribución de los incendios forestales del área de estudio. Los tipos de vegetación definen las áreas de riesgo, mientras que la topografía, en particular la orientación de ladera, intensifica el riesgo. Después de integrar todos los factores, se identificaron las áreas de máximo, alto, mediano y bajo riesgo. La clase de mediano riesgo fue la clase predominante; mientras que los riesgos máximo y bajo fueron identificados en proporciones similares. El área de bajo riesgo corresponde principalmente a áreas no arboladas, principalmente campos agrícolas, pastizales o ciudades. El riesgo mediano también lo conforman campos de agricultura y pastizales; sin embargo, se localiza rodeando vegetación natural, dado que los incendios que se inician en estos sitios por lo general se extienden a las áreas arboladas. Esta clase también incluye áreas con la vegetación natural localizada en áreas bajas como matorrales o en altitudes muy altas. Las áreas clasificadas como de alto riesgo se encuentran en cuevas escarpadas con vegetación natural, principalmente bosques de pino o encino. Por otro lado, las áreas de máximo riesgo son aquellas que cumplen todas las condiciones que favorecen los incendios forestales. Estos son pendientes escarpadas orientadas al sur y con vegetación natural como pino, encino o bosque tropical caducifolio. El submodelo de riesgo de combustible se puede observar en la figura 4-12 de la sección de resultados.

3.2.2 Submodelo Ignición

El modelo de ignición está relacionado con actividades humanas como la agricultura, la ganadería, o la presencia de asentamientos humanos o caminos. En la fase exploratoria se observó una relación directa entre estas variables y los incendios forestales. Debido a esto, en este submodelo fue incluida la categoría origen de riesgo, la cual incluye las áreas donde se llevan a cabo dichas actividades humanas. Los riesgos máximo y alto fueron localizados en áreas con vegetación natural limítrofes con

campos de agricultura, pastizales y carreteras. Por otro lado, el riesgo mínimo fue localizado en áreas de mayor altitud donde no hay presentes asentamientos humanos. El submodelo de riesgo de ignición se puede observar en la figura 4-13 de la sección de resultados.

3.2.3 Submodelo Detección

El submodelo de detección muestra las áreas donde un incendio no puede ser detectado durante un cierto período del tiempo. Ya que el área de estudio es un área altamente poblada, gran parte de la superficie es visible desde ciudades, caminos y torres forestales. Sin embargo, todavía existen algunas áreas que permanecen como no visibles. Las áreas no detectables pertenecen principalmente a áreas remotas con altitudes más altas o a barrancos. Asimismo, algunas áreas entre montañas o lejos de caminos tampoco son visibles. Este submodelo permite identificar estas áreas lo que puede ayudar en la toma de decisiones para la localización de nuevas torres o campos forestales.

3.2.4 Submodelo Respuesta

El submodelo de respuesta mostró que el 54% del área de estudio puede tener una capacidad de respuesta de máxima a alta, el 42% de media a moderada y el 5% de baja a mínima. Las distribuciones de las áreas de velocidad de respuesta no son al azar debido a la presencia de 15 centros forestales en el área, de los cuales las brigadas de bomberos acuden a extinguir el incendio. Casi todos los centros forestales se encuentran localizados en la parte del sur-oeste del área. Las zonas donde hay un tiempo más largo de respuesta son en general aquellos donde la altitud es mayor. Esto significa que áreas con altitudes altas y terrenos escarpados son más inaccesibles que áreas con altitudes bajas y terrenos llanos. Una cuestión importante de este modelo es que, consideró valores de fricción en el cálculo de la capacidad de respuesta. La variedad de respuestas depende de la pendiente, el tipo y densidad de la vegetación y el tipo de caminos, ya que, las cuestas escarpadas o los tipos de vegetación muy densos podrían ser difíciles de pasar por las brigadas. El mapa del submodelo respuesta se puede encontrar en la figura 4-15 de la sección de resultados.

3.2.5 Modelo estático de riesgo de incendio

Para construir el modelo de riesgo estático de incendio se evaluaron tres Ecuaciones:

1. Modelo estático = Combustible + Ignición + Respuesta + Detección
2. Modelo estático = (3 × Combustible) + Ignición + Respuesta + Detección
3. Modelo estático = (3 × Combustible) + (2 × Ignición) + Respuesta + Detección

La ecuación 1 es la suma de los cuatro modelos estáticos sin ponderación alguna, la ecuación 2 da más peso al submodelo Combustible y la ecuación 3 incluye al submodelo de Ignición como el segundo factor en importancia. A pesar de que las tres Ecuaciones dan pesos diferentes para el combustible y la ignición, la distribución de cicatrices quemadas es similar en la mayor parte de categorías usando las tres ecuaciones. La diferencia principal se observa en la distribución de cicatrices quemadas en las categorías de riesgo moderado y bajo. La ecuación 3 fue elegida para calcular el modelo estático, ya que da mayor peso a dos de los factores principales para iniciar un incendio: combustible y calor (fuentes de ignición).

El modelo estático de riesgo de incendio considera a todos los factores incluidos en los submodelos de combustible, ignición, detección y respuesta. El resultado global de la suma de todos los submodelos es el Modelo de Riesgo de Incendio final, pero estático. Según este modelo el 29% del área del bosque posee riesgo de incendio de máximos a alto, el 42 % es clasificado como medio-alto a moderado y el 30 % es clasificado como bajo a mínimo riesgo. Dado que el modelo de combustible posee mayor peso en el modelo, la topografía y el tipo de cobertura juegan un papel fundamental en la distribución de las áreas de riesgo. Las áreas con riesgo máximo y muy alto corresponden a laderas de orientación sur con bosque de pino, pino-encino y encino. Por otra parte el efecto de la fuente de ignición se refleja en un claro aumento del riesgo en áreas de vegetación natural limítrofes con caminos, campos de cultivo y pastizales. En cuanto a las áreas del riesgo medio, su distribución es más heterogénea en los tipos de vegetación presentes en altitudes medias. El efecto de los submodelos de respuesta y detección no es tan evidente en el mapa final del riesgo de incendio el modelo estático, ya que ambos ocurren una vez que el fuego ha comenzado.

3.2.6 Modelo multi-temporal de riesgo de incendio (Submodelo Clima)

El modelo de riesgo meteorológico se llevó a cabo para los 12 meses del año. El objetivo de este modelo fue comparar las diferencias entre la distribución de las áreas de riesgo a lo largo del año. Durante la temporada seca, se observó que las áreas clasificadas como de máximo, muy alto y alto riesgo aumentaron con respecto a los meses lluviosos. Las diferencias más contrastantes se observaron entre abril, el mes más cálido y seco, y agosto, el mes más húmedo y frío. Sin embargo, es importante considerar que el uso de valores promedio mensuales de temperatura y precipitación impide que el modelo prediga como cambiará el riesgo de incendio de un día a otro. Además el submodelo no comprende variaciones inter-anales, por lo que fenómenos climáticos relacionados con incendios forestales como “El Niño” no son considerados. No obstante, el modelo sí ayuda a identificar las áreas de mayor riesgo, principalmente durante la temporada de secas, lo cual podría permitir la elaboración de medidas de prevención. Además el modelo se puede modificar fácilmente si se cambian los parámetros climáticos.

3.3 FASE III. VALIDACIÓN

La validación del modelo de riesgo de incendio forestal se llevó a cabo cruzando el mapa de áreas quemadas con los mapas de los submodelos y el modelo de riesgo de incendio final. El modelo estático tuvo una alta coincidencia de las áreas de riesgo alto y la superficie quemada o escamas de incendio, ya que el 92 % de la superficie quemada fue localizada principalmente en las categorías de máximo a medio-alto riesgo. Por lo tanto, los esfuerzos en el manejo de incendios forestales, deben dirigirse principalmente a las áreas de riesgo muy alto a medio alto. Dado que este modelo incluye la información de los submodelos de Combustible, Ignición, Detección y Respuesta y constituye la base para el submodelo Clima, se aplicó un análisis ROC (Receiver Operation Characteristic) como prueba adicional para la validación. Dicho análisis reveló que el modelo estático fue muy bueno al clasificar las categorías de riesgo de incendio ($ROC = 0.8$). Por otro lado, en el caso del submodelo Clima tuvo un porcentaje alto de coincidencia de cicatrices de incendio en las categorías de riesgo alto para los meses de la temporada seca, mientras que para los meses de la temporada lluviosa el riesgo disminuye para las mismas áreas. Para abril el 98% de las cicatrices de incendio se localizó en las categorías de

riesgo alto, mientras que para agosto solo fue del 25%. Finalmente cabe la pena mencionar que en general la exactitud del modelo fue alta ya que casi todas las cicatrices de incendio se localizaron en la clase de riesgo alto.

4 CONCLUSIONES

El objetivo general de este estudio se cumplió, ya que se elaboró un mapa de riesgo forestal para una zona con frecuentes incendios en Michoacán. El modelo identificó apropiadamente las áreas de alto, medio y bajo riesgo de incendio forestal. El modelo estático mostró que 29% de la superficie forestal tiene un riesgo de máximo a muy alto, el 42% de medio alto a moderado y el 30% de bajo a mínimo.

Para desarrollar el modelo de riesgo se cumplieron los cuatro objetivos específicos planteados: 1) Detectar y mapear las áreas quemadas usando una imagen ASTER, 2) Analizar los principales factores relacionados con incendios forestales del área, 3) Desarrollar un modelo de riesgo de incendio forestal que identifique las áreas con mayor probabilidad de incendio, y 4) Validar el modelo de riesgo de incendio forestal. A continuación se presentan las conclusiones específicas.

La utilización de la imagen ASTER permitió mapear exitosamente las áreas quemadas utilizando una combinación de bandas 3, 2, 1. El área afectada por incendios forestales fue de 15,220 ha de un total de 339,330 ha. En base a este mapa los factores relacionados con incendios forestales tales como pendiente y tipo de vegetación fueron evaluados. Como resultado, se encontró que existe una clara relación entre la presencia de áreas quemadas y la distancia a campos de cultivo, pastizales, caminos y ciudades. Asimismo, la topografía tiene un efecto importante ya que la distribución de las áreas quemadas es predominante en áreas con pendientes pronunciadas y laderas orientadas al sur. Finalmente, los tipos de vegetación con mayor superficie quemada fueron los bosques de pino y encino.

Los submodelos de combustible, ignición, detección y respuesta constituyen el modelo estático. Los componentes tanto del modelo de combustible como el de detección fueron fundamentales para el correcto desarrollo del modelo de riesgo de incendio. Por otro lado, el mapa de detección mostró que aunque la mayor parte del área de estudio es visible, aún existen áreas en donde los incendios no son perceptibles desde su origen. De acuerdo con el submodelo de respuesta el 54% del área de estudio tiene una capacidad de respuesta de máxima a alta. Dicha capacidad se encuentra en función de la pendiente, la altitud, el tipo de vegetación y el tipo de camino. Por ejemplo, pendientes pronunciadas o con tipos de vegetación densos como el bosque tropical caducifolio oponen más resistencia al paso de brigadas que zonas planas con pastizal. Finalmente, los modelos de riesgo climático mostraron diferencias en la distribución del riesgo entre los meses más calidos y secos y los meses pertenecientes a la temporada de lluvias. Abril resulto ser el mes con mayor riesgo del año, mientras agosto es el mes con menor riesgo. Dichos resultados coinciden con las estadísticas de incendios oficiales (COFOM, CONAFOR) que muestran dicha tendencia de incendios forestales a lo largo del año.

Finalmente, la validación del modelo estático de riesgo fue satisfactoria para el área de estudio, dado que la mayor parte de los modelos presentó más del 92% de la superficie quemada en las áreas clasificadas como de muy alto a alto riesgo. Por lo tanto, los resultados de éste estudio son apropiados

para elaborar estrategias de prevención de incendios en el área de estudio. En resumen, el modelaje por medio de sistemas de información geográficas aplicado en este estudio permitió la elaboración de un modelo confiable de riesgo de incendios forestales. Asimismo, la simplicidad del modelo permite incorporar nuevas variables o realizar ajustes con el fin de mejorar los resultados ya obtenidos. En base a las observaciones hechas en este estudio, a continuación se citan las recomendaciones propuestas para futuros estudios en el tema:

- Se recomienda complementar la interpretación visual de las áreas quemadas con otra técnica como el análisis de índices de vegetación o valores de temperatura superficial.
- Se recomienda ampliamente incluir datos que proporcionen información del estado de humedad del combustible, dirección y velocidad del viento.
- Dado que los incendios se incrementan debido a fenómenos meteorológicos como “El niño”, se recomienda alimentar al modelo con información meteorológica actualizada de manera constante.
- La inclusión de información adicional relacionada con densidad de vegetación o biomasa puede mejorar los resultados encontrados en este estudio.

Algunas de las ventajas de utilizar el método aplicado en este estudio son que 1) El modelo se puede reproducir fácilmente para otras áreas, dado su sencillo manejo y operación y 2) El método aplicado es poco costoso dado que la mayor parte de los procesos se llevan a cabo en el software Ilwis, cuya licencia es gratuita, lo que permite que su aplicación se lleve a cabo fácilmente en otras áreas del país.

Abstract

The incidence of fires in size, frequency and intensity has increased significantly around the world. Mexico, a mega diverse country, has recurring forest fires, especially during the El Niño years. However, government efforts to the prevention of fires are still insufficient to reduce fire frequency and intensity. Moreover, fire risk maps at medium scale are still lacking for most of the country. Mexico needs to develop, fire prevention strategies with high efficiency in order to avoid the loss of natural resources. As any other natural disaster, fires have always influenced ecosystems provoking important abiotic and biotic changes. However, not all the ecosystems are adapted to the increasing frequency and size of forest fires. Fires cause the loss of local biodiversity and grave socio-economical damage. In Mexico, Michoacan state is among the first states with high fire frequency. Human activities such as grassland burning or campfires are the main cause. The general objective of this study is to model forest fire risk for a critical zone in Michoacan state. In order to do this, the method was divided in three phases: exploratory, modelling and validation. This study integrates biophysical and human variables into a fire risk model. There are four main factors that modify the fire risk model: 1) fuel, 2) physical environment, 3) causal factors and 4) prevention and suppression. Out of these factors, fuel was considered the most important since is indispensable for fire ignition and spreading of fires. In the first phase, these effecting factors were analyzed statistically. Likewise, in this phase, an ASTER image was used for visual interpretation to generate a burnt area map and to improve the vegetation type map. In the second phase, to detect the high, medium and low risk areas, five sub-models were developed: Fuel, Ignition, Detection, Response and Weather. These sub-models were constructed using logical indices based on a literature review and the opinion of the expert. Finally, in the third phase, the fire model was validated with a burn area map of the study site. The final outputs were a static fire risk model and twelve weather monthly risk models. The knowledge of the fire risk areas allow us to recommend the development of fire prevention plans.

The study revealed that factors included in the fuel and ignition sub-models play an important role to determine the fire risk. The vegetation types with more burnt surface were: Oak forest, Scrubland and Pine forest. The distribution of the burnt areas also shows a tendency on elevation, aspect and slope classes. Burnt areas were predominantly over medium altitudes, oriented to south and on steep slopes. Results also showed that in the proximity of crop fields, grasslands and road there is more burnt surface, but as this distance increases the burnt surface decreases. On the other hand, the detection sub-model revealed that a high percent of the study area is visible from cities, roads and forest towers. For fire risk management plans however, it is worth to consider the non visible areas. According to the Response sub-model 54% of the study area has a high to maximum response, 42% shows a medium to moderate response and 5% may have a low to minimum response. The results of the sum of these sub-models in its static version show that 92% of the forest's surface is in the medium high to high risk categories.

Key words: Forest fire, Fire risk, Fuel, Ignition, Weather, Detection, Response, México, Michoacán

1. INTRODUCTION

1.1 Background

1.1.1 Forest fires and influencing factors

A fire is a chemical reaction that needs heat, oxygen and fuel to start and carry on, as it is established in the “fire fundamentals triangle”[1]. When an uncontrolled fire starts in or spreads to natural vegetation it converts to a forest fire. Therefore, its probability of occurrence depends on the ignition causes and environmental preconditions [2]. Among these are the fuel’s quality and distribution, the weather, topography, and human factors [3,4]. The following are brief descriptions of these influencing factors.

- *Fuel’s distribution.* Fuel could be distributed vertically or horizontally; a vertical distribution means that the fuel is found perpendicular to the ground, meanwhile, if the fuel is found in a parallel arrange to the ground, its is said that its distribution is horizontal. Often fuel’s vertical distribution is found in a very uneven way, which causes variations in the intensity of fire [4]. On the other hand, the horizontal distribution will determine where the fire will occur or spread.
 - *Fuel’s quality.* The characteristics of a fire, like the intensity and the heat generated, are essentially determined by the quantity and composition of the available fuel [5,6]. Fuel could be either living organic matter (like grass, bushes, trees, or canopy) or dead organic matter (*i. e.* dead bark, branches, twigs, leaves, etc.) [5]. The arrangement, size density, distribution, moisture and chemical composition of these materials, are the factors that determines fire’s intensity. Therefore fire’s spreading speed and released energy are highly depending on the mentioned factors [6]. Such characteristics are due to vegetation type found in the areas where the fire is happening [5].
 - *Weather.* High temperatures, low relative humidity, and winds are the typical weather conditions for a fire development, because these conditions reduce fuel’s drying time and the spread of fire [3]. Nevertheless, local weather is determined, in part, by vegetation, for example a dense and close canopy reduces relative evaporation and maintains high soil humidity; yet in an area with less vegetation cover the opposite will occur [7].
 - *Topography.* Terrain’s shape has several effects on fire’s distribution. For example in the case of fire on a slope, the flames establish a strong contact with the ground surface, which heats up the
-

fuel and favours the fire's spread [5]. Therefore, the movement of a fire is slower if it begins on a summit and is faster if begins on a canyon. This behaviour can also explain why a rough topography can constitute a fire-breaker barrier [8]. In addition, the slope's orientation plays a key role in fire's behaviour. This is because in the Northern hemisphere, a southern slope is drier than the northern slope. Southern slope is more suitable to ignite than the northern slope that has more humidity and green cover. In contrast, despite that altitude is not considered a factor that directly increases the occurrence of fire, it does modify the climate, which is directly related with fires. For example, the temperature at higher altitudes is lower than low altitudes. Moreover, in temperate areas precipitation is higher than lower zones. This reduces the probability of fires due to the moisture of fuel.

- *Human factors.* Humans have always lived with fire [9,10], and were able to control it. Fire has been used by humans for many reasons, from cooking to agriculture or livestock farming. Due to negligent activities and misuse of fire in agriculture or grazing land management, human activities are a main cause of fires around the world and Mexico is not an exception [11,12]. Fires are also related to other indirect activities such as deforestation, use of non-timber forest products (NTFP) or socio-economic and political conflicts. Thus, the study of human's role and his/her activities is crucial to understand the distribution of fires and its control. In Mexico, from pre-columbine times to the present shifting cultivation or slash and-burn agriculture, has been a common practice in Mexico [13]. Each year new areas are deforested and incorporated to shifting agriculture and grasslands. This represents a real risk for the forested areas since farmers who use fires represents the poorest sector and do not have instruction on how to control fire during the preparation of the agricultural terrain and grasslands.

1.1.2 Classification of forest fire

There are two classifications of forest fire: by their origin or by the fuel stratum they affect. Each classification is useful to develop prevention or suppression actions in a forest management plan. To design a prevention plan it is important to know the potential origin of a fire. On the other hand, the affected fuel stratum determines the behaviour and intensity of the fire. Consequently, the actions to control an active fire could depend on it. The main characteristics of each classification are:

- By its **origin** a fire can be classified as to be started either naturally or by humans. A natural fire is usually provoked by lightening. Natural causes also includes: extreme heat, sparks created by the friction of falling rocks or volcanic eruptions. Nevertheless, as it was explained in the previous section, the main cause of forest fire around the world is human activity. Forest fires caused by human activity can be divided into: negligent, intentional and accidental [14]. The main human activities that provoke forest fires in Mexico are negligence activities. Agriculture and grassland burning represent 60%. Other negligent activities can be cigarettes and camp fires (18%) (Figure 1-1)). Intentional fires, which represent 12% of the forest fires, occur as a product of conflicts or inadequate land use (e.g. illegal deforestation). Finally accidental fires are product of non intention action as car or train crash or electrical failure.
-

- Another classification focuses on the **affected fuel stratum** [15]. A fire that spreads horizontally over a terrain consuming leaves, twigs, fallen trees, grasses and other low plants is classified as superficial [15]. If the fire reaches the tree crowns under the influence of wind and slope, then is converted to a crown fire [16]. These type of fires are considered very destructive and of difficult control [17]. On the other hand, ground fires are those which spread below ground, burning organic matter such as compacted dead leaves and roots [15].

1.1.3 Forest fires: Effects and consequences

After a forest fire, there are remarkable abiotic and biotic changes. Some are the direct consequence of the fire, such as bark singe or tissue disintegration. However, there are other indirect effects that remain once the fire is extinguished. The main abiotic changes after a fire are: increase or decrease in soil nutrients content [4,18,19], increase of light and soil temperature [4,18] and increase of wind speed as a consequence of vegetation removal [20]. Due to these changes soil erosion processes are usually catalyzed after fire [21]. Unless the ecosystem is adapted to fire, the frequent presence of fire decreases the species richness and alters of the species biodiversity and vertical structure [12,22,23]. There can be also big socio-economic impacts, such as wood burnt or house damages are the most frequent. In summary, among the forest fire damages can be found: 1) wood destruction, 2) increase on land erosion, 3) habitat destruction and flora and fauna lost, 4) tree weakness and illness, 5) increase of pollutants, 6) decrease of landscape beauty, 7) health damages as a consequence of respiratory problems and 8) human and animal deaths [12,14,24].

1.1.4 Fire hazard, risk and danger definitions

A known definition of risk is “the probability of an event and the expected outcome-typically expressed as damage of the event” [25]. In other words, “is the multiplication of costs, the vulnerability and the recurrence interval of natural damaging phenomenon” [26]. The last definition is commonly applied to study technological, landslides, volcanic and other catastrophic events. However, the terminology of fire danger, risk and hazard is not always completely clear as in other disciplines. The definition and use of the term fire risk varies widely among fire researches [2]. Some authors have discussed the heterogeneity of this terminology. Bachmann, after a extensive literature review [2] proposes that: “**Fire hazard** is the process leading to undesirable outcomes”, “**Fire risk** comprises the probability of an undesired event and the outcome of it” and “**Wildfire risk** is the probability of a wildfire to occur at a specified location and under given circumstances and its expected outcome as defined by the impacts on the affected objects.” In contrast, Hardy [25] considers the catastrophic and negative adjectives associated with fire risk as inadequate, since fire has always existed in nature and even for some ecosystems it is part of a natural and recurrent process. Therefore, this author proposes that “**Fire risk** refers only to the chance (probability) of ignition of a spreading fire, and does not address values or damages”, whereas “**Fire hazard** is a fire-centric term, and is independent of weather. The term hazard must only be used to express the state of the fuel complex”. Other concept used in fire management is fire danger. FAO [27] defines **Fire danger** as “A general term used to express an assessment of both fixed and variable factors of the fire environment that determine the ease of ignition, rate of spread, difficulty of control and fire impact –

often expressed as an index.” Besides, it considers that **Fire danger rating** is: “A component of a fire management system that integrates the effects of selected fire danger factors into one or more qualitative or numerical indices of current protection needs”.

1.1.5 The role of Remote Sensing and GIS in fire modelling

Today there are many tools which integrate the biophysical and social elements to study forest fires. GIS and remote sensing allow to monitor, analyze and predict forest fires activity from local to global scales [28-31]. The following points summarize RS/GIS applications in forest fires [30,31]:

- They allow to integrate hazard variables such as vegetation, topography and human infrastructure
- They help to identify fire risk areas since they can consider meteorological conditions, vegetation type and allow the detection of burnt area.
- They provide important information of human settlements, natural resources, etc.
- They allow evaluating the fire disturbance degree and to assess the damages of the burnt forest.
- They allow to model forest fire risk or risk, to monitor and manage active forest fire, to model or simulate fire growth or spread and to assess forest recovery after fire.

RS/GIS are widely used for fire management including prevention activities. Remote sensing techniques allow monitoring vegetation, susceptibility to the fire, detection of the thermal signal of active fires, and post-suppression tasks as burnt area assessment [32]. The detection of active fires allows the knowledge of the fire distribution pattern. This is particularly useful in areas in which accurate fire reports are not available. Moreover, remote sensing techniques become indispensable for big inaccessible forest areas. The study after fire effects is another important issue that is commonly used to assess damage or study vegetation recovery. On the other hand, GIS is a suitable tool to integrate risk factors and to construct scenarios of forest fire risk. In the next paragraphs a brief review will focus on active fire detection, burnt scar assessment and fire risk modeling.

1.1.5.1 Active fires

There are several remote sensors designed to detect and monitor active fires in different spatial and temporal scales. Among these we can cite the Advanced Very High Resolution Radiometer (AVHRR), the Infrared Spin-Scan Radiometer and Atmospheric Sounder (VAS), the Along Track Scanning Radiometer (ATSR), the Moderate Resolution Image Spectroradiometer, the Operational Linescan System (OLS) and the Bi-spectral Infrared Detection (BIRD). A complete list of these sensors can be found in Lentil *et al.* [28]. The main differences among these sensors are the resolution of the MIR channel the revisit time, the minimal detectable fire area, the capability for a quantitative retrieval of fire parameters and the general mission parameter [33]. For example sensors as MODIS, AVHRR and ATSR have 1 km² of resolution and a revisit time of 12, 24, 24 hours respectively. On the other hand, BIRD sensor with its 100 m² of resolution allows the detection of fires in an area 7 times smaller than MODIS, but its revisit time is based on experimental imaging of selected areas [34]. In order to distinguish hot spots from the rest of the environment numerous algorithms have been proposed [35,36]. Basically, the detection of active fires is based on the brightness temperature levels

in short wave and thermal infrared bands (MIR, TIR, VNIR) wavelength bands which must be above the background [37]. This temperature depends on the fire temperature and size which is in function on the specific characteristics of the fire as it is the affected vegetation type and the fire intensity levels. It is worth to notice that the active fire detection still present certain problems. The main limitation is the information gap caused by the temporal coverage of most satellites, which in some cases could be every 16 days. This lack of information produces errors of commission that give erroneous scenarios of what really happens [38]. However, the study of remote sensing is in constant development. It is likely that soon new methodologies will allow the get of more reliable information. Some authors have proposed alternatives to this problem combining remote sensing techniques for the detection of active fire pixels with methods of burnt area detection [38].

1.1.5.2 Burnt scars

After a fire, the vegetation disappears giving place to a black layer of ash and burnt material. The vegetation absence increases the sun exposition of the soil, increasing the temperature of the soil [18,39]. Both facts are clues for mapping burnt scars which can be done by visual interpretation [24,40] or by satellite image classification [40]. The selection of bands is crucial for good visual interpretation since burnt areas present low reflectance in red and near infrared. For example, Landsat bands 4 and 5 have a good performance on the direct identification of burnt areas [40]. Based on this principle, the normalized difference vegetation index (NDVI) is also used for mapping burned forested areas [41]. Other indices for burned land discrimination are the Burned Area Index, the Soil Adjusted Vegetation Index and the Global Environmental Monitoring Index [42]. On the other hand, surface temperature is an other accurate criterion to discriminate burned areas and surroundings. The value composite technique [43] compares maximum or minimum values of different data such as NDVI, temperature, channels or albedo from different dates in order to find changes on land cover and detect burned areas. Summarizing, some of the composite techniques on satellite image classification for burned land mapping are [44,45]: 1) Minimum reflectance of the red channel and Minimum reflectance of the NIR channel, 2) Maximum Surface/Brightness Temperature, 3) Maximum value composite of the date with the maximum NDVI, 4) Maximum temperature from the three minimum reflectance for channel 2 and 5) Minimum reflectance of channel 2 from the three maximum temperatures. Among these, the composites that uses thermal bands have better accuracy than those based on NDVI values due to its capacity of cloud and shadow discrimination [46]. Moreover the Burnt Area Index, which considers a spectral reference point in its calculation, shows also a great capacity on burnt area discrimination [42]. Finally is worth to say that the product MCD45 of the Moderate Resolution Imaging Spectroradiometer (MODIS) of 500 m pixel resolution have been developed to localize and assess spatially and temporally the burnt areas [35].

1.1.5.3 Forest fires modelling

According to Chuvieco [5] there are four main approaches to model forest fire risk: 1) Qualitative and quantitative models based on expert knowledge, 2) Quantitative models based on multi-criteria evaluation 3) Models based on statistics, which includes neural network models and 4) Meteorological or fire dispersion models. The quantitative models based on expert knowledge classify

fire variables using a numeric scale based on formula indices or weights derived from field observations, literature review and expert opinion. Then, the fire risk model is reclassified into a categorical scale into high, medium and low risk. The main advantage of this model is that it allows recognizing the risk areas to make appropriate management decisions. However, these models do not give ignition or spreading probabilities. Among these models we can find the studies of Chuvieco and Salas [31,47], Rathaur [48], Neeraj [49], Maselli *et al.* [50] and Roy [24]. In the other hand, the multi-criteria risk analysis also considers expert knowledge into the risk model. However, one of its objectives is to diminish the subjectivity on the selection on weights. This approach is useful when expert's opinions are diverse, helping to make agreements among experts. One example of the use of this method can be found on Chen *et al.* [51]. The statistic models are usually accurate models [52]. They are dependent on the spatial characteristics of the study area and therefore can not always be extrapolated to other areas. Among the statistic analyses used to model fire risk are: linear regression, logistic regression and Poisson distribution [31,52-54]. In the same way, neural network is a useful method when the fire patterns are very diverse or when the fire variables are not clear. Other types of models are those that simulate fire spreading. Some recognized models are the Behave, FARSITE and PYROCART models.

Under these criteria, models can be also divided according its time and spatial scale [5]. The long term studies take into account static variables such as topography, the road network and vegetation type. They show risk patterns and are useful for the development of prevention and management plans. On the other hand, the short term studies use weather data to calculate a daily or weekly risk. Its importance depends on the fire alert that these systems can give in real time. Some examples are the Canadian Forest Fire Danger Rating System (CFFDRS) and the National Fire Danger Rating System (NFDRS) from U.S.A.

1.1.6 Forest fires in Mexico

The occurrence of fires (size, frequency and intensity) have increased significantly world wide in the last decades as an effect of the El Niño periodic phenomenon, deforestation and other causes [55]. During 1998, an El Niño year, Mexico was extremely affected by these events, registering 14,445 fires which affected 919,000 ha, altering mostly the Pine-Oak forests [11,56,57]. Eight years later, in 2006, this trend continue registering 8,725 fires, which damaged more than 240,000 ha [58]. Michoacán was one of the most fire-affected states, especially in the year 2005 when 17,443 ha were affected [11]. The main cause of fire were human activities in a form of grassland burning for cattle feed and campfires [59].

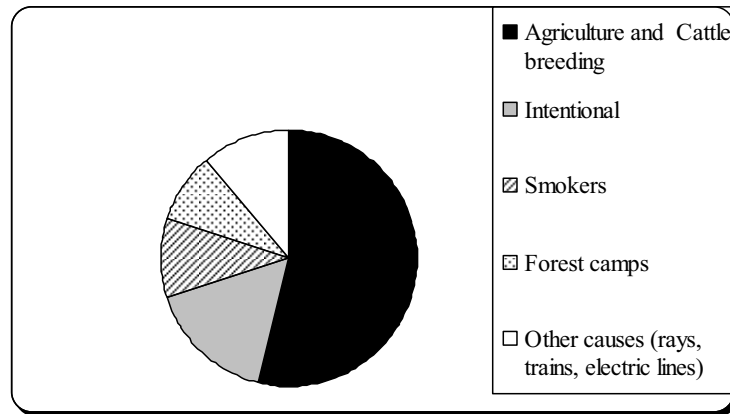


Figure 1-1. Main causes of forest fires in 1998, Mexico

The causes of fire are the result of an interaction between, biophysical and social elements. In Mexico, although, climatologic phenomena like “El Niño” or the dry season increase the frequency and intensity of fires, human activities are still their main cause, among these, agriculture is the most frequent fire-prone activity representing 48% of the total (Figure 1-1) [60].

The forest fire season is from January to June, being March and May the most fire intensive period [61]. Ninety percent of the fires are superficial, and most of them occur in the dry season caused by human activities [62]. For the centre of the country, where Michoacán state is located, the most important activities that promotes fires are grassland burning for cattle fodder and campfires [59]. Although it is true that natural fires are an important part of the dynamics of the ecosystems, they do not occur with the same frequency as fires caused by human activity.

1.1.1. Actual fire combating and prevention in Mexico

The actions to control and mitigate forest fires in Mexico are carried out by the National Program of Forest Fire Protection. Its target is to increase the prevention actions, detecting fires and reducing the response time and the affected area [58]. Three levels of government, civil organizations and volunteers contribute to the above mentioned activities. These activities are coordinated, since 2002, by the Ministry of Environment and Natural Resources (SEMARNAT) and the National Forest Commission (CONAFOR), which is the responsible institution of carrying out the anti-fire actions in Mexico [63]. At federal level, 18 agencies (13 State Departments and 5 federal dependencies) take part in a coordinated way in this program.

The main actions against fires considered in this program include the prevention, detection and fighting of fires. One of the primary actions is the detection of fires. To do this in a comprehensive way the actions are divided into four types [63]:

- Fixed Terrestrial Detection. It is carried out through the use of observation towers installed in forest camps. These towers are located in strategic points from which the staff observes and reports the occurrence of fires.

- **Mobile Terrestrial Detection.** Since there are areas or places where the observation towers are inefficient to detect fires; a different approach is needed to complement the previous detection type. To detect the occurrence in such places, this detection is realized by the Fire-Control Brigade patrolling in motorized vehicles, mainly in zones where there are a great visitor's inflow, or where the forest values are high.
- **Aerial Detection.** The use of flights to cover areas where there are no observation towers and roads for the access of ground personnel. However, this is an indirect strategy; given that there is much area to cover, and the agencies in charge of fire control are not able to afford flights in the whole area. Aerial reports are made by the Mexican Air Force, federal agencies, commercial and private airlines, which are required to warn flight controllers of airports once they have spotted a forest fire. The airport authorities in turn, report the fire to the State and National Center for Forest Fire Control.
- **Remote Sensing Detection.** The National Commission for the Knowledge and Use of Biodiversity (CONABIO), the Geography Institute of National Autonomous University of Mexico and of the National Meteorological Service (SNM) detect fires by using satellite images of NOAA-AVHRR, MODIS and GOES. CONABIO receives these images two times a day, whereas the national water commission (CNA) receives the images every 20 minutes. Then, these images are processed to allow the observation of possible fire occurrences using a Hotspot Algorithm. The detected hotspots in the previous step can be converted to a into map form for the purpose of publication and dissemination. In this case, CONABIO and SNM process the information and publish it in the internet as part of the Hot-Spot detection Program. Both agencies offer real-time interactive fire maps, in which can be observed the vegetation type where the fire happens. Moreover, the Canadian Forest Service produces a meteorological risk map (at a national scale) for the Mexican government. This spatial product reports the forest conditions and also the fire events. This map is updated daily.

1.2 Research problem

Although fires are beneficial for some ecosystems, they cause biological, social and economical damages, in addition to biological diversity losses [55]. In spite of all Mexican government efforts to prevent fire frequency and intensity, fires tend to increase every year [56].

The study area is one of the most affected zones in Michoacán state [64]. Nevertheless the risk areas and the important factors influencing fire have not been fully identified yet. The generation of fire risk maps at medium scale is still lacking for the major part of the country, with a few scanty academic contributions. For this reason it is urgently needed that Mexico develops, fire prevention strategies with high efficiency to avoid the loss of natural resources. It is necessary to integrate the available information and also generate more detailed information at large, medium and small scale, indicating the causes that favour the beginning and expansion of fires for their possible prevention. A forest fire risk map can help solve this problem because it shows fire probability in a given place [19]. The fire risk map would be of great value and essential in the management of forest resources for a more suitable response by the local authorities. For this reason the development of a database for fire risk seems to be a high priority project.

Many authors have focused their efforts on the fire risk assessment. The approaches are diverse, depending on the variable and the selected scale. In general, the final product is a prediction index of the fire risk in space and time [65]. Among the variety of fire prediction systems around the world we can mention: the Canadian Forest Fire Danger Index (CFFDRS), the National Fire Danger Rating System (NFDRS) and the Joint Research Center (JRC) [65]. Likewise, there are some known programs that simulate forest fires behaviour as Behave, FARSITE, or CSIRO. Although the fire risk models development in many countries has reached a very advanced level, in Mexico there are few works that evaluate forest fire risk. For instance we can cite Galindo and Barrón's work [66] which uses fuel, slope and fire frequency as input variables to create a fire risk index at small scale for the whole country. However, most of the studies in Mexico are focused on small areas due to lack of information, especially fuel data. For example, Villers-Ruiz and Lopez-Blanco [67] analyzed the fire risk in the Malinche volcano (706 km²) using the BehavePlus program developed by the US Forest Service. To accomplish this objective the fuel was classified according to the density of trees. The results describe which vegetation type has the highest fire dispersion rate. Other case study calculated a fire-risk index for the Chipinque Ecological Park (16.25 km²) [68]. The mentioned study used a fuel inventory, an IKONOS image, and land use information to determine fire risk index. The final result was a fire risk map. Both works have focused mainly on the fuel mapping to develop their fire models.

This study follows the approach used by Neeraj and Hussin [49] since it integrates biophysical and human variables. Fire probability depends on the ignition causes and preconditions, while, impact probability is associated with fire behaviour and suppression. Therefore, there are four main factors that modify the probability of a forest fire: 1) fuel, 2) physical environment, 3) causal factors and 4) prevention and suppression [48]. Based on this approach this study will add two new sub-models that will include ignition and weather variables. This integral approach, the use of a meso-scale and a weather multi-temporal sub-model are the main contributions of this study for fire risk modeling in Mexico. This model will not concern much with fuel mapping. Likewise, it is important to point out that the addition of an ignition sub-model will be crucial to the final forest fire risk model developed in this study, since human activity is the first cause of fires in Mexico.

Consequently, the main goal of this study is to develop a forest fire risk map, using remote sensing and GIS tools and all available data. This work will be focused on developing a method to generate a fire risk map for a Michoacán area based on physical, biological and social factors.

1.3 Rationale

Mexico is a mega diverse country [69,70], which annually loses thousands of hectares of forest due intentional or accidental fires [11] as consequence of burning of agricultural fields, grasslands, camping and other activities [57]. For this reason it is necessary to develop a strategy that can be used in fire prevention. Combating fire involves a considerable economical support and a huge amount of time, without mentioning the lives on risk to carry out this work. An example of this can be seen in 2003 when 252,882 man days were invested for fighting forest fires [63]. This study tries to contribute to fire prevention by developing a forest fire risk map. The contributions of this study are:

- Detecting burnt forests using medium and high spatial resolution satellite images.
-

- Analyze biophysical and social factors affecting forest fire in the test area of Michoacán, Mexico.
- Developing a forest fire risk model for the test area of Michoacán, Mexico.
- Supply a forest fire management recommendations for the test area of Michoacán, Mexico based on forest fire risk map.

1.4 Research objectives and questions

The general objective of this study is to model forest fire risk for a critical zone in Michoacán. In order to achieve this, the specific objectives and the research questions were divided in three phases.

| |
|---|
| Exploratory Phase |
| <p>1. To detect and map forest burnt areas using a high resolution ASTER image Q1. Can burnt area be detected using a high resolution ASTER image?</p> <p>2. To analyze the main biophysical factors related to forest fires in the study area Q2. Which of these factors are more related to fire through its relationship to burnt areas?</p> |
| Modeling phase |
| <p>3. To develop a forest fire risk model for the study area in order to identify the fire prone areas. Q3. Which are the fire prone areas (high, medium and low fire risk) in the study area?</p> |
| Validation phase |
| <p>4. To validate the forest fire risk model Q4. How accurate is the forest fire risk model developed in this study?</p> |

2 STUDY AREA

The study site is located in Michoacán state (Figure 2-1), one of the areas in Mexico with more forest fires. This state represents 3% of the entire country with 58, 643 km² of area and it is divided in 113 municipalities and 10 economical regions [71]. Due to its large area, its complex topography and the altitude range (0-4000 m a. s. l.) the climate varies from dry and hot to template and semiarid. Michoacán's vegetation includes Pine, Oak, Pine-Oak and fir forest, cloud forest, dry tropical forest, moist tropical forest, subtropical thicket, scrubland, spine thicket, natural grassland, induced grassland, cultivated grassland, palm tree forest, and mangrove. This is a high biodiverse area. There are more than 985 plant species, 88 mammal species, 460 bird species, 112 reptile species, 36 amphibian species and 38 fish species [72]. Nevertheless, it is among the states with highest deforestation rate in the country. The total number of inhabitants is 3 495 742 of which 113 166 belong to indigenous groups [73]. The official language is Spanish; however 12% of the indigenous habitants do not speak it. The most important indigenous groups are Purepecha, Nahuatl, Mixteca, Mazahua and Otomi [73]. These groups are generally characterized by high level of poverty. In accordance with the Index of Human Development calculation for Mexico, Michoacán is one of the states with less development and subsistence level [74].

2.1 Location

The selected study area is based on an ASTER image taken at the end of the dry season (May, 2006). The criteria selection of this image was: 1) Geographical location, 2) Temporally coincidence with dry season, 3) Null cloud cover, 4) Medium spatial resolution (15 m), and finally 5) a High frequency of fires. The exact location of the study area is between the coordinates 20.15 -102.5 NE, 19.59, -102.63 SE, 20.07, -101.92, NW, 19.51, -102.5 SW. The area of this test site is 3942 km², which includes 23 municipalities of Tepalcatepec, Lerma-Chapala, Purepecha and Bajío regions (Figure 2-1). Its highest point is 3400 m, and its lower point is 1110 m.

2.2 Climate

Due to the altitudinal difference there are two general climates: subtropical and temperate. The average temperature and rainfall values of the warm and the template areas can be seen in Figure 2-2.

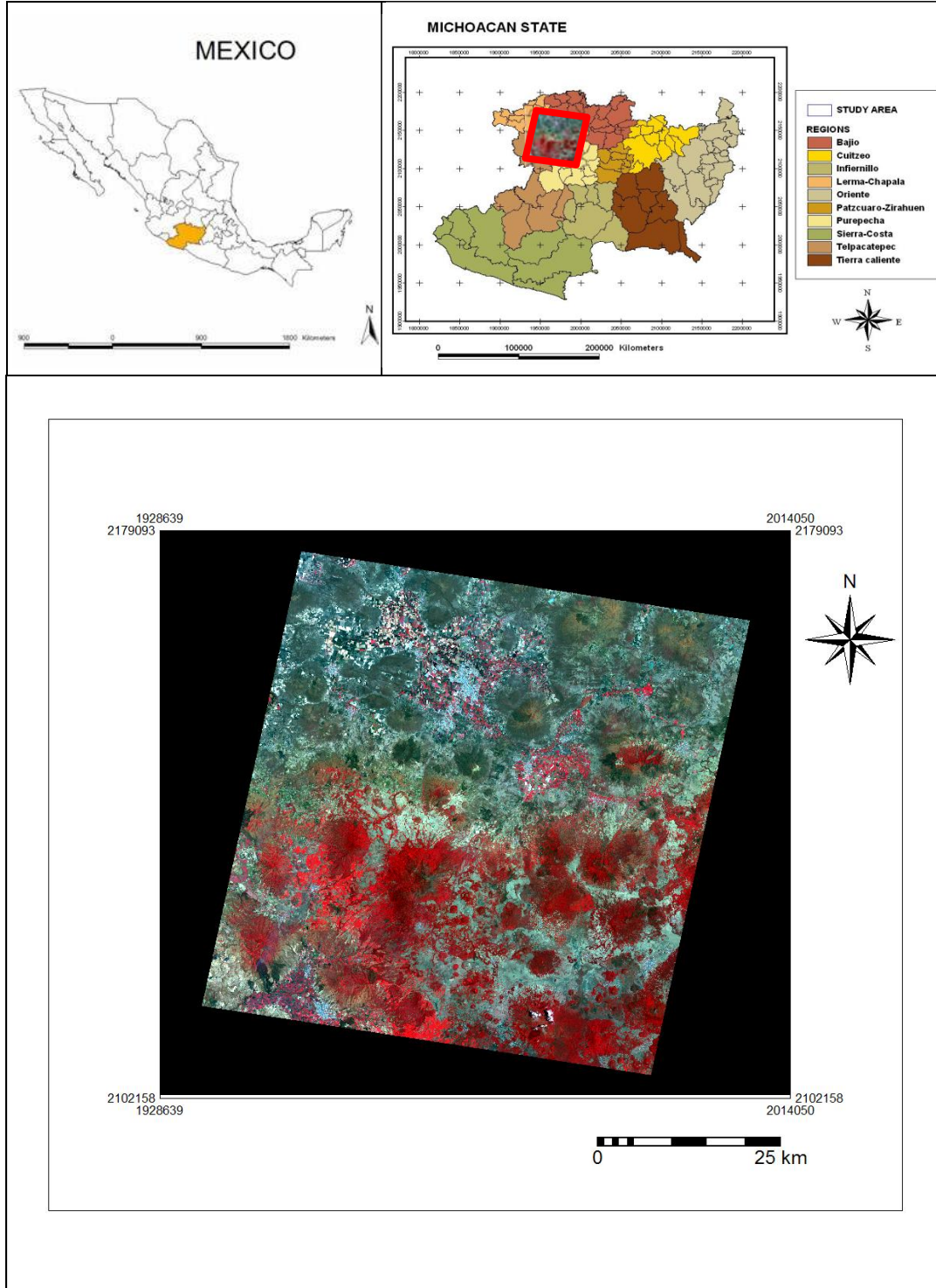


Figure 2-1 Study area localization in an ASTER image of Michoacán, Mexico

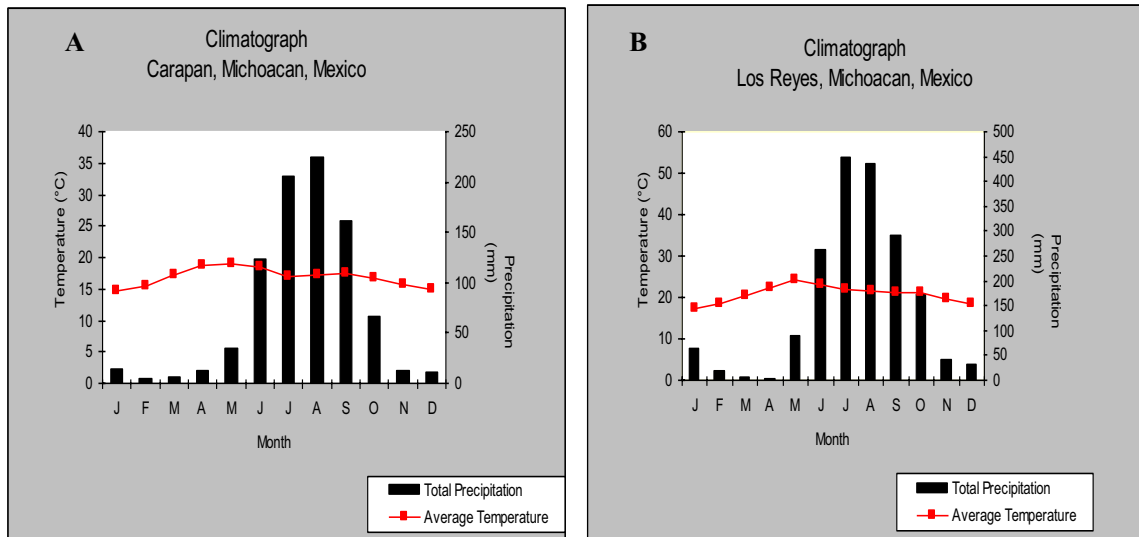


Figure 2-2. Climatographs from (A) Los Reyes station (subtropical) and (B) Carapan station (temperate) in Michoacán, Mexico

2.3 Vegetation

There are 7 types of vegetation distributed in the whole area: Pine forest (17.1%), mixed Pine-Oak forest (13.8%), secondary scrubland (11.5%), grassland (9.8%), Oak forest (7.1%), dry tropical forest (1.2%), and hygrophilous vegetation (0.1%). This area also includes a National Park named “Parque Nacional Lago de Camecuaro” in Tangancicuaro municipality. In the following paragraphs we describe each type of vegetation according to Rezdowski (1978) and Labat (1995) floristic studies. This information will be very useful later in the creation of the fuel risk model

Pine forest. The Pine forest is one of the most representative vegetation communities of Mexico. Usually it is found in climate with temperature range of 10-20°C and 600-1000 mm of total annual precipitation. This geographic distribution is related to the presence of mountains and high elevation topography. In the west of Michoacán state, Labat (1995) classified the Pine forests using the species temperature preference. These categories are termophilous and mesophilous forests. The termophilous Pine forests are located in the Sierra Tarasca between 1400 and 2100 m a. s. l., over extrusive Igneous Rocks and Andosols. The Pine trees of these forests are from 15 to 20 m height, but it is possible to find trees of 25 m. The tree canopy percentage is from 60 al 80% and the trees mean density is about 692-860 tree/ha, with diameters no higher than 70 cm. The dominant species for this termophilous forest are: *Pinus oocarpa* (493.3 trees/ha), *P. douglasiana* (173.3 trees/ha), *P. michoacana* var. *corneta*, *P. ayacahuite* var. *veitchii* and *Pinus pringley*. However there are many other associated pine species present. One particular case is *P. oocarpa*, which is adapted to fires.

The Mesic Pine forest is located in more humid zones between 2600 and 2700 m a. s. l over basaltic extrusive rock. Here the dominant species are: *P. montezumae* (45.2 trees/ha) and *P. pseudostrobus* (84 tree/ha), *P.teocote* (63.2 tree/ha). In the highest zones dominates *P. leiophylla* (181.2 tree/ha) and

in the lower zones (2500) the mesophilous species are mixed with the termophilous Pine forest. In this part it is usual to find it mixed with Oak and *Alnus* species. The height of the trees is from 15 to 25 m, whereas the tree mean density is 615 tree/ha with diameters of 5-100 cm. According to Rezdowski, this forest shows a lot of fire evidences. Other kinds of disturbances present in these areas are: illegal cutting, resin extraction, land use change to agriculture.

A high percent of Mexican Pine forests are under demographic pressure. This type of forest is cut and used for several purposes, from wood and pulp for paper making to land use change for agriculture and cattle breeding. In general from the mentioned activities, is important to highlight that agricultural and cattle breeding have a great influence on Pine forest. The use of fire is a common practice in agriculture whereas the burning of grassland is used constantly to renew the grass for the cattle. As a result, this forest shows intensive human disturbance and frequent fires. It is calculated that 80 percent of the forest is affected by fires. Nevertheless, it is not clearly known if fire is part of the Mexican Pine ecosystem dynamic. As Rzedowski mention, the forest response to a fire depends on its species composition. The presence of serotinous cones of some species as *Pinus oocarpa* shows that some Pines are resistant and favoured by fire. Other species as *Pinus patula* (which have serotinous cones too) are indirectly related with fires since they are commonly found in disturbed forests. Finally other Pine species, more sensitive to fire, cannot recover after a fire incidence. In this situation, fire contributes to the lost of forest areas. Moreover, in the case of the herbaceous stratum, the main family in this forest, the Gramineae, is favoured by fire. In some cases this fact leads to a positive forest fire feedback since grass presence induces or favours fires.

Oak forest. The Oak forests are characterizing Mexican mountainous areas. They are found in climates from temperate to subtropical with temperatures of 10 to 20°C and 350-2000 mm of annual precipitation. In the subtropical climate Oaks appear as a scrubland. According with the floristic study of Labat, the Oaks in this area of Michoacán are distributed between 1950-2300 m a. s. l. However, they can also be found up to 2400 m a. s. l. In its highest distribution they are close or mixed with the mesophilous Pine forest. In addition, the Oak forests grow on soils derived from Andesite and Basaltic rocks.

The Oak forest is one of the high diversity communities in Mexico since there are more than 150 species of Oaks. This implies an enormous floristic, physiognomic and ecologic diversity. We can find two types of vertical structure in this forest, one from 10-15 m and the other from 4-9 m. This difference is reflected also in the two tree diameter classes (55-75 and 20-55 cm). In the Oak forest trees density is of 2160 tree/ha (5075-280 trees/ha), with dominant tree species: *Quercus sideroxylla* (378.4 trees/ha), *Q. obtusata* (399.6 trees/ha), *Q. deserticola* (497.5 trees/ha), *Q. subspathulata* (289.3 trees/ha), *Q. castanea* (275.6 trees/ha) and *Quercus laeta* (132.5 trees/ha). The Oaks are deciduous; however the leaf off period is very short during the year (less than a month). Even some species never lose their leaves. The herbaceous stratum depends on the density of the forest. It is composed mainly of grasses and plants from the family Compositae, but also includes a great diversity of other families.

Moreover, other kind of trees that can be found in these forests as *Arbutus*, *Cercocarpus*, *Crataegus*, *Cupressus*, *Juglans*, *Juniperus*, *Pinus* and *Psedotsuga*.

As a result of its low height and thin logs, the Oak forests are more used locally than industrially. Its use is restricted to furniture and post construction, handcrafting or fuel. In the same way as the Pine forest, they are affected by the land use change, mainly to agriculture fields and grasslands for cattle. Fires are a common practice in the driest and hottest months. This fact leads to changes in the composition and the structure of the forest, and finally to its disappearance. It is worth noting that Oak trees have a slow growth. This process in a long term produces a shift in which Oak forest is converted to a scrubland or grassland; both are more useful for cattle breeding. After that the ecological and hydrological consequences are severe, observing high rates of erosion. The presence of regular fires favours the growth of the shrub (or short tree) *Eysenhardtia polystachya*.

Mixed Pine-Oak forest. Since both genera grow in similar environment, this type of vegetation is composed by a mix of Pine and Oaks distributed in different percentages. The Pine-Oak forest is considered as a separate vegetation type because its distribution is as wide as the pure Pine or Oak forest. Consequently, the coincidence of both species is not necessarily seen as a transition. This community is an evergreen forest, given that pines never lose their leaves.

Tropical deciduous forest. This vegetation is typically found in subtropical climate (temperature of 20-29°C) located in areas of altitudes of among 0-1900 m a. s. l. The mean annual precipitation is from 600-1200 mm. But should be noted that there are two major seasons: dry and wet. Therefore, this vegetation type is characterized by its dominant tree species, which lose their leaves in the dry season of the year (5-8 months). In addition it is usually found in thin and rocky soils of the slope of the hills.

The preserved forest has a high density of trees between 5 and 15 m of height and 50 cm of diameter. In Michoacán state the original vegetation is disappearing. As this type of vegetation is affected by agriculture, cattle breeding, forest fires, and selects illegal logging. Therefore, the height of the trees of Michoacán's tropical deciduous forests is not more than 4 to 6-7 m with diameters of 15-30 cm. The family Leguminosae is dominant in the tree stratum, but the genus *Bursera* is a common one. Moreover, it consists of cacti species, plants from the genus *Beaucarnea* and *Yucca* and other shrub species. The most important tree species are: *Acacia pennatula* (178 trees/ha), *Heliocarpus terebinthaceus* (128 trees/ha), *Ipomoea murucoides* (62 trees/ha), *Bursera cuneata* (84 trees/ha), *Zanthoxylum affine* (76 trees/ha), *Eysenhardtia polystachya* (54 trees/ha), *Opuntia cochineria* (20 trees/ha), *Manihot caudata* (42 trees/ha), *Lysiloma mycrophyllum* (46 trees/ha), *Mimosa rhodocarpa* (50 tree/sha), *Euphorbia fulva* (20 tree/sha) and *Opuntia chavenia* (16 tree/ha).

Secondary scrubland. The tropical deciduous forest is one of the vegetation communities most affected in Mexico. Areas covered by this vegetation type are used for agriculture. However, they are abandoned quickly because the scarce soil and high percent of rocks are typical characteristics of the areas where this forest grows. Its regeneration just occurs in the absence of disturbance. Hence, disturbance takes place by cattle, fires and selective cutting; thus tropical deciduous forest is converted to a permanent scrubland. In the composition of this scrubland remains many of the species of tropical forest. Among the most frequent species are: *Acacia spp.*, *Heliocarpus terebinthaceus*, *Ipomoea murucoides*, *Bursera spp.* and *Erithrina spp.* species. In the dry season the remnant of cacti characterize the appearance to the area.

Grassland. All the grasslands located in this area are cultivated or induced for cattle breeding. The grasslands areas take the place of the other types of vegetations cited above. For its maintenance fire is frequently used as a method of grass renewal. When grassland is established, the original vegetation cover hardly comes back due to the frequent use of fire and the presence of grazers. However, if these areas are abandoned, the vegetation starts an ecological succession process within the intermediate vegetation which is the scrubland. Grasslands derived from Pine or Oak forests are dominated by genera like *Andropogon*, *Aristida*, *Bouteloua*, *Bromus*, *Deschampsia*, *Hilaria*, *Muhlenbergia*, *Stipa*, *Trachypogon* and *Trisetum*.

2.4 Land use

The main land uses are seasonal agriculture (23%), irrigation agriculture (6.2%), and livestock farming (9.8% of grasslands). The percentage of these activities varies according to the municipality. In general agriculture is the most important economical activity in the study area. Some of the crops that grow here are: corn, beans, wheat, chickpeas, broad beans, sorghum, lentil, alfalfa, oat, sugarcane, tomatoes, strawberries, cucumbers, zucchinis, pears, peaches, plums, limes, avocados, chilli peppers, onions, potatoes, blackberries, apples, guavas and coffee beans [75]. Grasslands are mainly used for livestock farming. The livestock farming mainly include the care and breeding of cows, pigs, chickens and sheep [75]. The industry is not very developed in all the municipalities. However, Uruapan municipality is among the most industrial developed municipalities of Michoacán state. Finally, it is worth to mention that there are forestry activities in this area. The degree of intensity of these activities also varies according to the municipality. For example in the municipalities of Tocumbo, Los Reyes, Uruapan, Cheran and Charapan forestry is the main activity [75]. In other municipalities forestry is carried out in lesser degree. In Mexico, particularly in the State of Michoacán, the deforestation due to illegal logging is the main activity on forests land. Bocco et al. [76] report that Michoacán temperate and tropical forests lose every year about 1.8% and 1% of its area, respectively. Of particular interest in this study is the analysis of deforestation rate per municipality. For example, the municipality of Churintzio, located in the north-western of the study area, had a forest coverage

lost of 12.8% between 1975 and 1993. According to the same study the municipalities of Jacona, Villamar and Tocumbo lost their forest cover in the same period of time. This fact highlights the seriousness of the problem in the area. The main activity that contributes to the deforestation is the illegal logging. However, forest fires also contribute to the loss of forest coverage. Moreover, natural burned areas does not recover and are clandestinely occupied for agriculture, fruticulture and pasture [57,77]. In the Meseta Purepecha the forest decrease is caused mainly by the establishment of new avocado (*Persea spp.*) orchards [57,78]. México is the world first avocado producer and Michoacán state produces 85% of the national production generating \$750,000 (Mexican peso) per year [79]. This situation strengthens the economic incentive for converting forests to avocado orchards [77]. The main avocado producer municipalities in Michoacán state are: Uruapan (15,373 ha), Tancítaro (14,122 ha), Peribán (12,779 ha), Tingüindin (3,630 ha), Los Reyes (2,692 ha).

2.5 Population

Over the study site are 426 settlements, from which the most important are Zamora de Hidalgo, Jacona de Plancarte, Los Reyes de Salgado, Paracho de Verduzco, Tangacicuaro de Arista, Purepero de Echaiz, Santiago Tangamandapio, Ario de Rayon, Tarecuato y Capacuaro. All the settlements located in the Meseta Purepecha have indigenous population, from which a great part suffers economic poverty.

3 METHOD

Modeling forest-fire risk is an important tool for the prevention of disasters. Throughout this work I intend to develop a fire risk model and then produce a forest fire risk map for the study area in the state of Michoacán. The production of this map will be the result of a research focused on three main phases: 1) Exploratory, 2) Modeling and 3) Validation. The methodology for each phase will be explained in the following paragraphs.

3.1 Exploratory phase

3.1.1 Literature review and selecting factors influencing forest fire

The first phase consisted on literature review on forest-fires and available databases in order to obtain actual information related to previous studies on forest-fire, data records and a list of the institutions (both, local and federal) in charge of the fire monitoring and prevention, and their strategies for fire-prevention. This review will provide a better knowledge of the main factors affecting forest fire and helped on the factor selection. As it was mentioned in the introduction, the variables that influence the beginning of a forest fire and its development are: 1. fuel availability, 2. weather, 3. topography and 4. human activities. These factors integrated in the GIS model were: vegetation type, temperature and precipitation, elevation, slope and aspect, and land-use, road network and human settlements data.

During this phase, a new fire-event database was built for the study purposes using COFOM records and MODIS hot spots from 2003 to 2006 and 2004-2006 respectively.

3.1.2 Data processing

MODIS hot spot data were obtained from CONABIO, while the ASTER image was downloaded from the Earth Observing System Gateway website (<http://edcimswww.cr.usgs.gov/pub/imswelcome/>). The ASTER image was geometrically corrected using ILWIS ver. 3.31 relating georeference tie points of the image with a topographic map scale 1:50,000. The transformation used for the geometrical correction was the Affine method [80]. The root mean square error (rmse) of the georeference was ± 0.66 pixel due to the quality of the topographic map. According to the Ilwis Reference Guide [81], “The value of Sigma (in millimetres) for the current data indicates the accuracy with which the control points have been digitized. If the value of sigma is much larger than 1, this indicates that an error was made when digitizing the points or

when entering the coordinates. Sigma is the standard deviation calculated from the difference between the digitized and the calculated control points”.

The thematic maps of land cover, roads and hydrology of scale 1:250,000 and topographic map of scale 1:50,000 were used in this study. All the thematic maps were obtained from INEGI digital database. From each attribute, six maps in scale 1:50,000 were used and merged in order to cover the complete study area. Likewise, the fire ground records and fire headquarters location were obtained from CONAFOR and COFOM databases. All maps were converted to the Alberts Conical Area projection.

The Digital Elevation Model (DEM) was derived by interpolation of contour lines (which are every 20 m) from the topographic map. The aspect and the slope map were calculated from the DEM. Nevertheless, due to missing data in mosaicing two topographic sheets and to avoid false information, it was necessary to apply a 5 x 5 majority filter on those maps (for more information on this process refer to [80]).

1. Study area demarcation

The demarcation of the study area was made on the basis of the of the ASTER image that fulfilled the following premises: 1) To be an area with a high frequency of fires, 2) to be composed in its majority of natural vegetation, and 3) that possess (within possible) a representation of the majority of Michoacán state’s diversity; this means: an area that includes most common vegetation types found in the state.

In order to detect which areas in Michoacán state are the most affected by forest fires (i. e. condition 1), CONABIO’s MODIS hot spots and COFOM’s ground records were used. Hot spots are detected by remote sensing while ground records are points taken after a fire is spotted and extinguished. Both information sources come from governmental institutions. More over, the COFOM records are part of the official report of forest fire in the state of Michoacán and are continuously published in the newspapers as these areas with more forest fires incidence. CONABIO hot spots, are used to warn foresters about the fires in the country. These two sources complemented each other and allowed us to visualize which areas are more frequently burned. However, since both databases come from a different source; there were some differences among the COFOM fire frequency reports and MODIS hot spots. While the COFOM’s report shows Oriente, Bajío and Cuitzeo as the most forest fire affected regions, hot spot data indicates that Sierra-Costa, Telpacatepec and Tierra Caliente are the regions with the most high frequency of fires (Table 3-1).

Table 3-1 Comparison between COFOM reports and MODIS Hot spot

| Fires | COFOM report | Hot spot day | Hot spot night |
|-------|----------------------|----------------------|----------------------|
| - | Sierra-Costa | Patzcuaro-Zirahuen | Patzcuaro-Zirahuen |
| ↓ | Infiernillo | Cuitzeo | Lerma-Chapala |
| ↓ | Tierra caliente | Purepecha | Bajio |
| ↓ | Patzcuaro-Zirahuen | Lerma-Chapala | Cuitzeo |
| ↓ | Telpacatepec | Infiernillo | Infiernillo |
| ↓ | Lerma-Chapala | Bajio | Purepecha |
| ↓ | Purepecha | Oriente | Oriente |
| ↓ | Cuitzeo | Tierra caliente | Telpacatepec |
| ↓ | Bajio | Telpacatepec | Tierra caliente |
| + | Oriente | Sierra-Costa | Sierra-Costa |

There are many reasons that could explain the differences between these two sources. The efficiency of COFOM brigades were not the same in all the municipalities or could be biased to more populated areas with easy access. Other explanation could be that reliability of MODIS data for Michoacán is not known. Also it is probable that the forest fires indicated by MODIS hot spots are agriculture fires which are not attended by the fire brigades. Nevertheless, it is not possible to determine the origin of these differences analyzing the available data in this study. In spite of this, the data give an overview of the municipalities most affected by forest fire. For example, the Purepecha region is one of the most affected regions as it shows the COFOM reports [64] and newspaper news [82,83]. The COFOM reports allows knowing which are the regions and municipalities with more forest fires in the state. The municipalities with more fires according to this source are Morelia, Tacambaro, Chilchota and Uruapan (Figure 3-1). The Tepalcatepec region also coincides with the MODIS hot-spot most fire affected regions (Table 3-1).

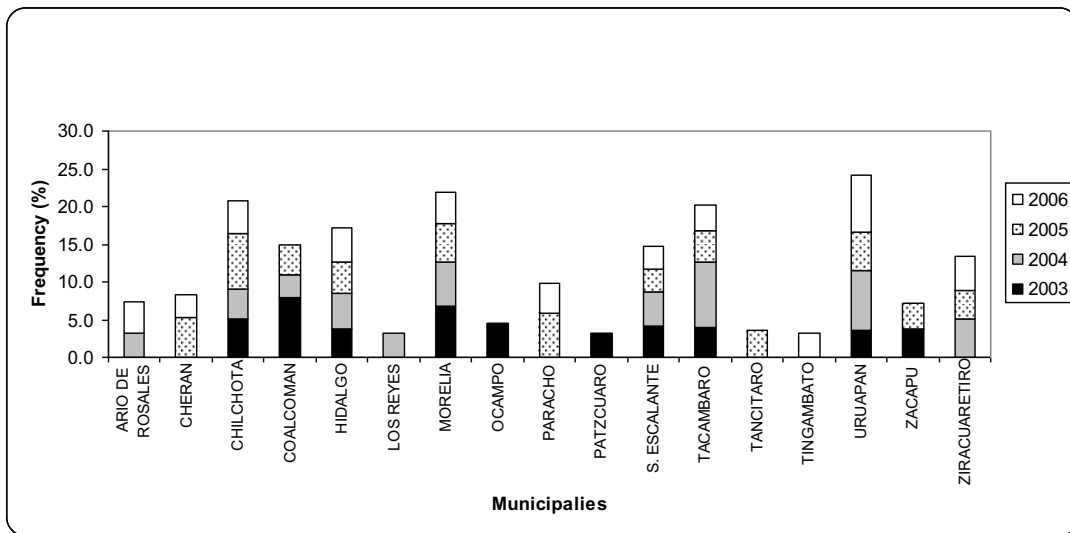


Figure 3-1. Michoacán's municipalities with highest percentage of forest fires in four years (COFOM)

3.1.3 Vegetation type map improvement

To fulfil conditions 2 and 3 (natural vegetation, and to represent Michoacán state's diversity), the National Forest Inventory map at scale 1:250,000 was used. This map organizes information in four hierarchic levels, from the most general to particular data are: Formation, Type, Community and Sub-community. The reliability of this map for the Formation level is of 70% or more [84]. However, as mentioned by Velázquez et al. [35], at a larger scale and lesser level aggregation in the legend, the probability of making a mistake increases. Moreover, the minimum mapping unit of this map is 1 km². Thus, the use of this information at a more detailed level must be done carefully. In this study the level of community was employed, consequently, it was necessary to improve the quality and detail of this Forest Inventory map. Therefore, the polygons of the map were revised and they were corrected digitally by overlaying with the ASTER image. Finally, a field trip was carried out to corroborate those areas in where the vegetation type assignation was unclear. As this map also includes the land use, as agriculture fields, grasslands and cities in the future it will be called Land cover map. Land cover map is shown in Appendix **¡Error! No se encuentra el origen de la referencia.**

3.1.4 Burnt area mapping

Once the study area was defined, a burnt area map was created. For this purpose an ASTER image was used, since such image is reported in the literature that it is useful for mapping historical or recent fires. Their high resolution and multispectral bands in the visible light, near infrared, shortwave infrared and thermal infrared wavelength [29], allow many compositions used to identify fire scars. In this study the bands 2, 3, 1 in red, green and blue were used, since it is a known composition that highlights burn scars well [36]. Given that the chosen image belongs to the final days of the dry season (January to June) it was possible to identify and map digitally the burnt scars. Non forested areas were masked in the mapping. Furthermore, MODIS data and ground records of four consecutive years (2003- 2006) were available for additional information.

3.1.5 Analysis of factors influencing forest fires

In this phase, factors affecting forest fire factors were analyzed (Figure 3-2). All the burnt areas were related with an attribute map to visualize the relationship among them. Crossing burnt area map with all available maps lead us to understand which are the main factors and their classes that promotes fires. For the analysis of mentioned factors, variance homogeneity was determined (Bartlett's test), and then the ANOVA test was applied. A Tukey test was applied to see difference among variables. In heteroscedastics data were analyzed by the Kruskal-Wallis test. The means were compared visually using box-and-whiskers plots at a significance of 0.05 [85]. These factors were used to have a better understanding of the final forest fire risk model.

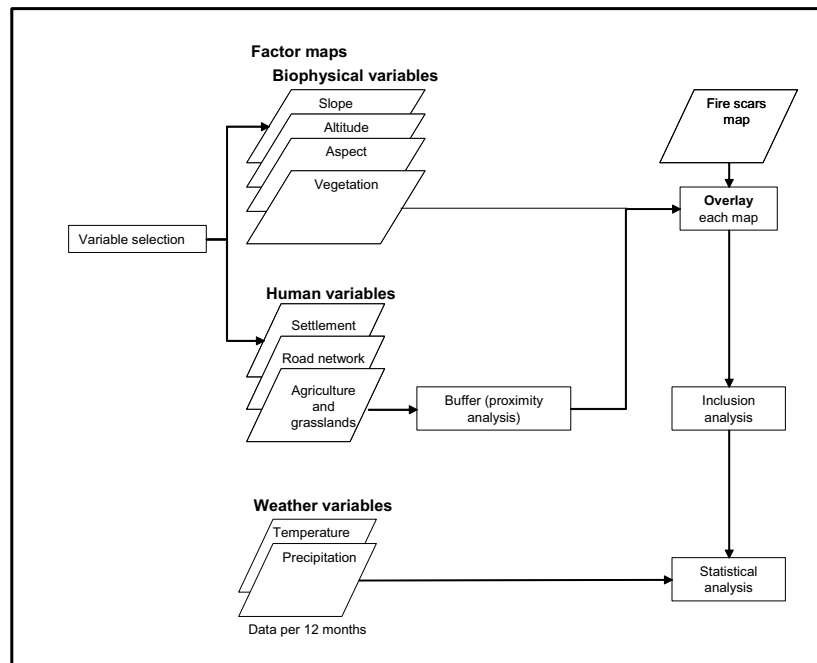


Figure 3-2 Factor Analysis

3.2 Modeling phase

In order to know the forest fire risk for the study area, in the second phase, all the factors analyzed in the previous phase were introduced in a five step model. Every step (or sub-model) emphasizes the most important factors related with the forest fires. These sub-models are: Fuel risk, Ignition risk, Weather risk, Detection and Response.

In order to model fire risk, the sub-models variables were divided in static and weather. The first 4 sub-models are composed of static variables but since fire behaviour varies along the year depending on climatic conditions, the fifth sub-model is multi-temporal.

The construction of the sub-models was based on the maps of the factors selected in the exploratory phase. The analysis of the spatial properties such as proximity, adjacency, direction, inclusion and exposition, helps to facilitate the modeling phase since it allows evaluate the spatial relationship between the variable and the fire event. In order to determine the categories with more fire incidence, a risk map from each variable was created using logical indices based on the literature review. In most of the cases the maps were reclassified with the index in classes according with the histogram or distribution of the data. In summary, all sub-models were combined by the adding each individual fire risk map. The sum of all sub-models will make the final Fire Risk Map for the study area. The following sections describe each sub-model and the creation of the indices.

3.2.1 Fuel risk sub-model

Fuel is one of the main variables that determine fire's occurrence and spread. Without fuel, a fire cannot occur. Therefore, the probability of a forest fire is determined in its majority by fuel quality and quantity [12, 13]. For these reasons fuel must be incorporated in the fire risk model. In order to build this sub-model, topographic and land cover information were used (Figure 3-3). The input maps for this model were: Slope, Altitude, Aspect and Land cover. All the factor maps were reclassified using indices.

This led to individual risk maps which finally were merged to obtain the Fuel risk sub-model. In the final sum, the land cover index was multiplied by 3, since this is the essential element for fire. To add the topographic factor to the fuel-submodel, the sum of aspect, elevation and slope was multiplied by 2. The indices of each factor were based on an extensive literature review and the particular characteristics of the study area. In order to give a general panorama to the reader the next section is focused on the factors description and its relationship with forest fires.

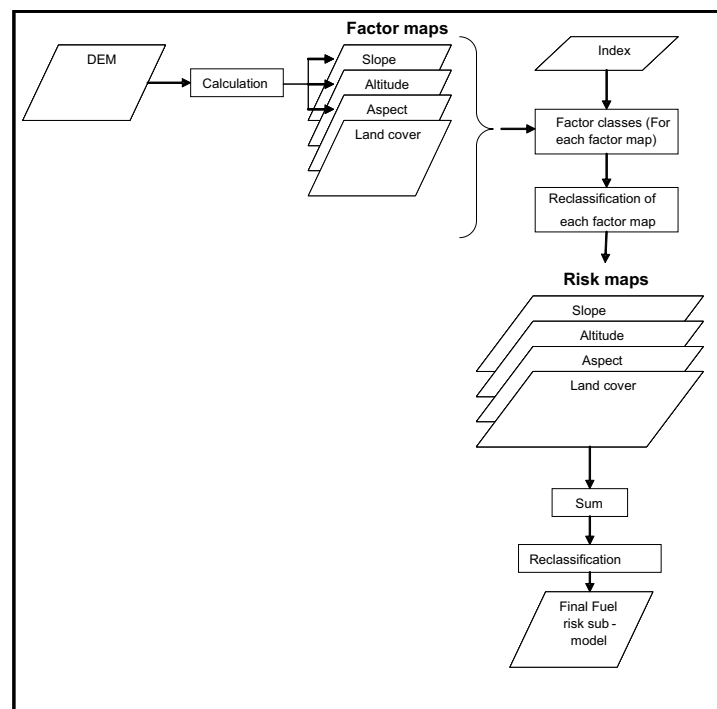


Figure 3-3. Fuel risk sub-model

3.2.1.1 Land cover index

The vegetation ranking was made according to the vegetation type characteristics. Table 3-2 shows the variables that were taken into account to generate this index (such as density and biomass). Also it shows the results of a workshop organized by CONABIO, where a group of experts ranked the vegetation depending on the probability of a fire and the recoverability of the vegetation. The Pine forest was ranked with high risk based on its fuel biomass, height and tree density. In addition, other features like flammability were considered in this ranking; for instance pine wood and resins are highly flammable [86]. Furthermore, tropical deciduous forest has the highest rank, since in the dry season this vegetation type presents many fine dry fuels (e.g. leaves and twigs) that favour an easy ignition in the appropriate hot weather. Moreover, this vegetation type has a low post-fire recoverability [87]. On the other hand, in the study area scrublands are secondary vegetation that are highly resistance to disturbance and have a high degree of recovery. Finally, Oak forests were considered as middle risk vegetation type, because of its considerable amount of biomass, but they do not have the density and flammability that the Pine forest has.

Table 3-2. Characteristics of land cover types and land cover index rating.

| Land cover | Vegetation type | | Tree height (m) | Tree diameter (cm) | Tree density (ind/ha) | Mean above ground Biomass (MgC/ha) ^a | | | CONABIO Susceptibility category ^c | Land cover index |
|-----------------------|--|-----------------------------|--|--|--|---|-------------|-------------|--|------------------|
| | Pine forest | Termophilous Mesophilous | | | | Tree | Herb | Shrub | | |
| Forest | Pine forest | Termophilous | 15-20 | < 70 | 692-860 | 100.5 ± 10.4 | 0.15 ± 0.03 | 0.16 ± 0.03 | 4 | 5 |
| | | Mesophilous | 15-25 | 5-10 | 615 | | | | | |
| Forest | Oak forest | | 10-15 and 4-9 | 55-75 and 20-55 | 2160 | 112.8 ± 61.2 | 0.3 ± 0.1 | 0.31 ± 0.1 | 3 | 3 |
| Forest | Mixed Pine-Oak forest | | Intermediate between Pine and Oak forest | Intermediate between Pine and Oak forest | Intermediate between Pine and Oak forest | 91.5 ± 8.9 | 0.1 ± 0.03 | 0.31 ± 0.03 | 3-4 | 4 |
| Forest | Tropical deciduous forest ^b | | 4-7 | 15-30 | 178 (Acacia) | 13.6* | n.a. | n.a. | 5 | 6 |
| Forest | Scrubland | | | | | 28.7 ± 24.8 | 2.3 ± 0.42 | 1.7 ± 0.4 | 2 | 2 |
| Forest | Plantation | | n.a | n.a | n.a | 50.5 ± 11.9 | 0.04 ± 0.01 | 0.06 ± 0.01 | | 3 |
| Grassland | Induced grassland | | Without | Without | Without | Without | 0.09 ± 0.08 | 0.14 ± 0.1 | 1 | 1 |
| | Cultivated grassland | | Without | Without | Without | Without | 0.09 ± 0.08 | Without | 1 | 1 |
| Agriculture | | | Without | Without | Without | Without | 0.10 ± 0.09 | 0.21 ± 0.2 | 1 | 1 |
| | | | | | | | | | | |
| Urban | | | | | | | | | 1 | 1 |
| Water body and rivers | | | | | | | | | 1 | 1 |
| | | | | | | | | | | |
| Bare soil | | | | | | | | | 1 | 1 |

a : Source Labat [88]; b: Maas *et al.* [89] c: CONABIO [87]; fire susceptibility categories: 1) Null, 2) Low probability of fires with high recover, 3) Low probability of fires with low recover, 4) High probability of fire with high recover, 5) High probability of fire with low recover.

3.2.1.2 Slope index

The slope has a direct relation with fire spread. Fuel exposition is greater as the slope steepness is increased (Figure 3-4) [90]. The fact is that fires spreads quicker up slope than in flat areas. According to McArthur ([91] cited in [5]) the steep of the slope will increase significantly the spreading of a fire; for instance a slope of 10° will double fire spread rate and a slope of 20° will quadruple it. When present, wind is the main element that modifies the contact of the flame with the fuel surface. Hence, fire spread depends on both slope and the wind force and direction [5,90,92,93]. Nevertheless, in absence of wind, slope is the main factor effecting fire spread. Having said that, a slope index was rated as it is shown in Table 3-3. The slope fire risk index is higher in steep slopes than in flat terrain.

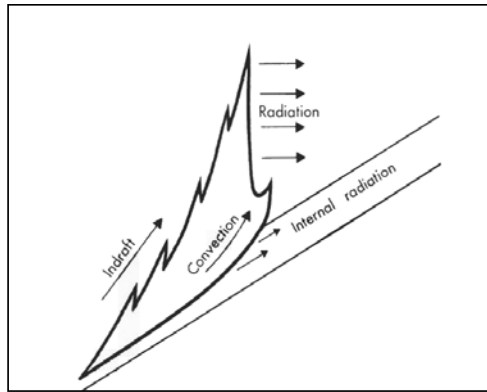


**Figure 3-4. Schematic of a fire on a slope.
Taken from Burgan [1]**

Table 3-3. Slope index

| Slope class (degree) | Index |
|----------------------|-------|
| 0-3 | 1 |
| 3-15 | 2 |
| 15-30 | 3 |
| 30-90 | 4 |

3.2.1.3 Elevation index

Vegetation type, temperature and humidity are correlated with altitude [94]. In temperate forests, higher areas are more humid and cooler than lower ones. Due to this geographical condition, vegetation types change with altitude. In the study area, for example Pine forest distribution is limited to highest zones while grasslands, tropical deciduous forest and scrubland are found in lower altitudes. The elevation index relates this information with forest fires, since high temperatures, low humidity and fuel quantity and quality increases the chance of ignition. Elevation indices are showed in Table 3-4.

Table 3-4. Elevation index

| Elevation class | Index | Elevation class | Index |
|-----------------|-------|-----------------|-------|
| 1050-1250 | 3 | 2250-2450 | 5 |
| 1250-1450 | 3 | 2450-2850 | 4 |
| 1450-1850 | 4 | 2850-3050 | 3 |
| 1850-2050 | 6 | 3050-3250 | 2 |
| 2050-2250 | 5 | 3250-3500 | 1 |

3.2.1.4 Aspect index

Soil humidity and vegetation distribution are influenced by slope aspect [94-96]. In the Northern Hemisphere the south slope receives more sun hours than the northern aspect, making it hotter [95,97]. This produce a drier condition that is also responsible for differences on vegetation distribution [94-96]. For instance, the vegetation more adapted to dry conditions, as some grasses and Pine species, are favoured in southern slopes [94]. On the other hand, eastern aspect is longer exposed to the sun therefore, receives more time the perpendicular rays of the sun. Hence the fuels located in south and eastern aspects are more prone to get burnt. Table 3-5 shows the aspect risk indices associated to each aspect.

Table 3-5. Aspect index

| Aspect class | Index |
|---------------------|--------------|
| N-NE | 2 |
| NE-E | 1 |
| E-SE | 3 |
| SE-S | 4 |
| S-SW | 5 |
| SW-W | 6 |
| W-NW | 2 |
| NW-N | 1 |

3.2.2 Ignition risk sub-model

As it was mentioned before, humans cause more than 90% of fires in Mexico [11,62]. In this model the human activities that can cause a fire in Michoacán state were included. These are agricultural burns and grassland burns (Figure 3-5). From January to May the burnt of grasses and some agricultural practices are carried on, these activities coincide with the dry season. As a result, the forest fire season occurs mainly in the first half of the year. The expansion of fires from these particular areas to forest covers is common. Also the closeness to roads and settlements could be a factor that promotes fires. In fact, it has been proved that there is an edge effect of roads in the forest. Changes like; increase of temperature and light, occurs as an effect of a decrease of the forest cover [98]. Near the roads, the composition of species is different from the original too; exotic and/or invasive plants, many of them pyrophilum, can be found in the borders of highways.

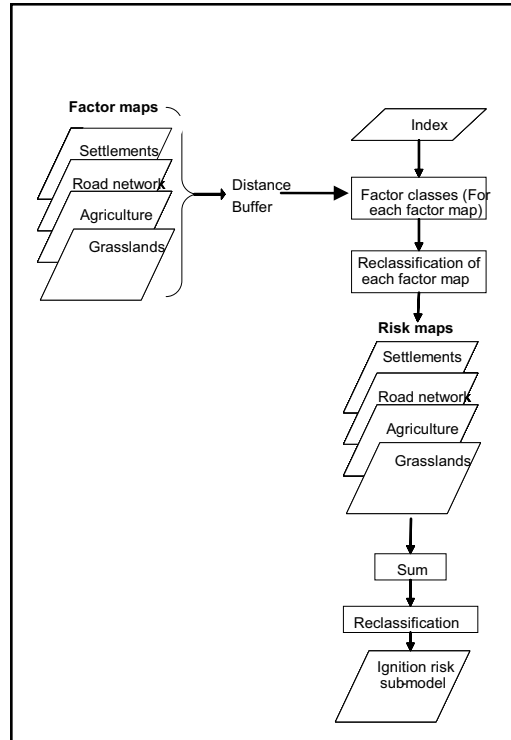


Figure 3-5. Ignition risk submodel

Keeping this into account, the data to be considered in the development of this sub-model will be maps of distance to 1) roads, 2) settlements, 3) agriculture fields and 4) grasslands. The distance category it is based on Hernandez-Leal [53] proximity to road categories. These maps were reclassified and rated by a risk index value (Table 3-6). Finally the maps were combined and resulted the final ignition risk map.

Table 3-6 Distance to roads, agriculture fields and grasslands indices

| Distance (m) | class | Risk value |
|--------------|-------|------------|
| 0-15 | | 7.0 |
| 15-50 | | 6.0 |
| 50-100 | | 5.0 |
| 100-500 | | 4.0 |
| 500-2000 | | 3.0 |
| 2000-5000 | | 2.0 |
| 5000-100000 | | 1.0 |

3.2.3 Fire detection risk sub-model.

This sub-model considers the visibility of a fire from forest towers, settlements and roads (Figure 3-6). For this purpose, a viewshed analysis was carried out using the extension 3D Analyst from the program ArcGIS 9.2.[80] and exported to Ilwis 3.1. A viewshed analysis is a complex calculation that takes into account the DEM information and view point location to determine the visibility taking into

account the offset, azimuth, vertical angle and radius [99]. In this case, in order to improve the visibility model, the mean vegetation height was overlaid to the DEM (See Table 3-2). This analysis can be performed from points or lines. The calculation from lines is made for each vertex of the line [100]. However, due to the complexity of the road map it was necessary to convert the road map into a point map. Each point was located every one kilometre over the road line.

In order to calculate the visibility, a 5 km threshold, or radius, from roads and/or forest towers; and one of 6 km from the centre of cities were used. However, it is worth to mention that the forest towers used in this study are located in the boundary of the study area and not inside it. Once the overall visibility was calculated, the hidden areas were considered of more risk; since the fires started in this zone can cause more damage to the forests. Visible areas have less risk, because they will be detected and stopped faster. Detection risk indices can be seen in Table 3-7.

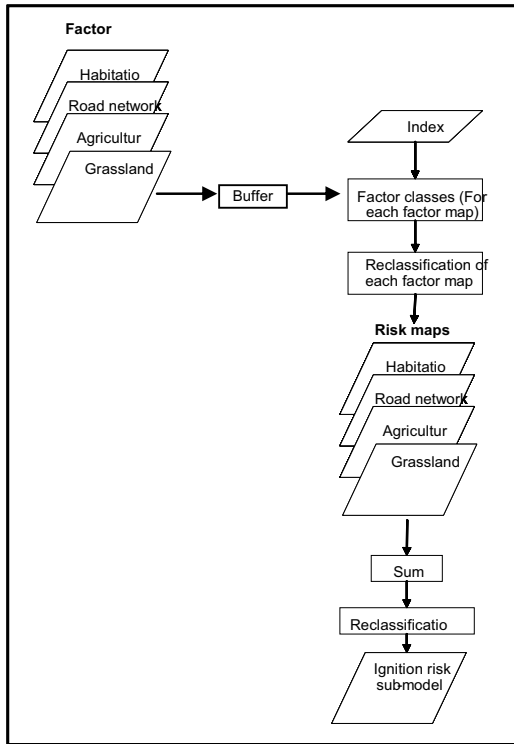


Figure 3-6 Detection risk sub-model

Table 3-7. Detection risk index

| Detection class | Detection risk index |
|-----------------|----------------------|
| Visible | 1 |
| Invisible | 3 |

3.2.4 Response risk sub-model

Once the fire has been detected and announced, foresters and fire-fighters have to move to stop the fire. The response to a fire is the time between the detection and the extinguishment. In this case, the fire response will be considered as the fire suppression force reaction time to a specific fire event anywhere in the area. This response is in a function of the speed of reaction divided by the distance to fire (i. e. everywhere). It is simple and direct to measure the time of on and off-road travel. However off-road travel can be more complex and indirect to measure. Thus for measuring off-road travel time

DEM, land cover and the road network was used to create a friction map that allow us to know the response reaction time for a fire (Figure 3-7).

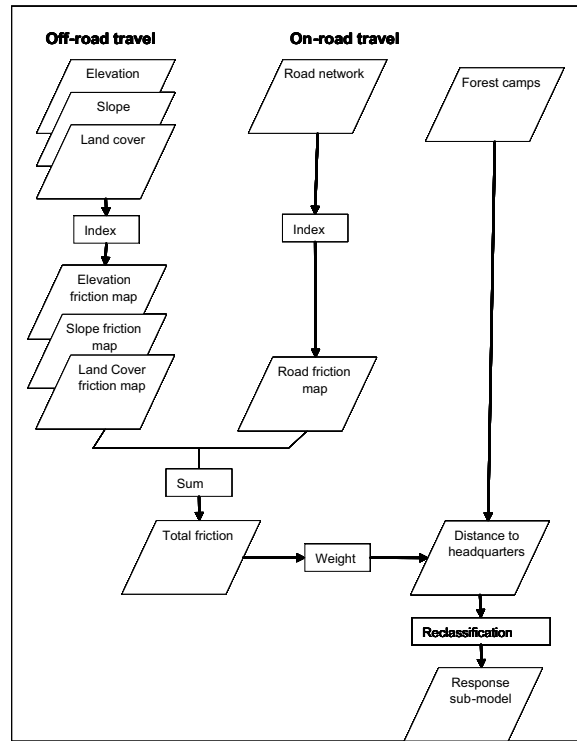


Figure 3-7 Response risk sub-model

3.2.4.1 On-road response

For the initial response, fire-fighters usually approach to fire by car; therefore, roads play a key role in the response time. In the study area roads are classified depending on the type of transport supported. The on-road travel was calculated using this road classes (Table 3-8). Time travel response depends on velocity. In this way, the quality of the road is very important. Highways are paved roads designed to drive at higher speeds than urban roads, unpaved roads and paths. Urban roads are narrower and usually present more traffic than highways. Conversely, unpaved roads and paths have a more local use, and its maintenance is less frequent than the more transited roads, though paths can be transited by cars. Particularly for unpaved roads, it is difficult to drive at high velocities. Finally footpaths are paths where the vegetation have been removed and are just used by people and animals.

Table 3-8 On-Road response index

| Road type | Characteristic | Index |
|--------------|-------------------------|-------|
| Highway | 4-2 lanes | 1 |
| Street | Urban road, 1-2 lanes | 2 |
| Unpaved road | 2 lanes | 3 |
| Path | 1 lane | 4 |
| Footpath | Only people and animals | 5 |

3.2.4.2 Off-road response

Once it is not possible to keep going by car, the approximation should be made by walking. The mean walking velocity is 5 km/h (After [2] and [3]). However, considering the resistance or friction, given by the slope, altitude and land cover the velocity could be modified.

- Slope. As the slope is increased, there is an increased effort to go up (Figure 3-9). Considering this fact, slope was classified according the friction force to the fire response. Slope friction index is showed in the Table 3-9.

Table 3-9. Slope friction index

| Slope percent | Slope friction Index |
|---------------|----------------------|
| 0-10 | 1.0 |
| 10-25 | 2.0 |
| 25-40 | 3.0 |
| 40-55 | 4.0 |
| 55-65 | 5.0 |
| 65-75 | 6.0 |
| 75-85 | 7.0 |
| 85-95 | 8.0 |
| 95-105 | 9.0 |
| 105-110 | 10.0 |
| 110-115 | 11.0 |
| >115 | 16.0 |

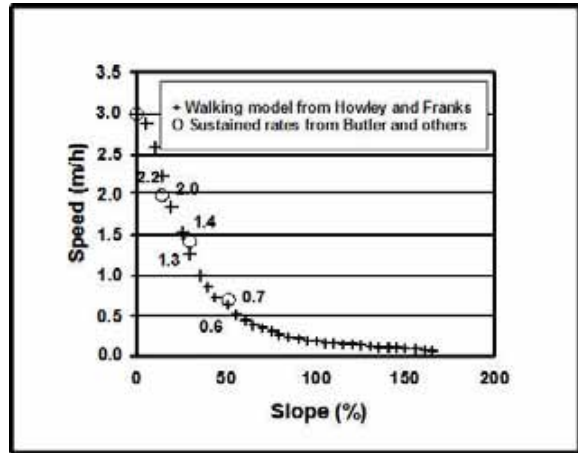


Figure 3-8. A comparison of walking model estimates of a fire fighter's sustainable walking speed with sustainable walking speeds (After [2] and [3])

- Elevation. The elevation can be considered as other factor that delays the response. It can cause negative physiological effects, as reduce supply of oxygen. Therefore, the elevations were reclassified into friction classes and converted to friction values (Table 3-10).

Table 3-10. Elevation friction index

| Elevation (m) | Index |
|---------------|-------|
| 1050-1250 | 1 |
| 1250-1450 | 2 |
| 1450-1850 | 3 |
| 1850-2050 | 4 |
| 2050-2250 | 5 |
| 2250-2450 | 6 |
| 2450-2850 | 7 |
| 2850-3050 | 8 |
| 3050-3250 | 9 |
| 3250-3500 | 10 |

- Land cover- Arriving to the fire site in absence of roads implies crossing through natural vegetation. Keeping this in mind, land cover was reclassified according the vegetation characteristics described in the previous section into land cover friction values. The land cover friction index is shown in the Table 3-11.

Table 3-11 Land cover friction index

| Land cover | Index |
|---------------------------|--------------|
| Bare soil | 1 |
| Settlement | 2 |
| Grassland | 5 |
| Agriculture | 6 |
| Pine forest | 7 |
| Pine Oak-forest | 7 |
| Plantation | 7 |
| Oak forest | 8 |
| Scrubland | 9 |
| Tropical deciduous forest | 10 |
| River | 12 |
| Lake | 15 |

Once the friction is calculated, a response map was generated. For this, first it was calculated a distance map from the headquarters, using the values of friction as a weight map. Finally, this map was reclassified in homogeneous ranges of 3 km. And reclassified, the more is the distance between headquarter and the fire, the less capacity of response.

3.2.5 Static fire risk model

The static fire risk model is composed by sum of the fuel, ignition, detection and response risk sub-models. In order to determine which is the best combination of sub-models three Equations were compared. Equation 1 is defined by the sum of the models with out weighting. Equation 2 gives more weight to fuel, since this is the element factor for fire ignition and spreading. And finally, Equation 3 gives importance to fuel, but also to ignition since human is the first cause of fires in the study area.

Equation 1. Static fire risk model

$$\text{Static fire risk model} = \text{Fuel} + \text{Ignition} + \text{Response} + \text{Detection}$$

Equation 2. Static fire risk model

$$\text{Static fire risk model} = (3 \times \text{Fuel}) + (\text{Ignition}) + \text{Response} + \text{Detection}$$

Equation 3. Static fire risk model

$$\text{Static fire risk model} = (3 \times \text{Fuel}) + (2 \times \text{Ignition}) + \text{Response} + \text{Detection}$$

3.2.6 Weather risk sub-model.

Since the ideal atmospheric conditions for a fire are low humidity and high temperatures [10], the variables considered for the construction of this model were temperature and precipitation. Initially it was planned to develop a model including also the variables of relative humidity and wind (Figure 3-9). However, given the quality of the available data, this model was built using only temperature and precipitation data. It should be mentioned that the probability of a fire's ignition is greatly influenced by the fuel's moisture [86]. The latter is divided into two types: Living fuel and dead (non living) fuel. Dead fuel consist mainly on the organic material (this is non living organisms) deposited on the ground. Its moisture level depends on the surrounding weather and it is considered that as drier as it is found, the higher the probability of a fire's ignition [24,101]. Alternatively, living fuel (living organism, mostly plants, in the surroundings) favour fire spreading more than ignition [101]. Its moisture level could be calculated from the NDVI [102,103]. Given that, one of the main goals of the present study is to solve the question of which are the zones with higher, lower and medium risk of forest fires in the study area. The Weather sub-model can give us indirect information about the moisture level (i. e. how moisture of the dead fuel components could be). Yet, it is highly recommended for further studies the inclusion of fuel's moisture data and wind direction, in order to obtain a more accurate weather sub-model.

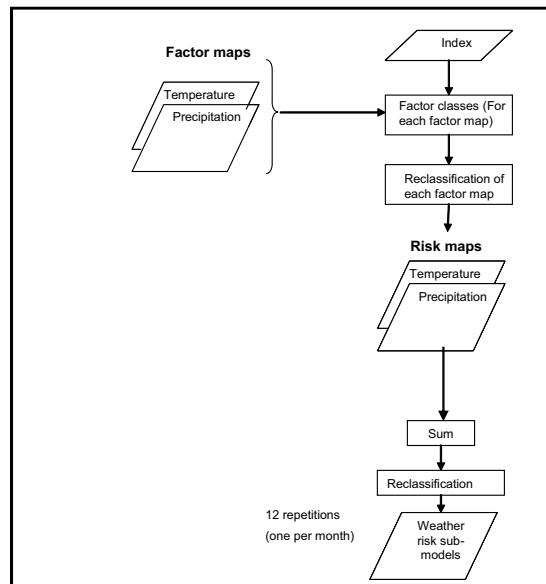


Figure 3-9. Weather risk sub-model

This model tries to consider temperature and precipitation changes on time. (e. g. dry season and rainy season). The model was considered for each month of the year. For this, data obtained from 32 meteorological stations was used; of which 13 stations are located within the study area and the remaining 19 are located in the surroundings areas. Both data series were obtained from the National Meteorological Service (in Spanish: Servicio Meteorológico Nacional) website (www.smn.cna.gob.mx). Moreover, the precipitation and temperature data are the monthly normal mean average of the data recorded between the years 1977 to 2000. The years with available data varies according to the records of each meteorological station.

Given that, as the altitude increases the temperature reduces, to obtain the general maps of temperature, all the information of every meteorological station was interpolated using a linear regression between the temperature and the altitude for every month of the year (Figure 3-10 and Figure 3-11). Similarly, in the case of precipitation an attempt to find a linear regression between this and the altitude was made. Yet for this study area there it was not possible to develop such relation between these two variables. Precipitation is much more complicated to interpolate than temperature because of its high variability [104]. This could be explained because in Mexico there is a strong influence of other phenomena like tropical storms and hurricanes in the summer or cold fronts in winter [105]. Therefore, an interpolation of the type Moving Average of Inverse distance was carried out to obtain the maps of precipitation. There are other different types of point's interpolation, like the following: Nearest point, Moving average, Moving surface, and Trend surface. Concerning this matter, ILWIS 2.1 Reference Guide defines the method of Moving Average as "The moving average operation is a point interpolation which performs a weighted averaging on point values and returns a raster map as output. In short, the output value for a pixel is calculated as the sum of the products of weights and point values divided by sum weights" [81]. The interpolation method of Moving Average was considered the best for this study, given that there are a considerable number of meteorological stations in the study area. Therefore, the fitting of this method represents the precipitation in a suitable way. This method was compared with the trend surface method with a function of second order and the results are comparable. Yet the trend surface method only shows more general tendencies. Also this method is the most similar to the statistical method of Kriging [106], which is other statistic method used in climatology to interpolate weather variables [106]. Finally, it is important to recognize that the interpolation type applied in this study may be subjected to a certain (but acceptable) error degree, since one of the disadvantages of this method is the lack of knowledge of the fitting accuracy, especially in such variable factors as the precipitation.

To generate the temperature and precipitation fire risk indices the monthly maps were classified homogeneously according to the following simple logic: the hotter and drier areas have the higher fire risk. Table 3-12 shows the temperature indexes and Table 3-13 shows the precipitation indexes. The lower limit for precipitation coincides with the beginning of the dry season. To obtain a map that represents the weather risk, the temperature index and the precipitation index were summed. Finally these maps were summed with the static fire risk model and reclassified homogeneously to obtain the weather sub-models per each month.

Table 3-12 Temperature index

| Temperature (°C) | Index |
|-------------------------|--------------|
| 0-13.7 | 1 |
| 13.7-17.1 | 2 |
| 17.1-20.5 | 3 |
| 20.5-23.9 | 4 |
| 23.9-28 | 5 |

Table 3-13 Precipitation index

| Precipitation (mm) | Index |
|---------------------------|--------------|
| 0-24.44 | 10 |
| 24.44-71.56 | 9 |
| 71.56-118.68 | 8 |
| 118.68-165.79 | 7 |
| 165.79-212.91 | 6 |
| 212.91-260.03 | 5 |
| 260.03-307.15 | 4 |
| 307.15-354.26 | 3 |
| 354.26-401.38 | 2 |
| 401.38-450 | 1 |

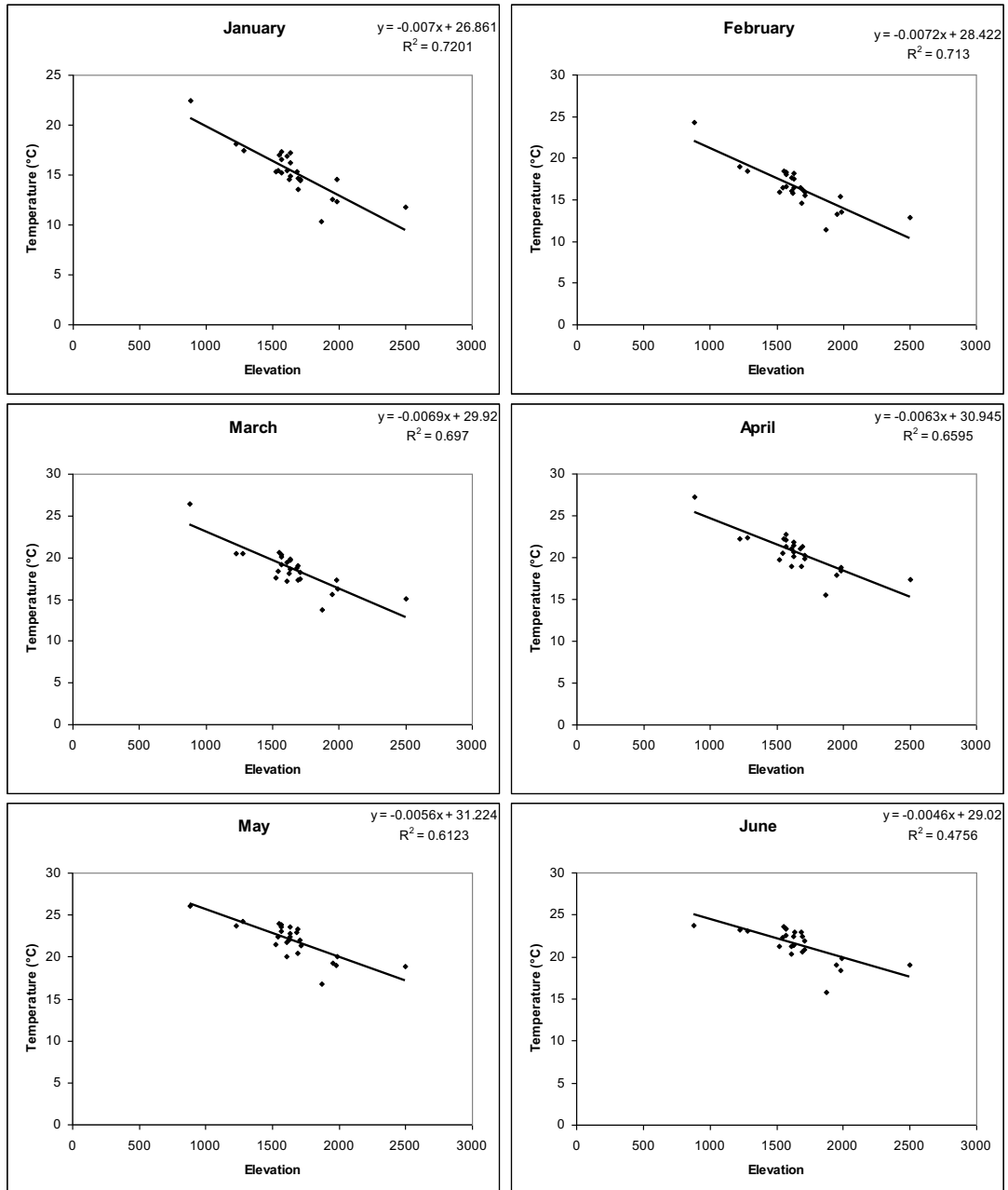


Figure 3-10. Linear regression between elevation and temperature for the months January to June

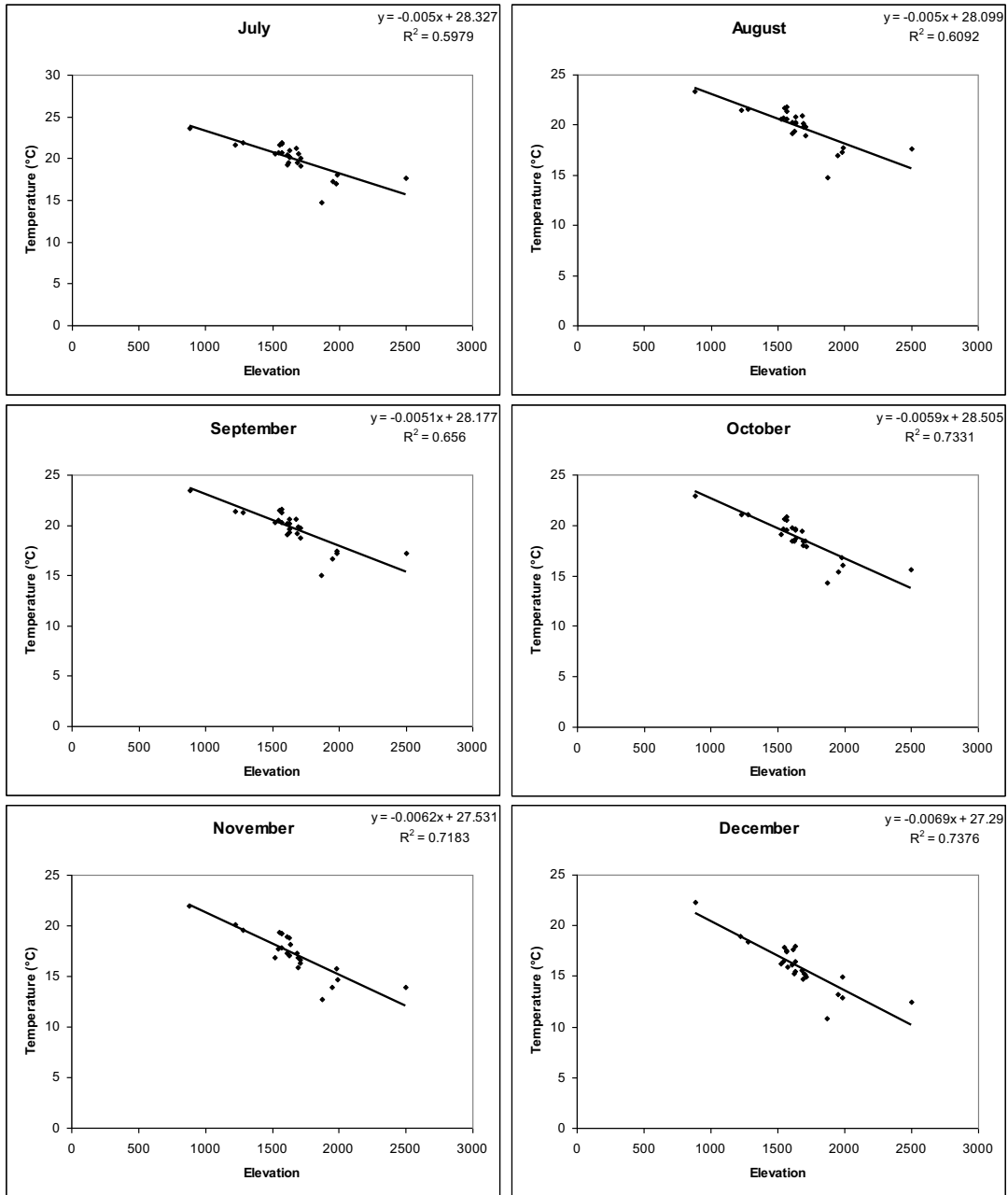


Figure 3-11. Linear regression between elevation and temperature for the months July to December

3.3 Validation phase

The accuracy of this model was validated using the burnt area map. This was done for all the sub-models and the final fire risk model, crossing them with the burnt area map. This allowed comparing the real fires with the high, medium and low fire risk areas of the model. The coincidence of burnt scars with the categories will show the level of accuracy of the sub-models. If a high percentage of the burnt scars area coincides with the high risk categories the model will be considered functional. This procedure allows assessing the agreement of burnt area with the forest fire risk model. The obtained results were summarized in tables. In addition, it was applied the Receiving Operating Characteristic analysis (ROC) in the Idrisi Andes v. 15 [107]. The ROC analysis is used to measure the performance of the model and to evaluate classification accuracy. This analysis predicts the location of the fire's occurrence by comparing the probability of fire's occurrence map and a Boolean image that shows where the fire really existed [38]. The ROC analysis shows how the fires are concentrated in a high probability category, and the ROC curve is a plot of the probability of having a true or false forest-fire event [38, 39]. This analysis has been performed with success to assess classifications with ground binary data. ROC analysis has been used in other studies to validate deforestation models [108], land cover change models [109], habitat suitability models [110] among others. Moreover, the Idrisi help [107] states that:

“The Relative Operating Characteristic is an excellent method to assess the validity of a model that predicts the location of the occurrence of a class by comparing a suitability image depicting the likelihood of that class occurring (i.e., the input image) and a Boolean image showing where that class actually exists (i.e., the reference image)...ROC offers a statistical analysis that answers an important question: ‘How well is the category of interest concentrated at the locations of relatively high suitability for that category?’ The answer to this question allows the scientist to answer the general question ‘How well do pair of maps agree in terms of the location of cells in a category’ while not being forced to answer the question ‘How well do the pair of maps agree in terms of the quantity of cells in each category’ Thus the ROC analysis is useful for cases in which the scientist wants to see how well the suitability map portrays the location of a particular category but does not have an estimate of the quantity of the category”.

3.4 Materials

3.4.1 Cartographic Data and Imagery

In order to develop the fire risk model the following maps and images were employed Table 3-14:

Table 3-14. Cartography and Imagery used in the study

| ITEM | DATE | 3.4.1.1.1.1 CHARACTERISTICS |
|----------------------|---|-----------------------------|
| Imagery | | |
| CONABIO MODIS MOD_14 | January to July, 2003, 2004, 2005, 2006 | Pixel size: 1 km |
| ASTER | May, 2006 | Pixel size 15 m |
| Thematic Maps | | |
| Topography | | Vector map, esc. 1:250000 |
| Land cover | | Vector map, esc. 1:250000 |
| Highways and roads | | Vector map, esc. 1:250000 |
| Human settlements | | Vector map, esc. 1:250000 |
| Headquarters | | Point map |
| Fire ground record | | Point map |

In this study three sources of information were used: NASA MODIS images processed by CONABIO, an ASTER image and COFOM's ground records. MODIS hot spots and ground records were required to define the study area. Whereas the ASTER image was used to improve the vegetation map and create a burnt area map. In the following sections are described the characteristics of each one.

3.4.1.2 IMAGES

a) MODIS images

Moderate Resolution Imaging Spectroradiometer (MODIS Spectroradiometers) Terra and Aqua, were launched to space as part of NASA's Earth Observing System in 1999 and 2002, with the purpose of generate information about Earth's surface from specialized products [111,112]. Part of this data are the thermal anomalies products, developed to monitor fires MOD_14 and MOD_40, which are designed to detect active fires and to calculate the burned areas [111,113]; this characteristics (Table 3-15) made these products useful tools to understand the spatial and temporal distribution of fires [113].

Table 3-15 EOS MOD_14, and MOD_40 satellite image's characteristics [113]

| | MOD_14 | MOD_40 |
|--------------------------------|-------------------------------------|-----------------------------------|
| Cover | Day and night | |
| Space-temporal characteristics | 1 km and 10 km and 0.5 degrees /day | 1 km and 10 km every 8 or 16 days |
| Level of process | 2 and 3 | 4 |

Fire detection is carried out using an algorithm that uses temperatures from the thermal channels 21 and 22 of 4 μm (T4) and channel 31 of 11 μm (T11); channel 21 saturates at 500°K (230°C) meanwhile channels 22 and 31 saturates at 331°K (58°C) and 400°K (130°C) respectively [111]. Fire's temperature usually varies depending on the intensity, type and quantity of fuel, and the burning frequency of a determined place; for example, on a prairie in the state of Kansas, USA, a fire's temperatures oscillate between 235.5°C, in a red oak habitat, to 78.7°C in a microclimate of the forest's ground [114].

Since 1998 the National Commission for the Knowledge and Use of Biodiversity (in Spanish CONABIO), has been monitoring forest fires by the implementation of the "Program for the detection of hot spots by the use of remote perception techniques". According to this program there are four stages for the fire monitoring, these are: reception and processing of images, fire detection, and publication of information.

MODIS images were incorporated from 2002; first the images from the sensor Terra were received and incorporated and soon after, those from sensor Aqua were incorporated too. Both kind of images are calibrated and georeferenced. Once MODIS images are received, they are processed using MOD14 algorithm, developed by the University of Maryland and by NASA, to detect the hot spots. Later in order to remove the possible false hot spot, different layers (masks) are used in the process. Among the masked layers are: clouds, earth-water boundaries, stable lights and some geographic stable points (*e. g.* Mines, Nitrogen plants, oil wells, etc.). In addition, CONABIO offers thematic cartography to locate the Possible-Fire Points. Finally the fire points are daily uploaded in the CONABIO website, as well as annual, monthly and daily statistics of the occurrence of fires. All the information offered by this institute is contained in a table that shows the exact location of fire events, some of the locality features, visualization of every fire event on a terrain digital model and also over a vegetation model; also they present a map of the fire events' distribution in the country and all this maps are available in format for download to commercial GIS [56].

B) ASTER images

The ASTER sensor (Advanced Spaceborne Thermal Emission and Reflection Radiometer) is also aboard the satellite Terra in December 1999 as a part of NASA's Earth Observing System (EOS) designed and manufactured by the Japan's Ministry of Economy, Trade and Industry (METI) and the Japan's Earth Remote Sensing Data Analysis Center (ERSDAC) [115]. The purpose of this sensor is to obtain information about land surface temperature, emissivity reflectance and elevation [115]. An ASTER scene is a 60 km swath composed by 15 bands divided on three different resolutions: three in the visible and near infrared (0.52-0.86 μm) (VNIR), six in the short wave (0.6-2.43 μm) (SWIR) and five thermal bands (8.125 and 11.65 μm) (TIR) with 15, 30 and 90 m of resolution respectively [116]. These characteristics make ASTER images ideal to study active fires and burnt scales [117]. Composition 6, 3, 1 of bands is also useful to identify the burned areas [37].

3.4.2 Ground records

C) COFOM records

The Michoacán's State Forest Commission (COFOM) is the state's government department in charge of taking action in every aspect related to conservation, encourage, and use of forest resources, according to the law; prevent and fight forest fires through its Department of Forest Fire-fight [14]. Among its functions are the update of the fire's fast detection system, gathering and systematizing of all the fire-related info and elaborate statistical briefs of fire events [118]. Every year this office elaborates and provides a database which contains the records of every fire that they fought within the year. This database provides a lot of information like the location site, municipality, date of the fire's beginning and finishing, fire's length, the vegetation's growing shape (tree, bush, herbaceous), and the name of every person who participated in the fight and control of the fire. Also the COFOM has elaborate maps of the fire critical zones and the location of all the fire fight infrastructure.

4 Results and Discussion

4.1 Exploratory phase

4.1.1 Burnt Area map

The digital interpretation is a direct method to locate and map areas that have been burnt in past events (burnt scars), using different spectral band combination. Sunar [44] found that the spectral signatures from bands 1, 2, 3 and 4 have a high ability to separate burnt areas from other land cover classes. The selected band combination used in this work (2, 3, 1) has allowed distinguishing the burnt areas easily because of its black tones (Figure 4-1); and finally had lead us to obtain a final burnt map for the study area, shown in Figure 4-2. An advantage of using interpretation and digitalization of burnt areas over supervised classification is that avoids confusion among areas with similar reflectance. This confusion could be present in shadowed areas or in volcanic cone's summit; nevertheless, since mapping burnt areas is not a trivial aspect, it would even better to consider other analyses that could complement the visual interpretation, like NDVI or surface temperature analysis [41], [46]. Burnt area interpretation in scrublands and Oak forests is particularly difficult, due to these areas appeared in greyish to brownish tones. Moreover, due to the frequent burning history of the study area, it is possible to appreciate a considerable number of greyish zones, which they probably not due to recent fires. However, in order to evaluate this, a more detailed database and a more thorough study with extensive field work are needed. However these were not the objectives of the present study. One of the interesting issues that should be mentioned is that most of the burnt areas mapped are beside agriculture fields and grasslands.

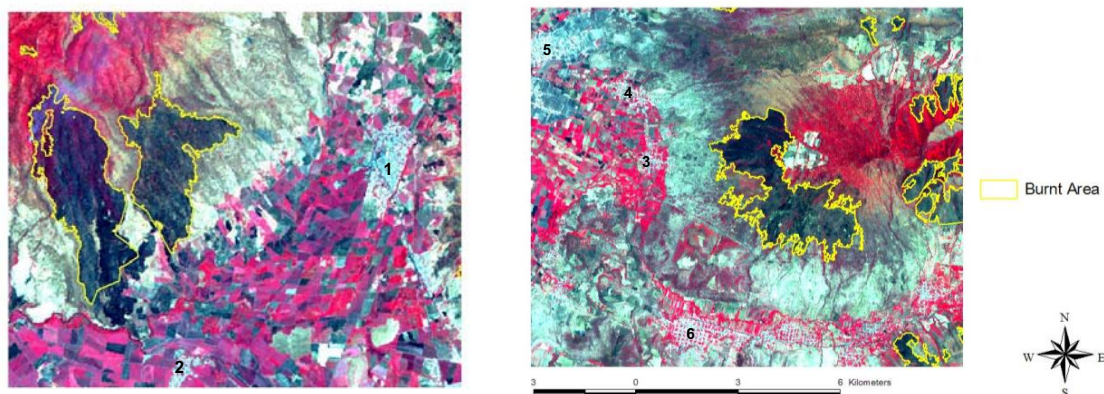


Figure 4-1. Two examples of a digitalized burnt area. Settlements shown in this picture: 1) Santa Clara de Valladares, 2) Los limones, 3) Etucuario, 4) Valle de Guadalupe, 5) Gómez Farias 6) Chilchota

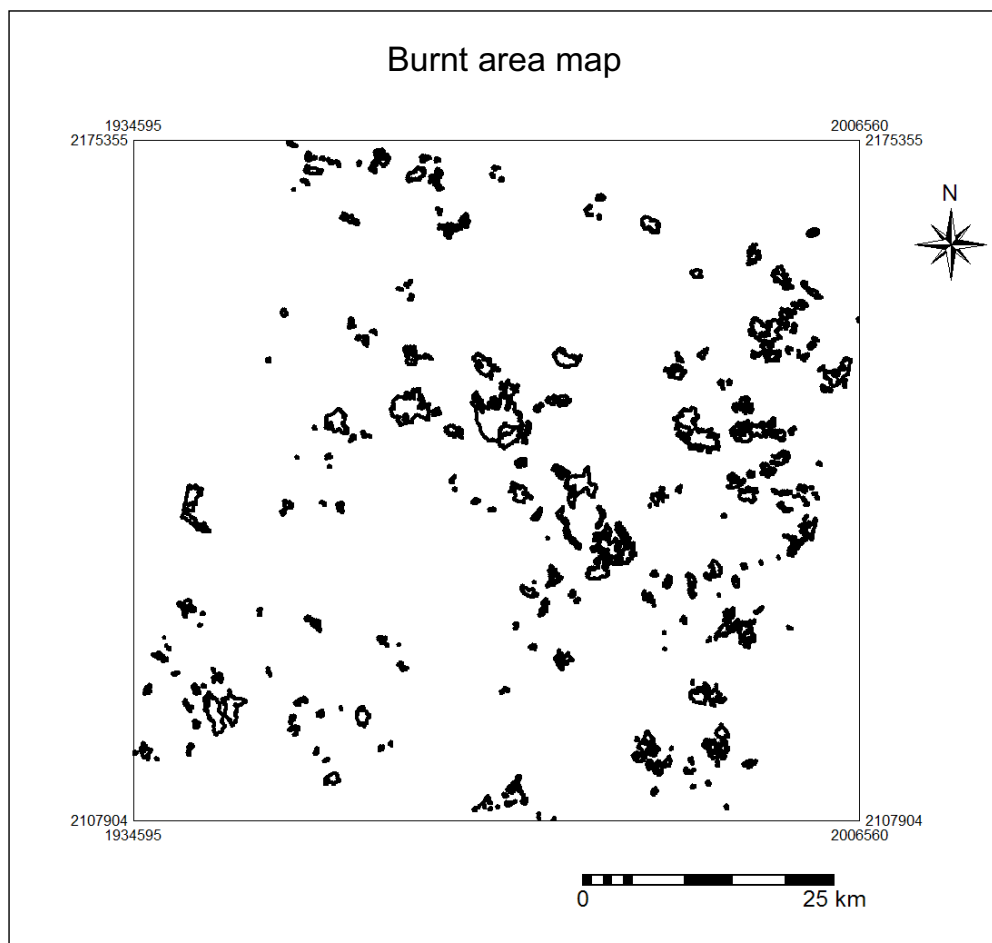


Figure 4-2 Study area Burnt area map

4.1.2 Analysis of biophysical factors influencing forest fire

4.1.2.1 Vegetation type

The presence of fuel is indispensable to generate a fire. Therefore, the characteristics of the vegetation type have big influence on forest fires developing. In the study area the predominant vegetation type is the Pine forest with a total area of 84 250.2 ha. Considering the total burnt area in the different vegetation types, the most affected one are the scrublands, the Oak and the Pine forests (Table 4-1). The burnt surface among them is similar, and it must be considered as an important sign of forest degradation in this area. However, considering the burnt area proportion of Pine forest only a total of 4% was affected by fires, while in the case of Oak and tropical deciduous forests, almost 19% and 17% respectively, of their proportional surface was burnt (Table 4-1). Hence, proportionally to its area Oak forest was significantly more burnt than the other vegetation types ($H = 21.84, P = 0.0002$).

During CONABIO's fire susceptible areas workshop [87] it was stated that the habitats with the higher probability of fire occurrence in Mexico, are the Pine and tropical deciduous forests. Moreover, as it was commented in the introduction in Mexico pine forests are commonly affected by

fires [119]. Conversely Oak forests and scrublands are considered to be the type with a lower probability of fire occurrence. The latter differs from the results obtained in this work. This could be explained because Oak forests and tropical deciduous forests are located at low altitudes where they are in contact with agricultural fields and grasslands for cattle breeding. On the other hand, Pine forest is located in higher altitudes. If the fires come from agriculture fields they first have to cross Oak forests, which usually are located below Pine forests. Moreover, during the dry season the presence of dead leaves over the soil of the Oak forests can favour fire spreading. In the case of scrublands, although they are located in lower altitudes too, its ability to recover after a fire is high. Moreover, it is known that tropical deciduous forest is one of the most affected vegetations by deforestation and fires [119]. Therefore, the difference between CONABIO workshop and the present results could be explained by the elevation factor.

Table 4-1. Burnt scars per vegetation types

| Vegetation type | Total surface (ha) | Burnt surface (ha) | % Affection |
|---------------------------|--------------------|--------------------|-------------|
| Oak forest | 23665 | 4388 | 18.54 |
| Pine forest | 84250 | 4185 | 4.97 |
| Oak-pine forest | 23521 | 2151 | 9.14 |
| Scrubland | 57902 | 4316 | 7.45 |
| Tropical deciduous forest | 1009 | 168 | 16.67 |

4.1.2.2 Elevation

Figure 4-3 shows distribution of the land cover classes in relation to its altitude. Pine forest is located in the highlands, while at low and intermediate altitudes is possible to find agriculture fields, grasslands and settlements. The Oak forest is also distributed in this low to medium range. Alternatively, the tropical deciduous forest is located only in areas of less than 1450 m a.s.l altitude.

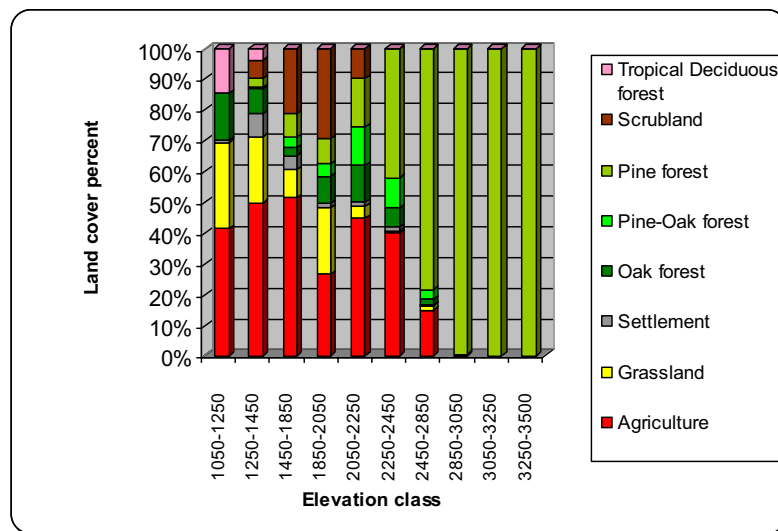


Figure 4-3. Altitudinal distribution of land cover classes

The distribution of burnt areas in relation to altitude are located mainly between the 2000 and the 2800 m a.s.l. (Figure 4-3). As mentioned earlier in methodology, the burnt scar mapping was made excluding the fires that occurred in non-forested areas (*i. e.* agriculture fields, grasslands and/or settlements). Considering that the original vegetation cover has been modified for human activities at lower elevations, there are less burnt areas at this altitude classes. It also happens that agricultural and grassland fires from the lower areas expand to higher elevations; this occurs because the fire direction; that in absence of wind always goes up-slope [90]. Therefore a great part of the burnt area is located in the elevation classes between 1850 and 2850 m a.s.l. (Figure 4-4). Conversely, at higher altitudes, a fire could extinguish and not arrive to these areas. In addition, the increase of altitude provokes changes in the temperature and humidity that may be influencing this behaviour too.

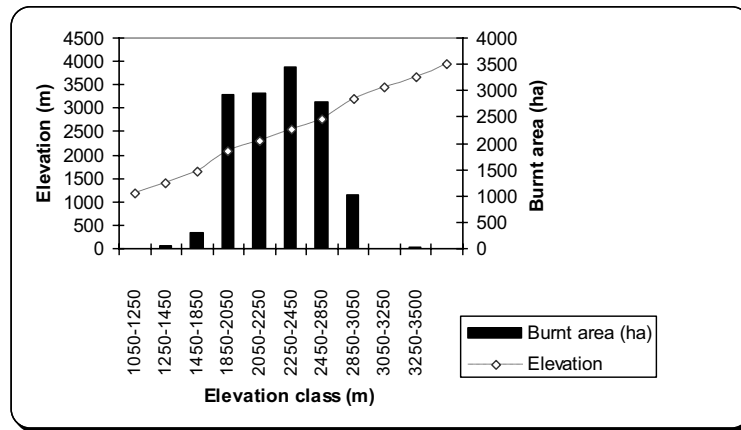


Figure 4-4. Altitudinal distribution of burnt areas

4.1.2.3 Slope

The distribution of burnt scars through different slopes was according to the expected system except for the very steep category (See section **¡Error! No se encuentra el origen de la referencia.**) [90]. The burnt area increases as the slope becomes steeper (Figure 4-5). However, in this case the very steep categories have less burnt area, because this is the category with less total area (Table 4-2) ($H = 139.2$, $P = 0.0001$). Also it is important to consider that in these areas human accessibility is more difficult.

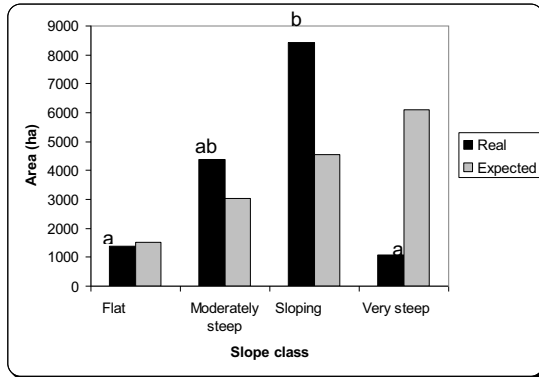


Figure 4-5. Burnt scar distribution per slope class. Letters indicates significance differences among groups

Table 4-2. Burnt scars per slope class

| Slope class | Total area (ha) | Burnt area (%) |
|------------------|-----------------|----------------|
| Flat | 336778.27 | 0.41 |
| Moderately steep | 68313.13 | 6.39 |
| Sloping | 219072.65 | 3.84 |
| Very steep | 34899.64 | 3.07 |

4.1.2.4 Aspect

The burnt area distribution was significantly different among the different orientation types ($F_{(7,1671)} = 2.79, P = 0.0069$). According to the Tukey test, there are no significant differences among the areas exposed to the south, but among the categories W-NW, NW-N and NE-E. Figure 4-6 shows that the observed burnt area distribution is similar to the expected, except for the N-NE category. As it was expected (See section **;Error! No se encuentra el origen de la referencia.**) [95,97], the more burnt areas are those sloping to the SW-W and S-SW (Figure 4-6).

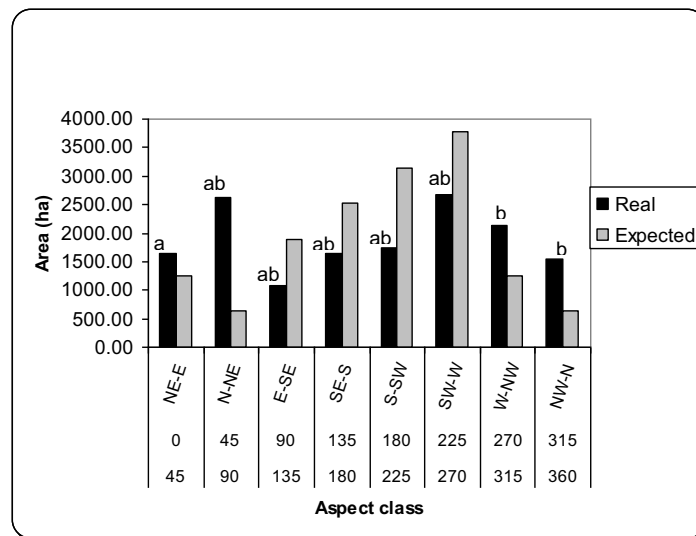


Figure 4-6 Burnt scar distribution per aspect class. Letters indicates significance differences among groups

4.1.2.5 Ignition factors

Official reports in Mexico consider human activities as the primary cause of fires [11,17,64]. As mentioned earlier, in the State of Michoacán the burning of grasslands is the main activity that provokes forest fires; leaving the crop field burning as the second cause of fires. In the study area both activities take place during the dry season. Figure 4-7 A and B represents the distribution of the burnt scars in relation to the distance to growing fields and grasslands. In both figures is possible to observe that in close proximity of crop fields and grasslands there is a more burnt surface, but as this distance increases the burnt surface decreases. For example in the first 500 m following to crop fields and grasslands a burnt surface of about 2500 to 5000 ha were recorded. As agriculture is the main economic activity in the zone, this appears to influence the distribution of the burnt areas.

In contrast, the border effect that exists in the surroundings of roads and highways produces a reduction in the vegetation cover that causes an increase in the ground temperature [98]. Moreover, these highways give people access to natural or remote areas. In the study area, the closeness to roads and highways increases the areas of forest fires. For instance in the first 500 m close to roads and highways, a total burnt surface of 4000 ha was found (Figure 4-7 D). Nonetheless, it is important to mention that roads and highways usually cross crop fields as well as grasslands. Concerning the presence of human settlements, the relation is exist but it is showed after a distance since the fields of agriculture and grass are outside the settlement in a distance beyond 2 km; then the relationship is shown (Figure 4-7 C). However, more data is needed to analyze the degree of influence in the distribution of fires due to the presence of human settlements.

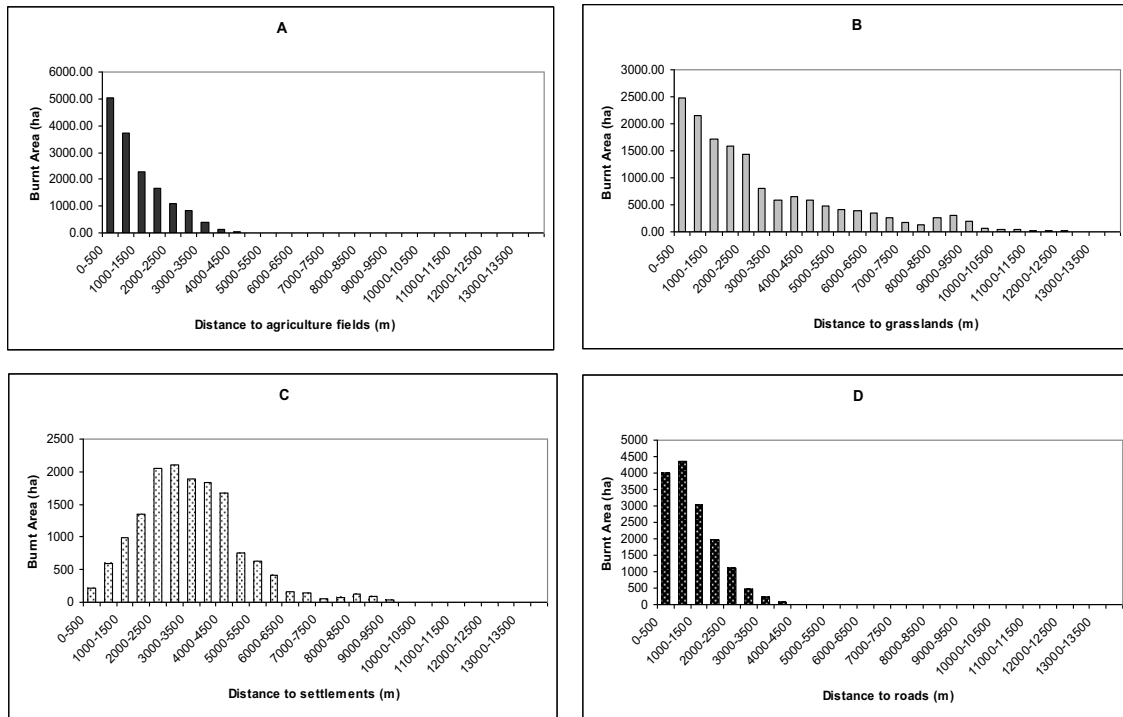


Figure 4-7. Burnt scar distribution according to distance to (A) Agriculture fields, (B) Grasslands, (C) Settlements, (D) Roads

4.1.2.6 Weather

The fire season takes place in the first half of the year (January to June) [61]. Of these, the most incidences of fires occur in April and May (Figure 4-8). Although the incidence of fires does not occur as a direct consequence of the climatic conditions in Mexico, it is clear that the high temperatures and the low precipitation that take place in the mentioned months (Figure 4-10 and Figure 4-9) make the fuel gets dry. Such condition favours that fires may spread to natural areas during the burning of crop fields and grasslands [3]. Moreover, it is known that fires originated by people have more influence when the natural conditions are appropriate to fires [120].

4.2 Modelling phase

4.2.1 Fuel risk sub-model

The fuel risk model is considered as one of the most important models since it includes indispensable variables for the forest fires like vegetation type, slope, aspect and elevation [82]. As stated in the previous section all these factors have a great effect on forest fires in the study area. The vegetation types define the risk areas, whereas the topography, in particular the southern aspect, intensifies the risk. After integrating all the factors, it was identified the maximum, high, medium and low risk areas were identified. Medium risk is the predominant class; whereas maximum risk and low risks were identified in similar proportions (

Table 4-3). The low risk area corresponds mainly to non forested areas such as agricultural fields, grasslands or cities. The medium risk is also composed of agriculture fields and grasslands; however it is located surrounding natural vegetation, since fires started in these places usually spread to forested areas. This class also includes areas with natural vegetation located in low areas such as scrubland or in very high altitudes. The areas classified as high risk have steep slopes and belong to natural vegetation, mostly Pine or Oak forest. Likewise, the maximum risk areas are those that fulfil all the favour conditions for a forest fire. This is southern steep slopes and natural vegetation as Pine, Oak or tropical deciduous forest. Finally, the no risk area belongs to water bodies, or bares soil. The fuel risk sub-model is showed in Figure 4-12.

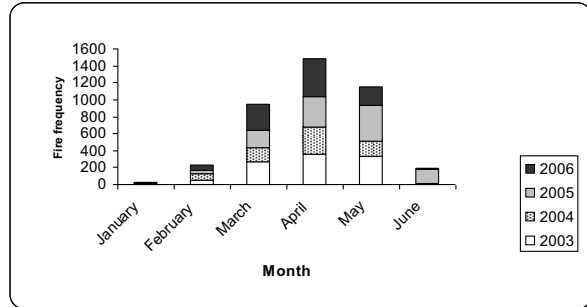


Figure 4-8. Fire frequency in the dry season from 2003 to 2006

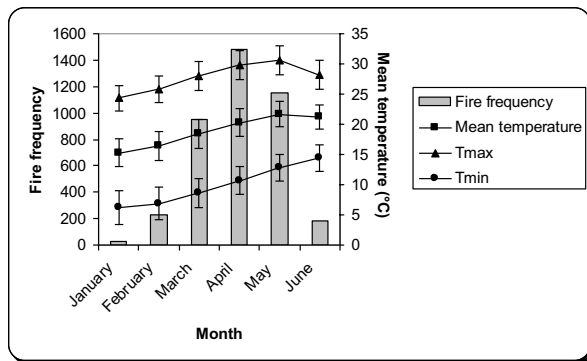


Figure 4-9. Fire frequency and temperature (°C), temperature of the first six months of the year.

Tmax = Maximum temperature and Tmin= Minimum

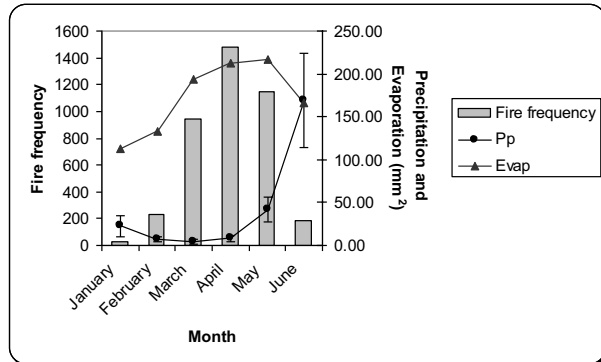


Figure 4-10 Fire frequency of the first six months of the year. Pp = mean precipitation (mm) and E= evaporation

Table 4-3. Area (%) per risk category of Fuel risk sub-model

| Fuel fire risk | Area (%) |
|----------------|----------|
| Maximum | 9.28 |
| High | 24.59 |
| Medium | 42.8 |
| Low | 22.99 |

4.2.2 Ignition risk sub-model

The ignition model is related with human activities like agriculture or stock farming or with human settlements or roads. In the exploratory phase it was observed a direct relation among these variables and forest fires. Due to this in this sub-model it was included a category source of risk based on these human areas. The percentage area occupied by the ignition risk categories is shown in Table 4-4. The maximum and high risks are located in areas limiting with agriculture fields, grasslands and highways. In the other hand the minimum risk is located in the highest areas where no settlements or human activities are present. The ignition risk sub-model is shown in Figure 4-13.

Table 4-4. Area (%) per risk category of the Ignition risk sub-model

| Ignition fire risk | Area (%) | Ignition fire risk | Area (%) |
|--------------------|----------|--------------------|----------|
| Maximum | 9.2 | Moderate | 9.8 |
| High | 11.2 | Low | 2.8 |
| Medium | 13.9 | Minimum | 1.3 |
| | | Source of risk | 51.5 |

4.2.3 Weather risk sub-models

As mentioned earlier, in Mexico the fire season occurs mainly from January to June, although sporadic fires may take place during the second half of the year. The weather risk model was made for the 12 months of the year as a comparative exercise. During the dry season, it is observed that the areas classified as maximum, very high and high risk increase with respect to the rainy months. An example of this is April, as this month is the driest and hottest month and is the month with the highest number of fires of the year. The map corresponding to this month shows the areas classified as high risk than the rest of the year (Figure 4-18). Conversely, in the rainy season the risk decreases as Figure 4-17 shows, which represents the risk of fire during August. A more detailed distribution of the risk zones through the whole year is presented in Appendix **¡Error! No se encuentra el origen de la referencia..**

The weather sub model developed in this study is a temporal model that provides twelve-month scenarios. It uses the average data for both temperature and precipitation, without considering the annual or daily variability in both features. Consequently, the model does not include the changes in temperature and precipitation caused by “El Niño” phenomenon, which has a high influence in the fire frequency in Mexico. It has been reported that, during the “El Niño” years the fire’s incidence increases significantly in contrast with other years. A clear example of this is 1998 when the national record of fires was of 14,445, causing severe ecological and economical damage to the country [11,57,60]. However, this model will not predict the change of forest fire-risk according to the daily or annual fluctuations in temperature and/or precipitation. It is worth to mention that including dynamic meteorological data represent a challenge in Mexico. The scarcity of meteorological stations as well as the insufficiency and the poor-quality of forest fire records, limits the application of predictive modeling to associate the fire’s incidence with the temperature and precipitation changes. Thus,

factor's correlation analyses from the data obtained from meteorological stations are ruled out in the modeling of forest fire risk. In addition, the location of these stations is biased to settlements instead of the forested areas. GIS allows to acquire meteorological data easily and of better quality. An example of this is the work of Manzo [121], who uses a Logit model in order to predict the fire's incidence from NDVI values and surface temperature for the years 1997 to 2000. Nonetheless, there is no climatic model so precise that could be continuously updated with information obtained from satellite and that can be incorporated to a fire occurrence predicting model. One of the virtues of the proposed sub-models of this study is that they show possible forest-fire risk scenarios throughout the whole year, pointing out the areas with the higher risk per month. However, their function is not predictive.

As mentioned before, the sub-models elaborated in this study show the distribution of the highest risk zones through the year. These sub-models highlight the high risk areas. For example, despite the fact that during the rainy season the occurrence of fires is low, it is worth to consider the zones classified as high risk during the whole year. The spatial location of the risk zones through the different seasons of the year, essentially on the dry season, may help to elaborate strategies to prevent fires or to minimize the damages caused by them. Nevertheless, it is important to consider that the present model only considers two variables: the precipitation and temperature. Therefore, in order to improve this model in the future it is highly recommended to include data for the fuel's humidity, air humidity, wind speed and direction.

Table 4-5. Area (%) per risk category of April sub-model

| April fire risk | Burnt Area (%) |
|-----------------|----------------|
| Maximum | 1.43 |
| Very High | 5.64 |
| High | 22.68 |
| Medium high | 16.41 |
| Medium | 11.44 |
| Moderate | 30.76 |
| Low | 11.63 |

Table 4-6. Area (%) per risk category of August sub-model

| August fire risk | Burnt Area (%) |
|------------------|----------------|
| Maximum | 0.0 |
| Very High | 0.0 |
| High | 0.75 |
| Medium high | 9.65 |
| Medium | 11.54 |
| Moderate | 15.39 |
| Low | 35.81 |
| Minimum | 26.86 |

4.2.4 Detection risk sub-model

The detection risk sub-model shows hidden areas for the human eye, where a fire cannot be detected for a certain period of time. Since the study area is highly populated a high percentage of the surface is visible from cities, roads and forest towers. However, there are still some areas that remain non visible (Table 4-7). The invisible areas belong mainly to highest altitudes or ravines. Some areas among mountains or far from roads are invisible. This sub-model allows identifying these areas and it can help in the decision making to locate new forest towers or forest camps.

Table 4-7. Area (%) per risk category of the Detection sub-model

| Detection | Area (%) |
|-----------|----------|
| invisible | 24.16 |
| visible | 75.84 |

4.2.5 Response risk sub-model

The response risk sub-model shows that 54% of the study area is in of maximum to high response, 42% shows a medium to moderate response and 5% appear to be in a low to minimum response, (Table 4-8) (Figure 4-15). The distributions of the response areas are not at random. Because there are 15 headquarters available in the area, from which the fire fighters brigades depart. Almost all the headquarters are located to in the southwestern part of the area. The zones where there is a longer time of response are in general those where the altitude is high. This means that there is more distance between the headquarters located at lower altitudes and flat terrains and the potential fires in high altitudes. An important issue of this model is that it also considers friction. The variety of responses depends on slope, type of vegetation cover and type of roads. Steep slopes or very dense vegetation types could be difficult to the access by brigades. Considering this friction values, the longest distance that should be crossed to arrive at the location of a fire would be 270 km, and considering that the average vehicle used reaches a constant speed of 60 km/hr, the estimated time of arrival would be of approximately 4.5 hours. According to the data obtained from CONAFOR, the national average time of fire's detection in 2005 was 37 minutes, with a time of arrival at the site of one hour and 12 minutes, and the average time of fire fight's duration of 13 hours and 40 minutes [11]. For the 2006 the same office reported that the average detection time was of 37 minutes, the average response time of one hour and duration time of 13 hours and 19 minutes [11]. Currently, Mexican government is making efforts to improve these average times with the purchase of more vehicles (mainly terrain trucks) and giving a much better capacity for the staff.

Table 4-8. Area (%) per response category of the Response sub-model

| Response | Area (%) |
|-----------------|-----------------|
| Minimum | 0.51 |
| Very low | 1.33 |
| Low | 3.18 |
| Moderate | 9.43 |
| Medium | 14.19 |
| Medium high | 17.85 |
| High | 23.09 |
| Very high | 21.30 |
| Maximum | 9.12 |

4.2.6 Static Fire Risk Model

In order to construct the static fire risk model three Equations were compared (Figure 4-11). Equation 1 is the sum of the four static models with out weight, Equation 2 gives more weight to fuel and Equation 3 includes ignition as the second factor in importance (See Section 3.25). In spite of the fact that the three Equations give different weights to fuel and ignition sub-models the distribution of burnt scars is similar in most categories. The main difference in the distribution of burnt scars among the three tested equations was concentrated in the moderate and low categories. Equation 1 shows more burnt area distributed in moderate risk, whereas Equation 3 had more burnt area in the low risk

category. Equation 3 adds more weight to ignition than the other two equations. Therefore, this difference between the low and moderate risk mentioned above can be explained because the model is having more emphasis in Equation 3 on agriculture fields and grasslands as a high forest fire risk zones. Ignition model consider that these areas are continually burned and fire can spread from them to forest. However, agriculture fields and grasslands are non forested areas, and are not of the interest of this study. Equation 3 was chosen to calculate the static model, since it gives high weight to the two of the main factors to start a fire: fuel and heat (ignition sources). In the following paragraphs the results of the static fire risk model are described.

The static fire risk model takes into account all the factors included in the fuel, ignition, detection and response sub-models (Figure 4-16). The global result of the sum of all sub-models is the final but static Fire Risk Model. According to this model the resulting percentages are: 29% of the forest's area considered in the maximum and high risk values, 42% is categorized as medium-high to moderate risk and 30% is categorized as low to minimum risk (Table 4-9). As it was mentioned in the introduction the basic elements to fire starting are fuel, oxygen and heat [1]. Once a fire starts, spreading occurs as an effect of fuel characteristics (mainly its accumulation), topography and weather conditions [122]. For both, starting and spreading, fuel characteristics are essential. As a result of this, the weight of fuel and ignition sub-models has a great importance in the final static fire risk model. The study area topography and cover types play a key role. In this respect, the areas considered in the very high risk category are those with a vegetation type of Pine, Pine-Oak and Oak forest, which are located in the lower zones of the highlands. Besides, some of the areas classified as maximum and very high risk correspond with the southern orientation of the slope. In contrast the areas with the lower risk values correspond with the absence of natural vegetation cover, like the cities, agriculture fields, and grasslands; which are also found in low and flat terrain. The fact that a large proportion of the study site is found among such land uses categories, explains the high percentage value categorized as low risk. On the other hand the effect of the ignition source reflects a clear increase of the risk in the boundary of the natural vegetation cover close to roads, crop fields and grasslands. As for the areas of medium risk, their distribution is more heterogeneous in the different vegetation types at medium altitudes. The effect of the detection and response sub-models is not so evident in the final map of the fire risk static model, since both occur once the fire is started.

Figure 4-11. Percentage of burnt area by fire risk class using Equations 1, 2 and 3

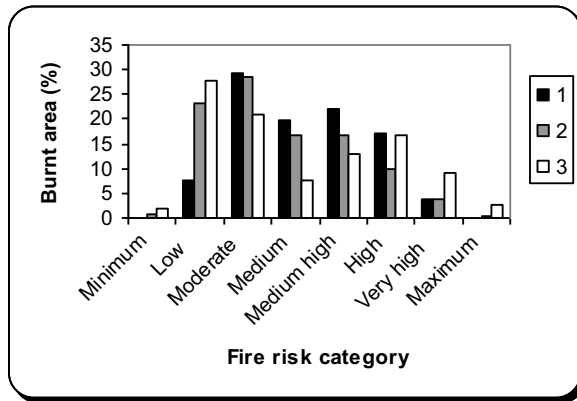


Table 4-9. Area (%) per risk category of Static fire risk sub-model

| Fire risk | Area (%) |
|-------------|----------|
| Maximum | 2.61 |
| Very high | 9.18 |
| High | 16.62 |
| Medium high | 13.12 |
| Medium | 7.58 |
| Moderate | 20.99 |
| Low | 27.87 |
| Minimum | 1.68 |
| No risk | 0.34 |

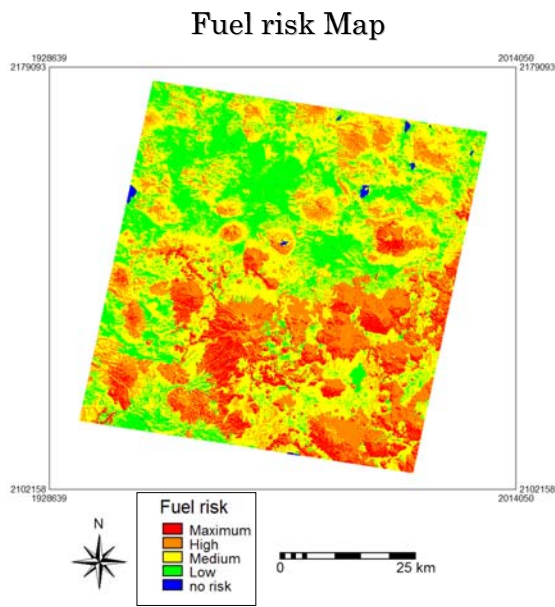


Figure 4-12. Fuel risk map
Detection Map

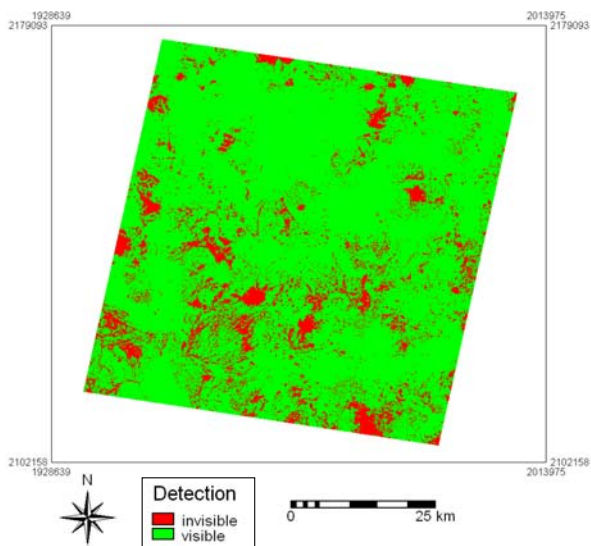


Figure 4-14. Detection map

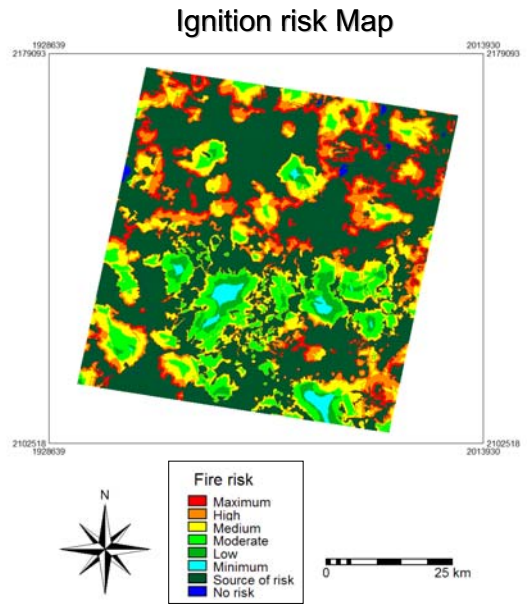


Figure 4-13. Ignition risk map
Response Map

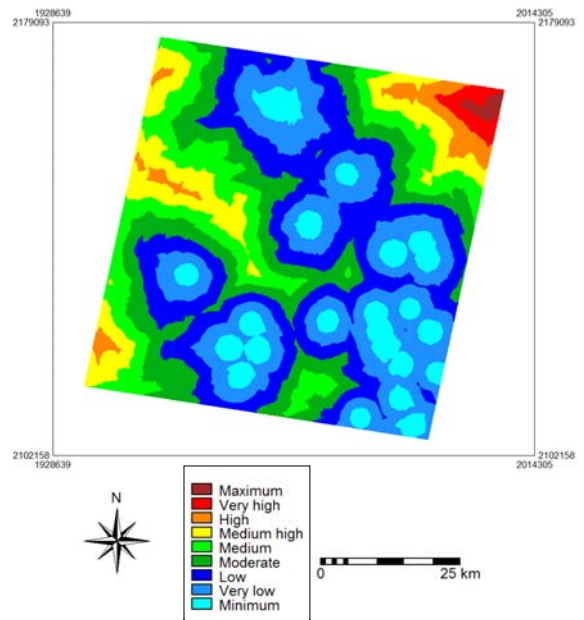


Figure 4-15. Response risk map

Static fire risk Map

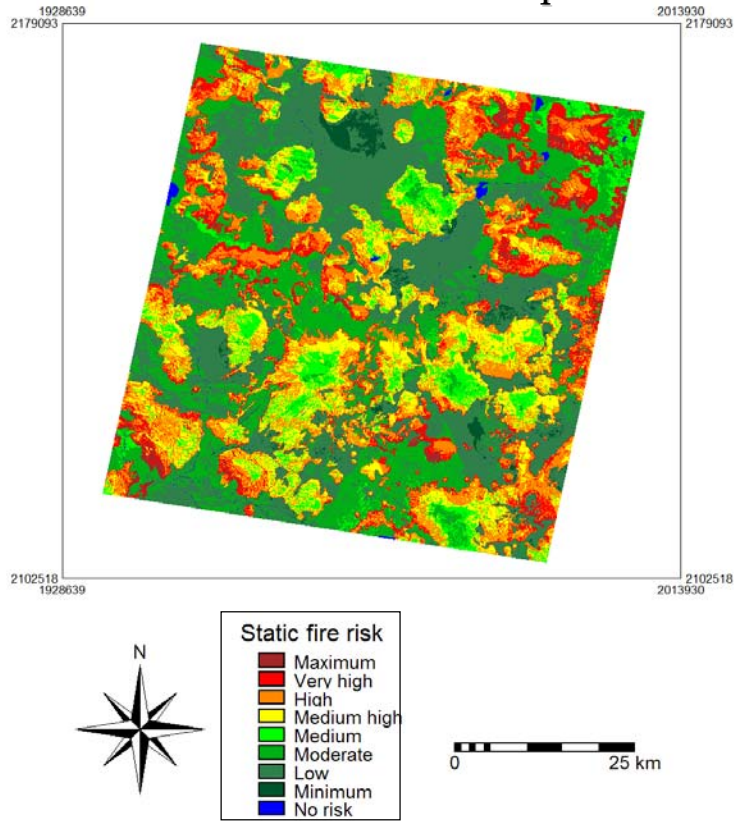


Figure 4-16. Static fire risk

August fire risk Map

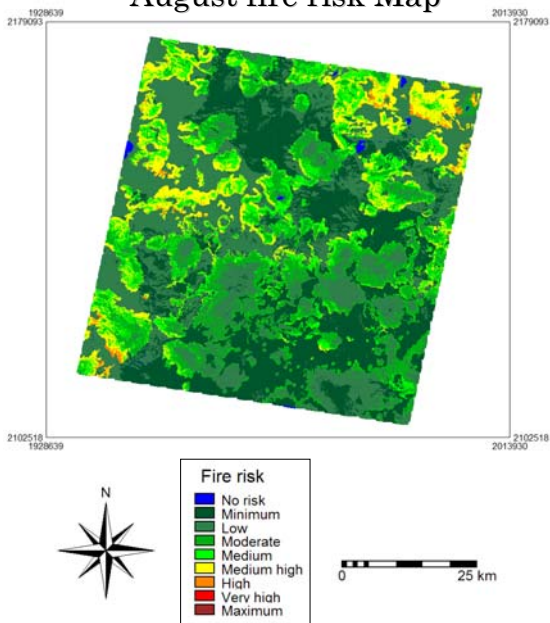


Figure 4-17. August fire risk

April fire risk Map

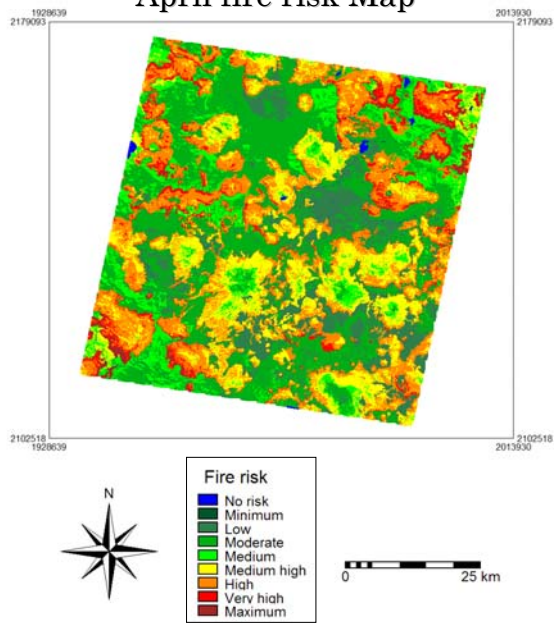


Figure 4-18. April fire risk

4.3 Validation

The validation of the forest fire map of risk sub-models was performed by crossing the burnt areas map with the sub-models maps and the final fire risk model. For the sub-models fuel and ignition the burnt scars were distributed mainly in the maximum to medium high risk categories (Table 4-10 and Table 4-12). On the other hand, the detection model shows that a great part of the burnt area was visible from certain point (Table 4-11). The high number of settlements and the complex road network can explain this fact. However, it is important to consider that the detection of forest fires is also a more complex issue. It can vary depending on the time of the day and also is important to consider that some roads are more passable than others. In the case of the response sub-model, 54% of the burnt scars were located in the areas classified as maximum and high response, 42% in the moderate to medium response and 5% in the low to minimum response (Table 4-13). The distribution of the burnt areas in the response model shows that just a few burnt areas were located in the most inaccessible areas, whereas the burnt area increases as the areas are more accessible. This coincides with the fact that the nearest places to roads are the areas with more percentage of burnt scars because fires are mainly associated with human activities.

The static model had a high coincidence with the burnt scars and the high risk categories, since 92% of the burnt scars were located mainly in the maximum to high medium risk category (Table 4-14). Based on Figure 4-19, we can say that the efforts of fire risk management should be directed mainly to medium high, high and very high risk areas because in the other categories the burnt area is very small. Since this model includes the information of the fuel, ignition, detection and response sub-models and is the base for the weather sub-models, a ROC analysis (Receiver Operation Characteristic) was applied to test the accuracy of the model. The static model was very accurate to classify the fire risk categories (ROC = 0.8). Figure 4-20 shows the ROC curve developed for this model. A ROC curve is constructed by contrasting the true positive rate against the false positive rate which corresponds to real burnt area and area by category of the static risk, respectively. This figure can be read in the following way: a) assuming that the 10% of the area has been burned, a perfect model would classify the same percentage of area as maximum or high risk, and therefore the ROC coefficient would be 1. This perfect prediction corresponds to the OA line of the graph; b) On the other hand, if the burnt area does not coincide with the high risk categories and its distribution is random, the curve would be under the line OM and the ROC coefficient would be 0 [108]; c) According to this, the ROC curve for the static fire risk model shows that the performance of the model is very good since 80% of the area below the curve OBM is over the diagonal OM. Here it should be mentioned that the role of the fuel and ignition model was fundamental in the elaboration and functionality of the static sub-model. In the cases where the weather sub-models had a high percentage of burnt scars in the high risk categories for the months of dry season, then for the months of rainy season the risk diminishes for the same areas. This result is in agreement with the expectation. For April 97% of the burnt scars were located in the high risk categories, whereas for August it was 60%. Moreover, Table 4-15 and Table 4-16 show the burnt area distribution of the months of April (driest) and August (wettest). To see other months, see the tables in Appendix **¡Error! No se encuentra el origen de la referencia.** Finally it should be mentioned that in general the accuracy of the model was considerably high since almost all the burnt scars were located in the high risk class.

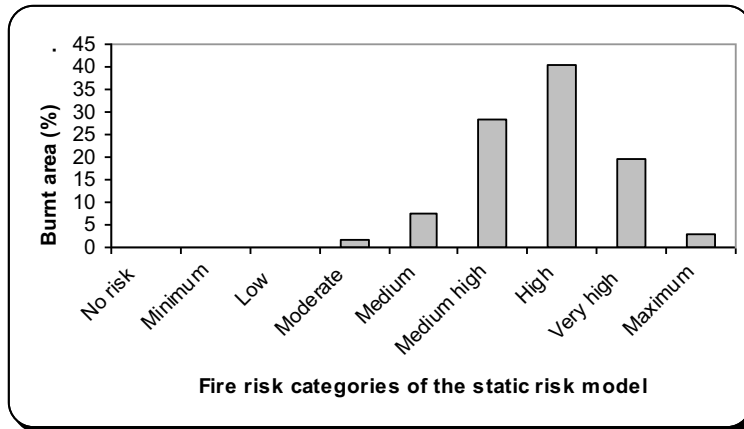


Figure 4-19. Distribution of the burnt scars in the fire risk categories of the static risk model

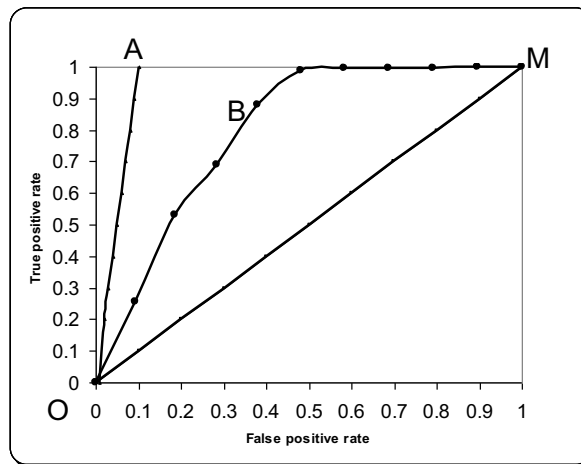


Figure 4-20. ROC curve. Lines OA correspond to a perfect model, OM to a null model and OBM to the static risk model.

Table 4-10. Burnt area (%) per fire risk category for the Fuel sub-model

| Fuel fire risk class | Burnt Area (%) |
|----------------------|----------------|
| Maximum to high | 63.0 |
| Medium | 34.3 |
| Low | 2.7 |

Table 4-11. Burnt area (%) per fire risk category for the Detection sub-model

| Visibility | Burnt Area (%) |
|------------|----------------|
| invisible | 17.9 |
| visible | 82.1 |

Table 4-12. Burnt area (%) per fire risk category for the Ignition sub-model

| Ignition fire risk class | Burnt Area (%) |
|--------------------------|----------------|
| Maximum to medium | 80.0 |
| Moderate to minimum | 20.0 |
| Source of risk | 0.0 |

Table 4-13. Burnt area (%) per fire risk category for the Response sub-model

| Response | Burnt Area (%) |
|---------------------|----------------|
| Moderate to minimum | 16.5 |
| Maximum to medium | 83.5 |

Table 4-14. Burnt area (%) per fire risk categories for the Static sub-model

| Static fire risk | Burnt Area (%) |
|------------------------|----------------|
| Maximum to medium high | 91.7 |
| Medium to minimum | 8.3 |

Table 4-15. Burnt area (%) per fire risk category for the month of April

| April fire risk | Burnt Area (%) |
|------------------------|----------------|
| Maximum to medium high | 97.77 |
| Medium to minimum | 2.23 |

Table 4-16. Burnt area (%) per fire risk category for the month of August

| August fire risk | Burnt Area (%) |
|------------------------|----------------|
| Maximum to medium high | 24.88 |
| Medium to minimum | 75.12 |

4.4 Relevance of the obtained results

The forest fire risk model proposed in this study is a very helpful tool to prevent forest fires, which can be a very helpful addition to the development of the national forest fire management program. The proposed model of this study was carried out in a similar condition to those found in several inter-tropical regions of Mexico. For instance, the burnt of agriculture fields and grasslands is a common practice in most of the country. Such activity is carried out mainly in the less developed and poorest areas. Therefore, this model would be of help to the people of this region, who requires a better strategy for monitoring, supporting and control of the fires.

It should be mentioned here that the development of this fire risk model will have more significance in a global climate change scenario, where high temperature and aridity conditions provoke an increase in the number of fires. As a consequence, their detection and prevention will be a priority. This model can be used easily to identify, with a relatively low cost, the areas more prone to fire, where the prevention efforts should be made.

The present model includes the more important biophysical and social variables. Comparing with other models developed for the detection of fire risk, this one coincides in using several variables like elevation, slope, aspect, vegetation type and the distance to roads, settlements and agriculture fields [1, 5]. Four approaches forest fire modeling presented by Chuvieco [5] are: 1) Qualitative and quantitative models based on expert knowledge, 2) Quantitative models based on multi-criteria evaluation 3) Models based on statistics, in which neural network models are included and 4) Meteorological or fire dispersion models. These approaches include an ample variety of methods for the development of risk's maps. However, since the actual information on the fire's records in Mexico does not include fire frequency or their precise location in geographic coordinates, it is not possible to built statistical models to correlate the occurrence of fire with other type of variables. For this reason, the significance of this model is that it can be applied to different regions, allowing identifying higher risk areas. Moreover, the validation of this model will allow its implementation in similar regions in Mexico.

5 Conclusions and Recommendations

5.1 Conclusion

The general objective of this study is to model forest fire risk for a critical zone in Michoacán, Mexico.

This objective was accomplished since the fire risk model, identified appropriately the high, medium and low fire risk areas. The static model showed that: 29% of the forest surface is in the maximum and very-high risk; 42% is categorized as medium-high to moderate risk and 30% is categorized as low to minimum risk. On the other hand, the weather sub-models showed the changes of fire risk through the year and high coincidence with the burnt areas.

In order to develop the fire risk model, four specific objectives were considered. The specific conclusions are summarized in the paragraphs below.

1. To detect and map forest burnt areas using a high resolution ASTER image

Q1. Can burnt area can be detected and mapped using a high resolution ASTER image?

The ASTER image successfully allowed detecting and mapping the burnt areas using the band combination 2,3,1. The estimated area affected by forest fires was 15,200 ha of the total area (394,200 ha). Based on this map the factors influencing forest fires were evaluated.

2. To analyze the main factors related to forest fires in the study area

Q2. Which of these factors are more related to fire through its relationship to burnt areas?

There was a clear relationship between distance to agriculture fields, distance to grasslands and distance from roads to forest areas, since burnt areas increases as distance decreases. Topography has an important effect too. The burnt areas are distributed mostly in steep slopes with southerly aspect and located in mid-elevations. Finally, Pine and Oak forests seem to be the most affected vegetation types. Areas that show all these characteristics were classified as high to maximum risk in the final fire risk model (See the following conclusion).

3. To develop a forest fire risk model for the study area in order to identify the fire prone areas.

Q3. Which are the prone fire areas (high, medium and low fire risk) in the study area?

The fire risk model was developed by integrating the fuel, ignition, detection and response sub-models. This model is considered as static fire risk model since it does not include weather variable. Ignition and Fuel sub-models are the most effective components of the final model, since their

components are essential contributing to fire start and spread. On the other hand, the detection sub-model shows that most of the study area is visible from cities, roads or forest towers. But it also highlights the areas where fires are not visible in the fire start stage. According to the response sub-model 53.51% of the study area has a maximum to high response, 41.47% a medium to moderate response and 5.02% is in a low to minimum response. The variety of responses depends mainly on slope, altitude, type of vegetation and type of roads. Steep slopes or very dense vegetation add more resistance to the fire brigade to pass through to the forest cover. In this case, the areas with less efficiency of response are those located at high altitudes. On the other hand, weather sub-models showed differences among the hottest and driest months and rainy season months. April is the month with more high risk of the year, whereas August is the month with least risk. These facts coincide with official fire statistics that show that temporal tendency of fires over the year.

4. To validate the forest fire risk model

Q4. How accurate is the forest fire risk model developed in this study?

The validation of the static and weather fire risk models was successful for the study area, since more than 92%, 97% and 60% of the burnt areas were located in the very high to high risk categories in the static, April and August models, respectively. Moreover, a ROC value of 0.8 supports the accuracy of the prediction. In summary the GIS modelling applied in this study allowed the elaboration of an accurate forest fire risk model. Consequently, the obtained results are appropriate to elaborate future prevention strategies in the study area. Moreover, the simplicity of this model allows the incorporation of new variables or the realization of adjustments in order to improve the obtained results.

5.2 Recommendations

Finally, the recommendations for further studies are:

- It is recommended that the visual interpretation is complemented with other techniques such as the analysis of NDVI values or surface temperature analysis.
- It is highly recommended to incorporate fuel's humidity, air humidity, wind speed and direction data in the weather sub-model.
- Fires frequency increases with meteorological phenomena such as "El niño". Therefore, for fire prediction it is recommended to incorporate updated weather data.
- The inclusion of additional data such as vegetation density or biomass maps could improve the results of this study.

Other recommendations:

- This model could be reproduced in other study area since it's operationally simple.
 - Since almost all the processes are carried out in the freeware software e.g., Ilwis, the applied method is cost effective and it could be easily implemented in other areas in the country.
-

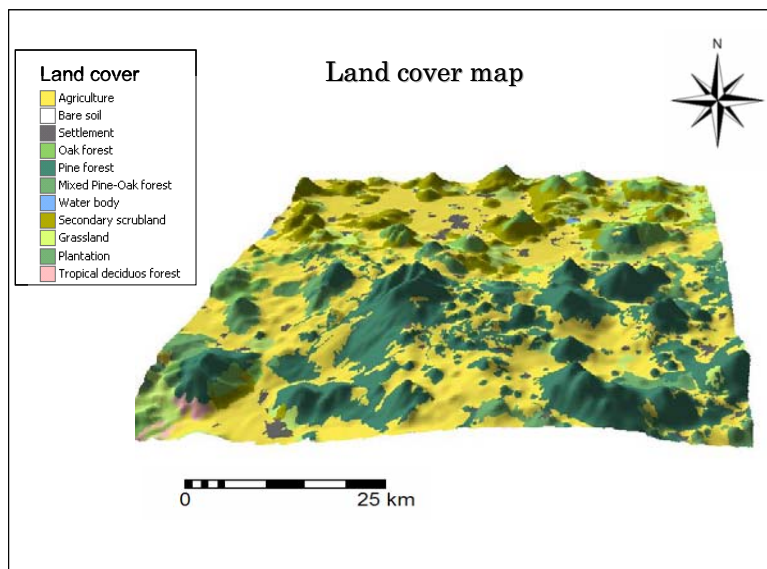
- Since human activity is the main cause of forest fires in Michoacán state it is recommended develop more prevention strategies with local people.
- The weather sub-models showed that there are areas located in constant risk the whole year. It is recommended to give higher consideration to these areas in a fire management plan.
- The implementation of fire-break lines is recommended for the high risk areas where brigade response is low.

Finally, the outputs of this study contribute to:

- Detect burnt forests using high spatial resolution of ASTER images.
 - Analyze biophysical and social factors affecting forest fire in the test area of Michoacán, Mexico.
 - Develop a forest fire risk model for the test area of Michoacán, Mexico.
 - Develop a multi-temporal dynamic sub-model for the above mentioned Forest Fire Risk Model.
 - Develop forest fire management recommendations for the test area of Michoacán, Mexico.
-

Appendices

a. Land cover map



b. Vegetation types



Pine forest



Oak forest



Tropical deciduous forest



Secondary scrubland



Grassland



Agriculture fields



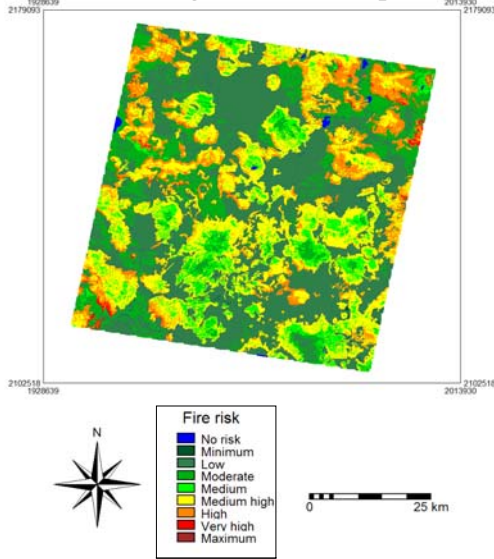
Unpaved road



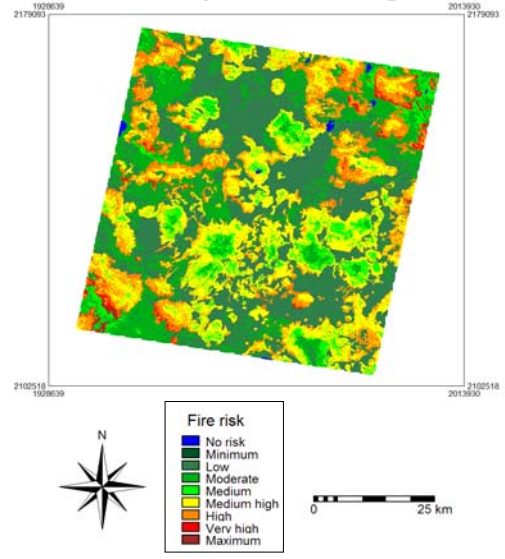
Path

c. Weather sub-models

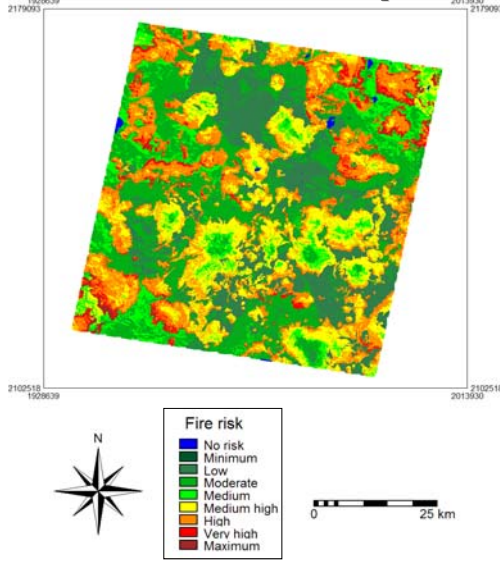
January fire risk Map



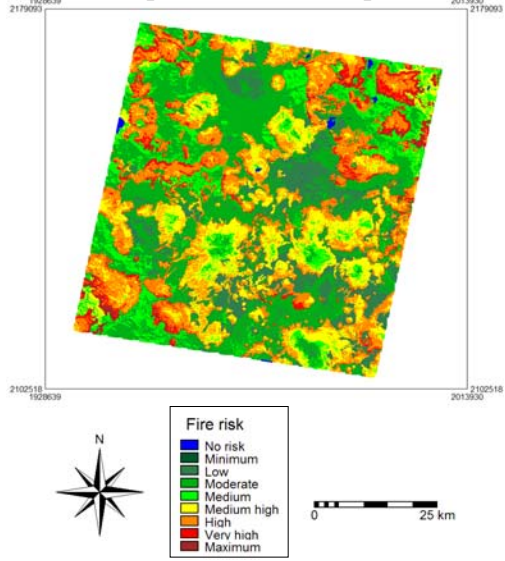
February fire risk Map



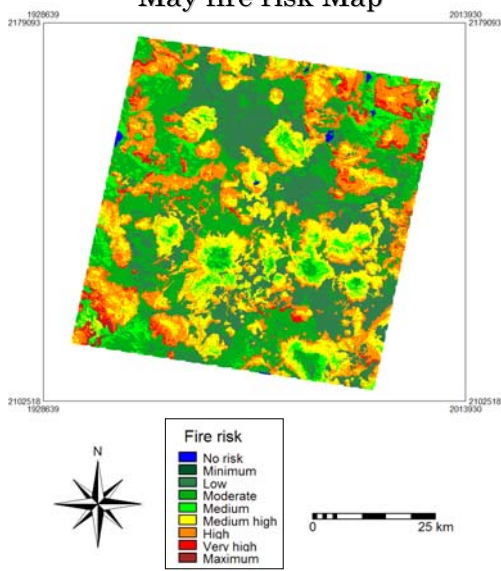
March fire risk Map



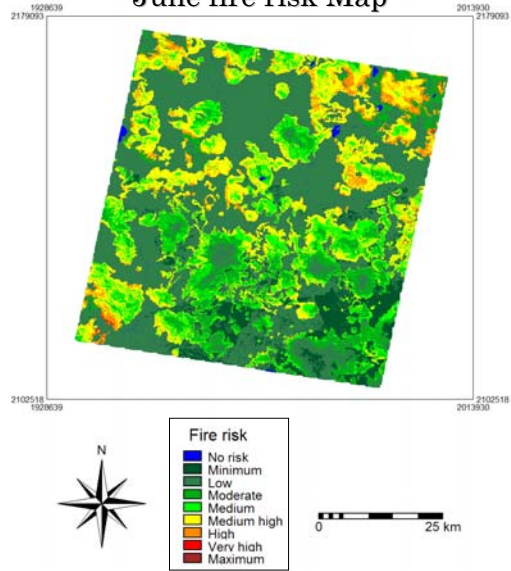
April fire risk Map



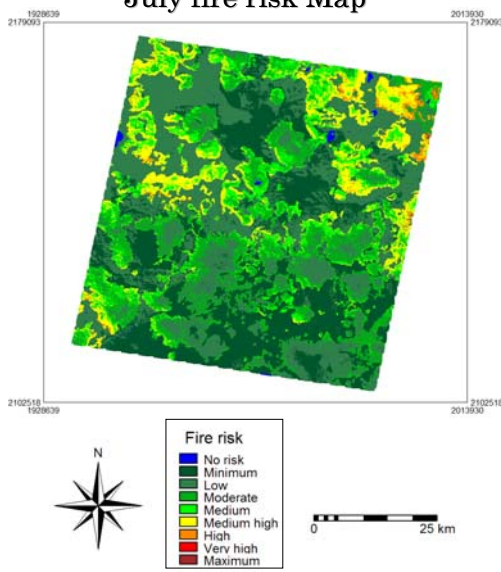
May fire risk Map



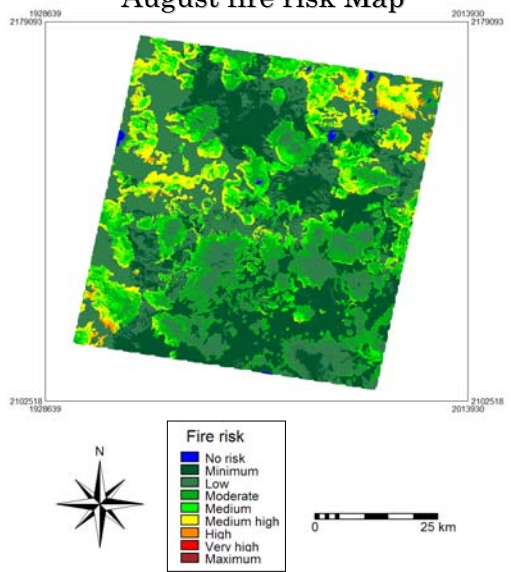
June fire risk Map



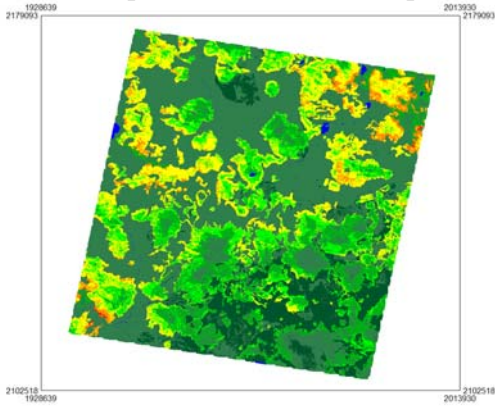
July fire risk Map



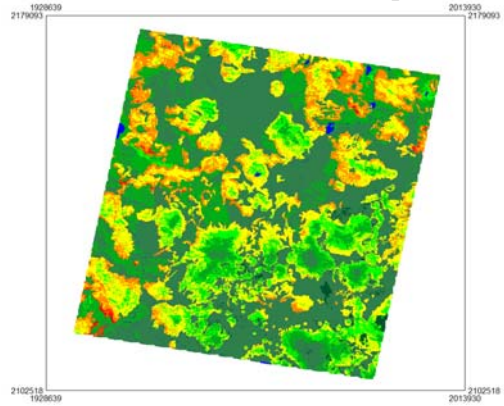
August fire risk Map



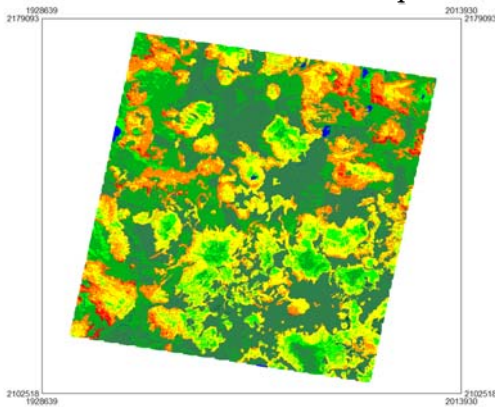
September fire risk Map



October fire risk Map



November fire risk Map



December fire risk Map

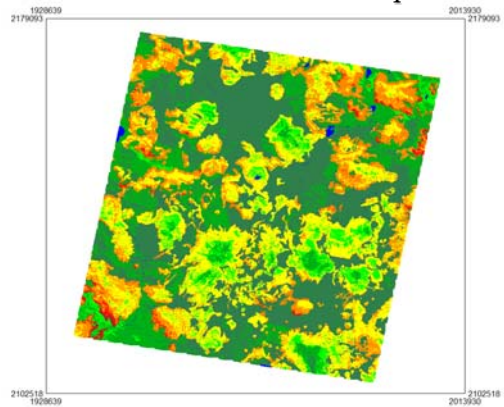


Table 0-1. Burnt area (%) per fire risk category for the month of January

| January fire risk | Burnt Area (%) |
|------------------------|----------------|
| Maximum to medium high | 85.25 |
| Medium to minimum | 14.75 |

Table 0-2. Burnt area (%) per fire risk category for the month of February

| February fire risk | Burnt Area (%) |
|------------------------|----------------|
| Maximum to medium high | 89.15 |
| Medium to minimum | 10.85 |

Table 0-3. Burnt area (%) per fire risk category for the month of March

| March fire risk | Burnt Area (%) |
|------------------------|----------------|
| Maximum to medium high | 96.47 |
| Medium to minimum | 3.53 |

Table 0-4. Burnt area (%) per fire risk category for the month of May

| May fire risk | Burnt Area (%) |
|------------------------|----------------|
| Maximum to medium high | 4.31 |
| Medium to minimum | 95.69 |

Table 0-5. Burnt area (%) per fire risk category for the month of June

| June fire risk | Burnt Area (%) |
|------------------------|----------------|
| Maximum to medium high | 57.14 |
| Medium to minimum | 42.86 |

Table 0-6. Burnt area (%) per fire risk category for the month of July

| July fire risk | Burnt Area (%) |
|------------------------|----------------|
| Maximum to medium high | 30.27 |
| Medium to minimum | 69.73 |

Table 0-7. Burnt area (%) per fire risk category for the month of September

| September fire risk | Burnt Area (%) |
|------------------------|----------------|
| Maximum to medium high | 46.85 |
| Medium to minimum | 53.15 |

Table 0-8. Burnt area (%) per fire risk category for the month of October

| October fire risk | Burnt Area (%) |
|------------------------|----------------|
| Maximum to medium high | 23.60 |
| Medium to minimum | 76.40 |

Table 0-9. Burnt area (%) per risk category for the month of November

| November fire risk | Burnt Area (%) |
|------------------------|----------------|
| Maximum to medium high | 11.84 |
| Medium to minimum | 88.16 |

Table 0-10. Burnt area (%) per fire risk category for the month of December

| December fire risk | Burnt Area (%) |
|------------------------|----------------|
| Maximum to medium high | 11.92 |
| Medium to minimum | 88.08 |

d. Study case: GIS FOREST FIRE RISK MODEL (in Spanish)

MODELO DE RIESGO DE INCENDIO

Un estudio de caso en Michoacán, México

1. Introducción

El estudio de caso a que continuación se presenta está basado en la tesis: “Un modelo de Riesgo de incendio en Michoacán, México” desarrollado por Sonia Juárez. Al finalizar el ejercicio, el estudiante modelará el riesgo de incendio forestal para una zona con incendios frecuentes en el estado de Michoacán, México. Para ello, el método se dividirá en tres fases: Exploratoria, Modelaje y Validación. En la primera fase, se analizarán los factores relacionados con incendios forestales. En la segunda fase con el objeto de identificar las áreas de alto riesgo de incendio forestal se desarrollarán cinco submodelos: Combustible, Ignición, Detección, Respuesta y Clima. Finalmente, en la tercera fase, se validará el modelo utilizando un mapa de las áreas quemadas del sitio de estudio. Los productos finales que se obtendrán serán un mapa estático de riesgo de incendio y doce modelos climatológicos de riesgo de incendio. Al final del ejercicio el estudiante habrá aprendido a: 1) Interpretar y digitalizar visualmente las áreas quemadas utilizando herramientas de sistema de información geográfica y percepción remota, 2) Analizar los factores biofísicos relacionados con los incendios, 3) Modelar el riesgo de incendio utilizando el programa ILWIS y 4) Validar los resultados del modelo.

El estudio de caso se llevará a cabo en el programa ILWIS 3.4. Por lo tanto, para poder acceder fácilmente a los datos del ejercicio se recomienda copiar la carpeta Firemod a una nueva carpeta en el disco duro de la computadora (p. e. C:\Firemod).

Antes de comenzar el ejercicio, familiarícese con el sitio de estudio. Esto le ayudará a tener una idea general a cerca de las características del área donde se está llevando a cabo este estudio. Posteriormente, haga una breve lista de los factores que usted piense estén relacionados con el riesgo de incendio forestal.

2. Antecedentes

La ocurrencia de incendios en tamaño, frecuencia e intensidad se ha incrementado significativamente en las últimas décadas alrededor del mundo debido al fenómeno periódico de El Niño, la deforestación y otras causas [55]. México es un país seriamente afectado por los incendios forestales [11]. Tan sólo durante 1998, durante un año de *El Niño*, el país registró 14, 445 incendios forestales que afectaron 919, 000 ha. Michoacán es uno de los estados más afectados por los incendios forestales. Las causas son resultado de la interacción de factores biofísicos y sociales. En México las actividades humanas aún son la principal causa de incendios. Entre las actividades más frecuentes que generan incendios forestales se encuentran la quema de campos agrícolas y pastizales y las fogatas campestres [60]. La temporada de incendios ocurre de enero a junio, siendo marzo y mayo, la

temporada más seca y calida del año, lo cual coincide con el período con mayor número de incendios forestales [61]. Durante estos meses los agricultores y ganaderos, toman ventaja de las condiciones climáticas y prenden fuego a los pastos y plantas secas con diversos fines, tales como, restaurar los nutrientes en la tierra o eliminar plagas. En numerosas ocasiones, dichos incendios se esparcen hacia los bosques, y aunque es verdad que los incendios naturales son una parte importante de la dinámica de algunos ecosistemas, los frecuentes incendios causados por actividad humana pueden producir diversos efectos negativos, tal como la pérdida de biodiversidad y la degradación del suelo [55].

En México, los esfuerzos para la prevención incendios aún no son suficientes para reducir la frecuencia e intensidad de los incendios [56]. El área de estudio es una de las zonas más afectadas por incendios en el estado de Michoacán [64]. No obstante las áreas con alto riesgo de incendio aún no han sido completamente identificadas. Por esta razón es de vital importancia desarrollar estrategias para la prevención incendios para evitar la pérdida de recursos naturales. El mapa de riesgo incendio elaborado en este estudio servirá para identificar las áreas de riesgo de incendio lo cual puede ser de gran ayuda para la creación de planes de prevención de incendio por parte de las autoridades locales.

3. Sitio de Estudio

El sitio de estudio se localiza entre las coordenadas 20.15 -102.5 NE, 19.59, -102.63 SE, 20.07, -101.92, NO, 19.51, -102.5 SO, cubriendo un área de 3942 km² en 23 municipalidades. El punto más alto en esta área es de 3400 m, mientras que el más bajo es de 1110 m. Debido a esta diferencia altitudinal se presentan dos grandes tipos de clima: subtropical y templado. Asimismo, hay siete tipos de vegetación distribuidos en toda el área: bosque de pino (17.1%), bosque de pino encino (13.8%), matorral secundario (11.5%), pastizal (9.8%), bosque de encino (7.1%), bosque tropical caducifolio (1.2%) y vegetación hidrófila (0.1%). Los principales usos de suelo son: agricultura temporal (23%), agricultura de riego (6.2%) y ganadería (9.8% de los pastizales). El porcentaje de estas actividades varía de acuerdo a la municipalidad. En general, la agricultura es la actividad económica más importante, seguida por las actividades ganaderas y las actividades forestales. El grado de intensidad de estas actividades también varía de acuerdo a la municipalidad. Por ejemplo en los municipios de Tocumbo, Los reyes, Uruapan, Cheran y Charapan las actividades forestales son la principal actividad económica [75]. No obstante, en otros municipios la actividad forestal se lleva a cabo en menor grado. En México, en particular en el estado de Michoacán, la tala de bosques ocurre como consecuencia de la tala ilegal. Bocco *et al.* [76] reportó que los bosques tropicales y templados de Michoacán pierden cada año cerca de 1.8% y 1% de su área, respectivamente. La principal actividad que contribuye a la deforestación es la tala ilegal. Sin embargo, los incendios forestales también contribuyen a la pérdida de cobertura de bosques. Las áreas naturales quemadas no se recuperan tan fácilmente de las quemadas frecuentes y suelen ser ocupadas clandestinamente por la agricultura, la fruticultura y los pastizales [57,77]. En la meseta purépecha el decremento de la cobertura forestal es causada principalmente por el establecimiento de cultivos de aguacate (*Persea spp.*) [77]. México es el primer productor de aguacate en el mundo, del cual, el estado de Michoacán produce el 85% de la producción nacional, generando 750 millones de pesos al año [79]. Esta situación fortalece la incentiva económica para convertir los bosques a cultivos de aguacate, siendo los incendios provocados una de las principales consecuencias [77].

En el sitio de estudio hay 426 poblaciones, de las cuales las más importantes son Zamora de Hidalgo, Jacona de Plancarte, Los Reyes de Salgado, Paracho de Verduzco, Tangacicuaro de Arista, Purepero de Echaiz, Santiago Tangamandapio, Ario de RAYon, Tarecuato y Capacuaro. Toda las localidades localizadas en la meseta purépecha tienen población indígena, de la cual gran porcentaje sufre de pobreza.

4. Fase exploratoria

Ahora que usted tiene un conocimiento general del sitio de estudio y del problema de investigación, puede comenzar con el estudio de caso. El modelo de riesgo incendio forestal es resultado de una investigación enfocada en tres fases principales: 1) Exploratoria, 2) Modelaje y 3) Validación. En la primera fase se exploraran las variables que van a ser incluidas en el modelo. Para ello será necesario crear un mapa de áreas quemadas. Éste mapa permitirá llevar a cabo un análisis para determinar si existe una relación entre las áreas quemadas y algunos factores biofísicos y sociales. Los factores que se considerarán en este análisis, por su importancia en el inicio y desarrollo de los incendios, serán: 1) combustible, 2) clima, 3) topografía y 4) actividades humanas.

4.1. Mapa de áreas quemadas

Un mapa de áreas quemadas es una herramienta útil para evaluar los daños en un bosque. La ausencia de vegetación y la presencia de ceniza incrementan la luminosidad y la temperatura del suelo [18,39]. Dichas características facilitan el mapeo de las áreas quemadas, el cual se puede llevar a cabo mediante clasificación de imágenes satelitales [40] o técnicas de interpretación visual [24,40]. Para esta última, la selección de bandas espectrales es crucial, ya que las áreas quemadas presentan baja reflectancia en el rojo e infrarrojo cercano.

En este estudio se mapearán las áreas quemadas utilizando una imagen satelital ASTER. Primero, el alumno practicará la digitalización de las áreas quemadas sobre la imagen utilizando diferentes combinaciones de bandas. Para ello se creará un mapa de segmentos, el cual a su vez se convertirá en un mapa de polígonos y finalmente en un mapa raster.

4.2. Detección de áreas quemadas

- **Actividad**

Para crear un mapa de áreas quemadas se utilizará una imagen ASTER ya que posee una alta resolución (15 m) y bandas multiespectrales en la luz visible, infrarrojo cercano, infrarrojo de onda corta e infrarrojo térmico que permiten diferentes composiciones para identificar escamas de incendio [29].

👉 Abra la imagen FinalA y utilice diferentes combinaciones de bandas haciendo clic en el icono en forma de monitor. Escoja la combinación de bandas (rojo, verde y azul) que resalte mejor el área quemada en la imagen y trate de reconocer áreas con bosque, campos de cultivo y ciudades.

4.2.1. Digitalización del área quemada

Para generar el mapa de áreas quemadas primero necesitará dibujar un mapa de segmentos. De acuerdo con la guía de usuarios de Ilwis " un segmento está compuesto por series de puntos intermedios, conectados por líneas rectas que empiezan y acaban con un nodo " (Figura 1).

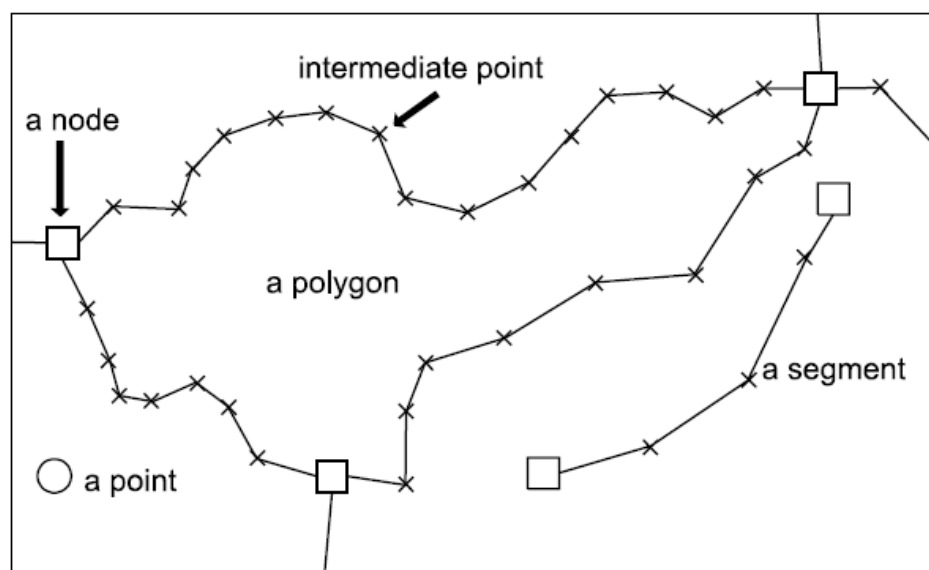






Figura 1. Puntos, segmentos y polígonos en Ilwis

Para digitalizar las áreas quemadas dibuje una línea haciendo clic en las inflexiones o manteniendo apretado el botón izquierdo del ratón y moviendo simultáneamente el cursor alrededor del área que se desea dibujar. Mientras realiza esta operación, no olvide que todas las líneas del polígono deben estar conectadas. Para cerrar el segmento, sólo necesita hacer doble clic sobre el nodo en donde comenzó a digitalizar. Debido a que la digitalización de toda la imagen llevaría mucho tiempo, practique digitalizar en sólo una pequeña área de la imagen.

Tip: si está usando la combinación de bandas 3, 2, 1, en rojo, verde y azul, las áreas quemadas aparecerán en negro en la imagen. Incluso podrá observar en algunas áreas donde humo gris sale de zonas con incendios activos.



- Abra la imagen `FinalA`.
- Desde el menú principal de Ilwis seleccione `Create` y `Segment map` para crear un mapa de segmentos.
- Nombre al mapa `BurntB` y acepte los otros valores predefinidos.
- Para digitalizar utilice las herramientas: Modo de inserción , Cortar y unión , y Mover puntos .
- Cuando haya terminado de digitalizar, se le recomienda revisar que no haya errores en los segmentos. Para ello desde el menú `File` seleccione `Check Segments` (chequear segmentos) y haga clic en las opciones de `Self Overlap`, `Dead Ends` e `Intersection` para hallar errores en el mapa de segmentos.
- Corrija todos los errores en su mapa segmentos y salga del editor de mapas  y cierre la ventana.

4.2.2. Conversión del mapa de Segmentos a un mapa de Polígonos

A continuación deberá convertir el mapa de segmentos en un mapa de polígonos. Un polígono es: " una área cerrada que consiste en uno o más segmentos. Todos los segmentos que forman un polígono están conectados por una intersección y cada intersección o fin de conexión tiene un nodo".



- Seleccione la opción `Segment to Polygon` (segmento a polígono) haciendo doble clic sobre ésta en la lista de operaciones de la ventana principal de Ilwis. La ventana para poligonizar el mapa de segmentos se abrirá.
- Seleccione el mapa `BurntB` como mapa de segmentos y deseccione las opciones de `Mask` y `Auto Correction` (máscara y autocorrección).
- Seleccione la opción de `Unique Identifiers` (identificadores únicos) y nombre `BurntB` al nuevo mapa de polígonos.
- Haga clic en el botón `Show` (mostrar), revise su mapa de polígonos y cierre la ventana.

4.2.3. Conversión del mapa de Polígonos a un mapa Raster

En esta sección convertirá el mapa de polígonos en un mapa raster. En un mapa raster los datos se organizan en celdas o píxeles. Esta organización permite hacer diferentes operaciones con sistemas de información geográfica (p.e. cruce de mapas y suma de mapas). Dado que en la fase modelaje trabajará con mapas raster, el mapa de áreas quemadas deberá ser convertido a raster.



- Seleccione de la lista de operaciones la opción `Polygon to Raster` (polígono a raster). Se abrirá una nueva ventana.
- Seleccione al mapa de polígonos `BurntB` y nombre `BurntB` al nuevo mapa raster.
- Seleccione la georeferencia `FinalA` y haga clic en el botón `Show`.
- Revise el nuevo mapa raster y cierre la ventana.

4.2.4. Exclusión de las áreas no forestales

Dado que estamos interesados en los incendios forestales, es importante discriminar las áreas forestales quemadas de las áreas no forestales quemadas (p.e. campos agrícolas). Algunas veces es difícil identificar donde inicia o finaliza un área forestal, debido a la tonalidad negra de la escama de incendio. Para excluir las áreas no forestales del mapa de áreas quemadas utilice el comando *iff*.



- Escriba la siguiente fórmula en la línea de comando de la ventana principal:

```
Burnttest:= iff(((Lcov="Agriculture") or (Lcov="Grassland") or  
(Lcov="Settlements") or (Lcov="Bare soil") or (Lcov="Water body") or  
(Lcov="Road") or(Lcov="River")),?,BurntB)
```

- Acepte los valores predeterminados y haga clic en el botón Show.
- Trate de explicar el significado de este comando con sus propias palabras.

5. Análisis de los factores relacionados con los incendios forestales

5.1. Inspección visual

- **Actividad**

En esta sección se analizarán los factores relacionados con incendios forestales.



Abra los mapas de pendiente, orientación, elevación, cobertura del suelo y distancia a campos de cultivo, pastizales, carreteras y localidades, llamados: slopeclas, aspectclas, elevclas, lcov, d1agric, d1grassd1, d1road y d1settle. Familiarícese con la topografía y la cobertura de suelo del área de estudio. Note que todos los mapas están clasificados. Cheque los rangos de las clases de cada mapa. Por ejemplo, el mapa de pendiente está clasificado de acuerdo al grado de inclinación en las categorías plano, pendiente ligera, pendiente moderada y pendiente elevada.

Pregunta:

¿La inclinación tiene algún efecto sobre los incendios? Observe la clasificación de otros mapas. Sobrelape el mapa de áreas quemadas BurntA con los mapas de pendiente, orientación, elevación, cobertura de suelo y distancia a campos agrícolas, pastizales, carreteras y ciudades. Cree sus propias hipótesis y discútalas con sus compañeros.

Al terminar este ejercicio usted tendrá una impresión visual de la distribución de las áreas quemadas.

5.2. Cruce de mapas: Obtención de tablas y gráficas

La exploración visual del área de estudio nos da una idea general de la condición del terreno y su relación con las áreas quemadas. No obstante, para encontrar algún patrón en la distribución de las áreas quemadas necesitaremos obtener algunos datos con cuantitativos. Cruce el mapa de áreas quemadas BurntA con los mapas de los factores (Tabla 1) que pueden influir en el inicio o esparsimiento de los incendios.



- Seleccione de la lista de operaciones la opción Cross (Cruzar) y elija los mapas raster BurntA y Slopclas.
- Nombre Slope_burnt a la tabla final y haga clic en Show.
- Esta tabla le mostrará en qué clases de pendientes se concentra la superficie quemada. Evalúe los resultados y repita los pasos con los factores de la tabla 1.

Tabla 1. Factores relacionados con los incendios y nombre de los mapas y tablas correspondientes

| Factor | Mapa | Tabla |
|-------------------------------|----------|---------------|
| Pendiente | Slopclas | Slope_burnt |
| Orientación | Aspeclas | Aspect_burnt |
| Elevación | Elevclas | Elev_burnt |
| Cobertura de suelo | Lcov | Lcov_burnt |
| Distancia a carreteras | D1road | Droad_burnt |
| Distancia a localidades | D1settle | Dsettle_burnt |
| Distancia a campos de cultivo | D1agric | Dagric_burnt |
| Distancia a pastizales | D1grass | Dgrass_burnt |

Las tablas que ha creado, le ayudarán a analizar la relación que existe entre estos factores y las áreas quemadas del área estudio. En estas tablas observará la distribución del área quemada por cada clase de los factores. Por ejemplo, si la clase pendiente moderada del factor pendiente tiene un valor alto de superficie quemada, el riesgo de incendio es alto para esa clase.



- Para convertir los resultados de la tabla en una gráfica, haga clic con el botón derecho del ratón en el icono de la tabla que desea usted convertir en gráfica.
- Seleccione la opción Create a Graph (crear gráfica). Se abrirá una nueva ventana, seleccione la columna del factor a analizar para el eje de las x y seleccione la columna de área para el eje de las y .
- Haga clic en OK. Repita éste ejercicio con todos los factores.

Tip: también puede importar los valores de las tablas a Microsoft Excel y hacer análisis estadísticos.

Piense en las gráficas y tablas que ha creado ¿existe alguna relación entre estas variables y la distribución del área quemada? Cree sus propias conclusiones y discútalas con sus compañeros ¿Es necesario hacer algún tipo de análisis estadístico? Algunas tendencias parece ser claras en las gráficas. Sin embargo una prueba estadística es un método científico que ayuda a obtener conclusiones claras de la información disponible.

Recuerde: estos factores serán usados para tener un mejor entendimiento del modelo de riesgo de incendio final.

6. Modelaje

6.1. Modelo de riesgo de incendio

Este estudio de caso sigue la aproximación usada por Neeraj y Hussin [49] dado la forma en que se integran las variables biofísicas y humanas. La probabilidad de incendio depende de las causas de ignición y las precondiciones del medio ambiente; mientras que la probabilidad de esparcimiento del incendio se asocia con el comportamiento del fuego y las acciones de supresión. Por lo tanto, existen cuatro factores principales que modifican la probabilidad de un incendio forestal: 1) combustibles, 2) medio ambiente, 3) factores de ignición y 4) prevención y supresión [48]. Los modelos cuantitativos basados en el conocimiento experto clasifican las variables relacionadas con los incendios utilizando una escala numérica de acuerdo a índices o pesos derivados de observaciones en el campo, revisión bibliográfica y la opinión de expertos [5]. Por lo tanto, el modelo de riesgo incendio se clasifica de acuerdo a una escala de categorías dividida en riesgo alto, medio y bajo. La principal ventaja de ese tipo de modelos es que permiten reconocer las áreas de riesgo para tomar las medidas de manejo forestal más adecuadas. Sin embargo, estos modelos no proporcionan información de probabilidades de ignición o de esparcimiento del fuego. Entre este tipo de modelos, podemos encontrar los estudios de Chuvieco y Salas [31,47], Rathaur [48], Neeraj [49], Maselli *et al.* [50] y Roy [24].

☞ Para identificar las áreas con riesgo de incendio forestal en el área estudio, en la segunda fase, todos los factores analizados en la fase previa serán introducidos en un modelo de cinco pasos o submodelos. Cada submodelo, enfatizará los factores más importantes relacionados con los incendios forestales. Estos modelos son: Combustible, Ignición, Clima, Detección y Respuesta.

Los cuatro primeros submodelos conformarán un modelo de riesgo estático. Sin embargo, dado que el comportamiento del fuego y el riesgo incendio cambia lo largo del año dependiendo de las condiciones climáticas, este modelo se convertirá en un modelo múltitemporal o modelo climático de riesgo incendio, el cual incluirá información de los cambios en la precipitación y temperatura mensual para los doce meses del año.

Para crear estos modelos se utilizarán índices lógicos basados en una revisión bibliográfica. En la mayoría de los casos los mapas serán reclasificados de acuerdo a los valores del histograma o a la

distribución de los datos. En resumen, todos los submodelos constituirán un mapa específico de riesgo incendio. La suma todos los submodelos creará el mapa final de riesgo incendio del área estudio.

En este estudio de caso se desarrollarán únicamente el submodelo de ignición y los modelos de riesgo de incendio Estático y Climatológico. Si desea aprender a desarrollar el modelo de combustible, detección y respuesta puede consultar el estudio de caso: "Modeling Forest Fire Hazard Using Remote Sensing and Geographic Information System GIS" desarrollado por Yousif Ali Hussin, Dirk Boon y Neeraj Sharma publicado por el ITC.

7. Submodelo Ignición

7.1. Introducción

Como se mencionó anteriormente, los humanos provocan más del 90% de incendios en México [11,62]. En este modelo se incluirán las principales actividades humanas que causan incendios en el estado de Michoacán. Estas son las quemadas de campos agrícolas y pastizales. La expansión de los incendios desde estas áreas a los bosques suele ser un fenómeno común. Asimismo la cercanía a carreteras y ciudades puede ser un factor que promueve la generación de incendios. De hecho, se ha observado que existe un efecto borde en los bosques que son fragmentados por caminos. La disminución de la cobertura vegetal en los bordes de caminos o carreteras produce cambios como el incremento de temperatura, y el aumento de luz en la superficie del suelo [98]. Esto permite que cerca las carreteras la composición vegetal de especies sea diferente a la original, pues plantas exóticas e invasivas, muchas de ellas pirófilas, pueden encontrarse en los bordes de carreteras y caminos.

Teniendo en cuenta toda esta información, los datos que serán considerados en el desarrollo de este submodelo serán mapas de distancia a: 1) campos de cultivo, 2) pastizales, 3) caminos y 4) localidades. Estos mapas serán reclasificados utilizando índices de riesgo. Finalmente los mapas serán combinados en el mapa final de riesgo de ignición de incendio.

7.2. Extracción del área de interés

- **Actividad**

Para elaborar los mapas de distancia, primero tendrá que extraer del mapa de cobertura del suelo, las áreas interés, es decir los campos de cultivo, pastizales, caminos y localidades. Para ello utilice el comando *iff*.



- Teclee la siguiente fórmula en la línea de comando de la ventana principal:

```
Agriculture:= iff((Lcov="Agriculture"),"Agriculture",?)
```

- Seleccione el dominio `Lcov` y haga clic en `Show` para evaluar el resultado. Repita el procedimiento para las otras coberturas, usando las siguientes fórmulas:

```
Grassland:= iff((Lcov="Grassland"),"Grassland",?)
```

```
Road:= iff((Lcov="Road"),"Road",?)
```

```
Settle:= iff((Lcov="Settlements"),"Settlements",?)
```

7.2.1.Cálculo del mapa de distancia

El siguiente paso es crear los mapas de distancia a campos agrícolas, pastizales, caminos y localidades.



- Haga doble clic en `Distance calculation` de la lista de operaciones de Ilwis. La ventana de calculo de distancia se abrirá.
- Seleccione el mapa `Agriculture` de la lista `Source Map`.
- Teclee `Dagric` para nombrar al nuevo mapa
- Acepte los otros valores predefinidos y haga clic en `Show`.
- Repita el procedimiento para los mapas `Grassland`, `Roads` y `Settle`.
- Nombre a los nuevos mapas `Dgrass`, `Droads` y `Dsettle`

Clasifique los mapas de distancia de acuerdo al riesgo de ignición. Recuerde que la distancia a los campos agrícolas, pastizales, caminos y localidades está directamente relacionada con la distribución de las áreas quemadas. En este caso, se asumirá que las áreas quemadas se incrementan a medida que estamos más cerca de la fuente de ignición. Por lo tanto el valor índice de riesgo será mayor en distancias cortas.



- Para elaborar los mapas de distancia primero se creará un dominio con clases de distancia.
- Cree el nuevo dominio seleccionando New Domain de la lista de operaciones y nómbrelo `Dclas`. Seleccione la opción Group y dé clic en OK. Una nueva ventana se abrirá. En ella usted podrá teclear el nombre de la clase y el valor superior de ésta.
- Use las funciones de edición: agregar item, editar item y borrar item cuando sea necesario para introducir los valores que continuación se presentan:

| Class name | Upper value |
|-------------------|--------------------|
| 0-15 | 15 |
| 15-50 | 50 |
| 50-100 | 100 |
| 100-500 | 500 |
| 500-2000 | 2000 |
| 2000-5000 | 5000 |
| 5000-100000 | 100000 |

- Cierre la ventana cuando haya finalizado.

El siguiente paso es clasificar el mapa de distancia, usando el nuevo dominio creado.



- Haga doble clic en la operación Map Calculation de la lista de operaciones de Ilwis. La ventana de cálculo de mapas se abrirá.
- Escriba la siguiente expresión:

$clfy(Dagric, Dclas)$ (Esto significa clasifica el mapa `Dagric` con el dominio `Dclas`)

- Teclee `Dagric1` para nombrar al nuevo mapa raster. Si lo desea escriba una descripción del mapa. Haga clic en Show.
- Acepte los valores predeterminados de la ventana de Display Options haciendo clic en OK.
- Evalúe el mapa y repita el procedimiento para los mapas `Dgrass`, `Droad` y `Dsettle`.
- Nombre a los nuevos mapas `Dgrass1`, `Droad1` y `Dsettle1`

Una vez finalizada esta operación, los mapas de distancia habrán sido reclasificados en siete clases. El siguiente paso, es asignarle valores de riesgo a cada una de las clases creadas. Cree una tabla con el dominio `Dclas` e indique con índices de riesgo que intervalo de distancia tiene mayor probabilidad de quemarse. Asigne 1 para el riesgo más bajo e incremente la numeración a medida que el riesgo se incrementa.



- Cree una tabla utilizando el dominio `Dclas`. Haga clic con el botón derecho del ratón en el dominio `Dclas` y seleccione la opción `Create table`.
- Escriba `Dclas` en el nombre de la tabla y acepte los valores predeterminados haciendo clic en `OK`. Una nueva ventana se abrirá.
- Seleccione en el menú la opción `Columns, Add Column` (agregar columna).
- Nómbrala a la columna como `Risk Value` y acepte el dominio `Value`. Cambie el intervalo a mínimo = 0 y máximo = 7. También cambie la precisión a 1.0. Haga clic en `OK`.
- Escriba las siguientes índices de riesgo.

| Class name | Risk value |
|-------------------|-------------------|
| 0-15 | 7 |
| 15-50 | 6 |
| 50-100 | 5 |
| 100-500 | 4 |
| 500-2000 | 3 |
| 2000-5000 | 2 |
| 5000-100000 | 1 |

- Cierre la tabla.

Usted ha clasificado los intervalos de distancia en clases de riesgo de ignición. El siguiente paso será crear un mapa de atributos donde las clases de distancia recibirán sus correspondientes valores de riesgo de ignición.



- En el catálogo de `Ilwis` haga clic derecho en el mapa raster `Dagric1`. Seleccione la opción `Raster Operations, Attribute Map`.
- La ventana del mapa de atributos abrirá. Seleccione la tabla `Dclas` y `Attribute Risk value`. Acepte el dominio `Value` (valor), así como el intervalo dado. Escriba `Dagric2` como nombre del nuevo mapa raster y de clic en `Show`.
- Después de que el mapa haya sido calculado, acepte los valores predefinidos de la ventana `Display Options` haciendo clic en `OK`.
- El nuevo mapa raster `Dagric2` se abrirá. Evalúe su contenido y cierre del mapa cuando haya terminado.
- Repita el procedimiento para los mapas `Dgrass1`, `Droad1` y `Dsettle1`.
- Nombre a los nuevos mapas `Dgrass2`, `Droad2` y `Dsettle2`.

En este momento usted ha creado mapas individuales de riesgo para cada fuente de ignición contemplada en éste estudio. A continuación, combine los cuatro mapas de riesgo utilizando pesos. Este procedimiento dará extra significancia a ciertos factores. Dado que la quema de pastizales es la principal causa incendios forestales registrados en Michoacán, asigne al mapa `Dgrass2` un peso mayor multiplicándolo por tres. Asimismo, el uso del fuego en campos agrícolas, es un uso común en el área. Déle un peso de 2 al mapa `Dagric2`. Sume los mapas de distancia a caminos y distancia a localidades

sin peso alguno. La suma de estos mapas resultará en el mapa de riesgo de ignición. Este mapa será reclasificado usando una tabla de atributos.



- De la lista de operaciones de Ilwis, haga doble clic en MapCalculation.
- Escriba la siguiente expresión en la caja de texto:

$$Dsettle2 + Droad2 + (2 * Dagric2) + (3 * Dgrass2)$$

- ¿Piensa que la suma ponderada de factores es necesaria para calcular este mapa?
- Nombre al mapa `Ignrisk` y seleccione el dominio Value. Cambie la precisión a 1.0 y acepte los valores predeterminados. Haga clic en Show.
- Acepte los valores predeterminados de la ventana de Display Options haciendo clic en OK.
- El nuevo mapa raster `Ignrisk` se abrirá. Evalúe el mapa y ciérrelo.

El mapa que usted ha creado contiene información fuera de los límites del área estudio. Use el mapa Polig para redefinir los límites.



- Teclee la siguiente fórmula en la línea de comando de la ventana principal:

$$\text{Ignrisk2} := \text{iff}(\text{isundef}(\text{polig}), ?, \text{Ignrisk})$$

- Presione enter y acepte los valores predeterminados. Haga clic en Show.

Evalúe el nuevo mapa. Los valores son el resultado de la combinación de mapas. Los valores más altos corresponden a un riesgo ignición alto y viceversa. Sin embargo, incluso los cuerpos de agua han obtenido un valor. Dado en los cuerpos de agua y el suelo desnudo nunca sufrirán un incendio, debemos reducir los valores localizados en estas áreas para obtener resultados coherentes.



- De la lista de operaciones de Ilwis haga doble clic en Map Calculation.
- Escriba la siguiente expresión en la caja de texto:

$$\text{iff}(((\text{Lcov} = \text{"Bare soil"}) \text{ or } (\text{Lcov} = \text{"Water_body"}) \text{ or } (\text{Lcov} = \text{"River"})), 0, \text{Ignrisk2})$$

- Nombre al nuevo mapa raster `Ignrisk3` y seleccione el dominio Value. Cambie la precisión a 1.0 y acepte los otros valores predeterminados. Haga clic en Show.
- El nuevo mapa raster `Ignrisk3` se abrirá.

El mapa Ignrisk3 muestra los valores de riesgo ignición para diferentes tipos de coberturas del suelo. Sin embargo, el interés este estudio se reduce únicamente a incendios forestales y no a las frecuentes quemas agrícolas. Por lo tanto se fijará un valor de 2 para los campos agrícolas y los pastizales. De ésta forma los valores más altos de riesgo ignición se distribuirán en las áreas con vegetación natural. Más adelante el valor de 2 identificará a las áreas con campos de cultivo y pastizales y se le asignará a estas áreas el nombre de fuente de ignición.



- Haga doble clic en Map Calculation de la lista de operaciones y teclee la siguiente expresión en la caja de texto:

iff(((Lcov="Agriculture") or (Lcov= "Grassland"))or(Lcov= "Road"))or(Lcov= "Settlements")),2,Ignrisk3)

- Escriba Ignrisk4 como nombre del mapa raster que va a crear. Seleccione el dominio Value y cambie la precisión a 1.0, acepte los otros valores predefinidos. Haga clic en Show.
- Acepte todos valores predefinidos de la ventana de Display Options.
- El mapa raster Ignrisk4 se abrirá.

Ahora que usted ha obtenido los valores finales de riesgo, abra el histograma de valores del mapa y evalúe su distribución. Para clasificar los valores de riesgo del mapa Ignrisk4 en ocho clases de riesgo de ignición cree un nuevo dominio.



- Cree un nuevo dominio haciendo doble clic en la operación New Domain de la lista de operaciones de Ilwis.
- Nombre al nuevo dominio Ignrisk y seleccione la opción Group (grupo). Haga clic en OK.
- Utilice los conocimientos aprendidos. Divida las clases de riesgo en ocho clases. Use la siguiente tabla:

| Class name | Upper value |
|------------------|-------------|
| Sin riesgo | 1 |
| Fuente de riesgo | 9 |
| Mínimo | 11 |
| Bajo | 13 |
| Moderado | 16 |
| Medio | 19 |
| Alto | 22 |
| Máximo | 48 |

- Cierre la tabla.

Los valores de riesgo de ignición han sido clasificados ahora en ocho clases de riesgo. Usted ha dado nombre a las clases de riesgo de ignición. Use el nuevo dominio para clasificar el mapa Ignrisk4, las clases que acaba de crear serán asignadas al mapa.



- Haga doble clic en la operación Mapcalc de la lista operaciones y escriba la siguiente expresión en la caja de texto:

$clfy(Ignrisk4, Ignrisk)$ *(Esto significa clasifica el mapa Ignrisk4 con el dominio Ignrisk)*

- Nombre al nuevo mapa raster Ignition risk. Seleccione el dominio Ignrisk. Haga clic en OK
- Acepte los valores predefinidos de la ventana de Display Options.
- Evalúe el mapa.

El submodelo de Ignición ha sido creado.

8. Modelo estático de riesgo de incendio

El mapa de riesgo incendio estático está compuesto por la suma de los modelos de Combustible, Ignición, Detección y Respuesta. Dicha suma se resume en la ecuación 1. En ésta ecuación se le da mayor peso al combustible, dado que es el elemento más importante para que inicie y se esparza un incendio. En segundo orden de importancia estará el submodelo de ignición, dado que el ser humano es la principal causa de incendios en el estado de Michoacán.

Ecuación 1. Modelo estático de riesgo de incendio

$$\text{Modelo estático de riesgo de incendio} = (3 \times \text{Combustible}) + (2 \times \text{Ignición}) + \text{Respuesta} + \text{Detección}$$



- Escriba en la línea del comando de la ventana principal la fórmula:

$Cstatic:=(3*Fueval)+(2*Ignval)+Detectval+Respval$

- Presione enter y acepte los valores predefinidos, haciendo clic en Show.
- Compare y evalúe los resultados del mapa estático con los mapas de valor de los cuatro submodelos: Fueval, Ignval, Detectval y Respval.
- Cierre los mapas cuando haya terminado.



- A continuación cree un nuevo dominio (Class group) llamado `Cfire`. Utilice la información de la tabla 2. Después cree una representación apropiada seleccionando Edit, Representation.
- Reclasifique el mapa raster `Cstatic` utilizando el dominio `Cfire`. Llame al mapa final `Cstatic2`.

Tabla 2. Categorías de riesgo para el mapa estático de riesgo de incendio

| Límite superior | Nombre de la clase |
|-----------------|--------------------|
| 14 | Mínimo |
| 18 | Bajo |
| 22 | Moderado |
| 26 | Medio |
| 29 | Medio alto |
| 32 | Alto |
| 35 | Muy alto |
| 42 | Máximo |

Evalúe el mapa estático de riesgo incendio forestal y compárelo con los otros cuatro submodelos ¿Dónde se localizan las áreas de alto riesgo de incendio forestal? ¿Está de acuerdo con los resultados obtenidos? ¿Cómo piensa que los resultados de éste modelo se pueden mejorar? Al finalizar este ejercicio usted habrá identificado las áreas de riesgo. Sin embargo, ¿cree usted que la variación en las condiciones climáticas pueden afectar los resultados? Imagine la probabilidad de incendio en diferentes condiciones: clima frío y húmedo y clima cálido y seco.

9. Modelo climático de riesgo de incendio

9.1. Introducción

Dado que las condiciones atmosféricas ideales para un incendio son baja humedad y altas temperaturas [10], las variables consideradas para construir este modelo son temperatura y precipitación. La probabilidad de ignición está fuertemente ligada a la humedad del combustible [86], el cual se puede dividir en dos tipos: combustible vivo y combustible muerto. El combustible muerto consiste principalmente en material orgánico muerto depositado en el suelo. Su nivel de humedad depende principalmente el clima y se considera que entre más seco se encuentre, mayor es la probabilidad de que pueda comenzar un incendio [24,101]. Por otro lado, el combustible vivo (organismos vivos, principalmente plantas) favorece la expansión del fuego más que la ignición [101]. Uno de los principales objetivos de este estudio es identificar las áreas con mayor riesgo para que comience un incendio. Por lo tanto, el modelo climático de riesgo incendio nos podrá dar un información indirecta acerca del nivel de humedad principalmente para el combustible muerto.

El modelo climático de riesgo de incendio considera cambios de temperatura y precipitación en el espacio y tiempo (promedio mensual). Debido a la diferencia altitudinal existen dos tipos de climas

generales en el sitio estudio: subtropical y templado. El modelo se calculó para cada mes del año. Para ello se utilizaron datos de 32 estaciones meteorológicas, de las cuales 13 se localizaron dentro del área de estudio y 19 alrededor de ésta. Los datos de precipitación y temperatura son la media normal mensual registrada entre los años 1977 y 2000.

- **Actividad**

9.2. Mapa de temperatura

En zonas alejadas de grandes cuerpos de agua, la temperatura se puede relacionar con la altitud, pues, a medida que ésta se incrementa, la temperatura disminuye. Para obtener los mapas generales de temperatura, la información de cada una de las estaciones meteorológicas se interpolará usando una regresión lineal entre la temperatura y la altitud de cada mes del año.

- Abra el modelo digital elevación y sobreponga el mapa de puntos de estaciones meteorológicas sobre el modelo digital de elevación. Esto le dará un panorama general de la distribución de las estaciones meteorológicas y las diferencias altitudinales del área de estudio.



- Seleccione el mapa de puntos *Simpst2* en catálogo de la ventana principal de Ilwis y arrástrelo sobre la ventana abierta del mapa raster *Demtotok*.
- La ventana de Display Options se abrirá. De clic en OK.
- El mapa de puntos que contiene las estaciones meteorológicas aparecerá sobre el modelo digital de elevación.

Para crear los mapas de temperatura se obtuvo una regresión lineal para cada mes. Se sustituyó la x por la elevación y la y por la temperatura. Dado que conocemos las diferencias de altitudes en el terreno con el modelo digital de elevación, use las ecuaciones de la tabla 3 y sustituya la x de la ecuación con el modelo digital de elevación para obtener el mapa de temperatura correspondiente a cada mes.



- Escriba la siguiente fórmula en la línea de comando de la ventana principal y presione enter:

$$Tmjan = (-0.007 * dem500) + 26.861$$

- Acepte los valores predeterminados y haga click **Show**.
- Abra el mapa y revise su contenido.

Tabla 3. Regresión lineal simple para obtener los mapas de temperaturas mensuales. $x =$ temperatura, $y =$ elevación

| Mes | Ecuación | R ² |
|------------|-------------------------|----------------|
| Enero | $y = -0.007x + 26.861$ | 0.72 |
| Febrero | $y = -0.0072x + 28.422$ | 0.71 |
| Marzo | $y = -0.0069x + 31.224$ | 0.70 |
| Abril | $y = -0.0063x + 30.945$ | 0.66 |
| Mayo | $y = -0.0056x + 31.224$ | 0.61 |
| Junio | $y = -0.0046x + 29.02$ | 0.48 |
| Julio | $y = -0.005x + 28.327$ | 0.60 |
| Agosto | $y = -0.005x + 28.099$ | 0.60 |
| Septiembre | $y = -0.0051x + 28.177$ | 0.66 |
| Octubre | $y = -0.0059x + 28.505$ | 0.73 |
| Noviembre | $y = -0.0062x + 27.531$ | 0.72 |
| Diciembre | $y = -0.0069x + 27.2$ | 0.74 |

Para crear los mapas de temperatura de los otros meses, puede crear un script. De acuerdo con la guía de usuarios de Ilwis, "un script es una lista de comandos y expresiones. Con ayuda de un script, se puede realizar un análisis de sistema de información geográfica o de percepción remota de manera automática."



- Para crear el script seleccione la opción Create Script del menú File de la ventana principal. El editor del script se abrirá. Escriba las siguientes líneas en la caja de texto:

Rem ILWIS script para calcular los mapas mensuales de temperatura

```

Tjan = (-0.007*Dem500) + 26.861
Tfeb = (-0.0072*Dem500) + 28.422
Tmar = (-0.0069*Dem500) + 31.224
Tapr = (-0.0063*Dem500) + 30.945
Tmay = (-0.0056*Dem500) + 31.224
Tjun = (-0.0046*Dem500) + 29.02
Tjul = (-0.005*Dem500) + 28.327
Taug = (-0.005*Dem500) + 28.099
Tsep = (-0.0051*Dem500) + 28.177
Toct = (-0.0059*Dem500) + 28.505
Tnov = (-0.0062*Dem500) + 27.531
Tdec = (-0.0069*Dem500) + 27.2

```

- Note que la primera línea empieza con REM. Esto indica que esta línea tiene un comentario, el cual no será ejecutado por Ilwis.
- Haga clic en el botón Save (Salvar) y nombre al script Tempmap.
- En la barra de herramientas del editor del script haga clic en el botón Run Script.

Una vez que haya terminado de correr el script, evalúe la distribución de la temperatura en el área de estudio a lo largo del año. Compare el mes más caliente (mayo) con el mes más frío (diciembre).

9.3. Mapa de Precipitación

La construcción del mapa de precipitación es más complicada que la del mapa temperatura, dado que la precipitación tiene mucho más variabilidad en su comportamiento debido a la influencia de otros fenómenos como tormentas tropicales o huracanes [104] [105]. En este caso, se interpolarán los datos de precipitación de las estaciones meteorológicas utilizando el método de *Moving Average of Inverse distance*. Sin embargo, es importante mencionar que este método de interpolación puede estar sujeto a cierto (pero aceptable) grado de error.

- Antes de comenzar el ejercicio, abra la tabla Panu (precipitación anual) y revise los valores de precipitación mensuales. Luego continúe con el ejercicio y cree el mapa de precipitación para el mes de enero.



- Haga clic en la operación Moving Average de la lista de operaciones. La ventana Moving Average de se abrirá.
- Seleccione el mapa de puntos Panualb en la lista de mapa de puntos y presione el símbolo + hasta que los nombres de las columnas aparezcan. Seleccione la columna PPJAN, que contiene los valores de precipitación del mes de enero.
- Escriba PPAN para el nombre del mapa de precipitación que se creará.
- Acepte la opción Inverse Distance as Weight Function. Seleccione Weather como georeferencia.
- Acepte los otros valores predefinidos y haga en el botón Show. Revise el contenido del mapa.

Para crear los mapas de precipitación para los once meses restantes utilice un script.



- En la ventana principal de Ilwis haga clic con el botón derecho del ratón en el mapa raster `PPJAN` y elija `Properties`.
- Haga clic en la pestaña `General` y copie la fórmula se presenta en la sección de `Description`. Esta fórmula es el comando usado para correr la función de promedios móviles.
- Copie la fórmula en un nuevo script y substituya los valores correspondientes a los otros meses, tal y como se muestra continuación.

Rem ILWIS script for calculating month precipitation maps

```
PPFEB=MapMovingAverage(panualb.PPFEB,weather.grf,InvDist(1.000000,37266.000000),plane)
PPMAR=MapMovingAverage(panualb.PPMAR,weather.grf,InvDist(1.000000,37266.000000),plane)
PPAPR=MapMovingAverage(panualb.PPAPR,weather.grf,InvDist(1.000000,37266.000000),plane)
PPMAY=MapMovingAverage(panualb.PPMAY,weather.grf,InvDist(1.000000,37266.000000),plane)
PPJUN=MapMovingAverage(panualb.PPJUN,weather.grf,InvDist(1.000000,37266.000000),plane)
PPJUL=MapMovingAverage(panualb.PPJUL,weather.grf,InvDist(1.000000,37266.000000),plane)
PPAUG=MapMovingAverage(panualb.PPAUG,weather.grf,InvDist(1.000000,37266.000000),plane)
PPSEP=MapMovingAverage(panualb.PPSEP,weather.grf,InvDist(1.000000,37266.000000),plane)
PPOCT=MapMovingAverage(panualb.PPOCT,weather.grf,InvDist(1.000000,37266.000000),plane)
PPNOV=MapMovingAverage(panualb.PPNOV,weather.grf,InvDist(1.000000,37266.000000),plane)
PPDEC=MapMovingAverage(panualb.PPDEC,weather.grf,InvDist(1.000000,37266.000000),plane)
```

- Salve el script con el nombre de `PPmap`, y corrálo de la misma manera que se le indicó para el script de los mapas de temperatura.

Usted ha generado los 12 mapas de precipitación. Evalúe a la distribución de la precipitación y compare el mes más húmedo (agosto) con el mes más seco (abril).

9.4. Índice de riesgo climático

En esta sección se crearán los índices de riesgo de incendio para los factores temperatura y precipitación. Para generar éstos índices los mapas mensuales de temperatura y precipitación serán clasificados homogéneamente de acuerdo a una lógica simple: entre más caliente y seco esté el ambiente, mayor es la probabilidad que hay de riesgo incendio. Las tablas 4 y 5 muestran los índices de riesgo de incendio para los factores temperatura y precipitación, respectivamente. Note que el límite inferior de la precipitación coincide con el inicio de la temporada de secas.

Tabla 4. Índice de riesgo para el factor temperatura

| Temperatura (°C) | Índice |
|------------------|--------|
| 0-13.7 | 1 |
| 13.7-17.1 | 2 |
| 17.1-20.5 | 3 |
| 20.5-23.9 | 4 |
| 23.9-28 | 5 |

Tabla 5. Índice de riesgo para el factor precipitación

| Precipitación (mm) | Índice |
|--------------------|--------|
| 0-24.44 | 10 |
| 24.44-71.56 | 9 |
| 71.56-118.68 | 8 |
| 118.68-165.79 | 7 |
| 165.79-212.91 | 6 |
| 212.91-260.03 | 5 |
| 260.03-307.15 | 4 |
| 307.15-354.26 | 3 |
| 354.26-401.38 | 2 |
| 401.38-450 | 1 |

Para obtener el mapa climatológico de riesgo de incendio, los mapas de los índices de riesgo para los factores de temperatura y precipitación se sumarán.

9.5. Mapa índice de riesgo para el factor temperatura



- Para clasificar los mapas de precipitación, un nuevo dominio debe ser creado.
- En la lista operaciones de Ilwis, haga doble clic en la operación New domain.
- Nombre al nuevo dominio *Trisk* y seleccione la opción Group. Haga clic en OK. Se abrirá una nueva ventana.
- Teclee los siguientes datos usando los comando Add item, Edit item y Delete item:

| Class name | Upper value |
|------------|-------------|
| 1 | 13.7 |
| 2 | 17.1 |
| 3 | 20.5 |
| 4 | 23.9 |
| 5 | 28 |

- Cuando haya terminado cierre la ventana.

Use el nuevo dominio para clasificar los mapas de temperatura. El mapa será dividido en clases de riesgo.



- Haga doble clic en Map calculation de la lista operaciones de Ilwis. La ventana de Map Calculation se abrirá.
- Teclee la siguiente expresión en la caja de texto:

$clfy(TJAN, Trisk)$ *(Esto significa clasifica el mapa TJAN con el dominio Trisk)*

- Nombre al nuevo mapa raster `TJAN1` y seleccione el dominio recién creado `Trisk`.
- Haga clic en o clic Show y evalúe el mapa.

Para continuar con el ejercicio se debe transformar el dominio `Trisk` en un dominio `Value`. Este cambio, permitirá realizar algunas operaciones matemáticas más adelante.



- Use los conocimientos que tiene y cree una nueva tabla llamada `Trisk` usando el dominio `Trisk`.
- Agregue una nueva columna con dominio `value`. Nombre la `Risk value` y cambie la precisión a 1.0
- Teclee los valores de riesgo que aparecen a continuación:

| Class name | Risk value |
|------------|------------|
| 1 | 1 |
| 2 | 2 |
| 3 | 3 |
| 4 | 4 |
| 5 | 5 |

- Cuando haya terminado cierre la tabla.

El siguiente paso será crear un mapa de atributos donde las clases de riesgo obtengan sus valores correspondientes.



- En el catálogo de Ilwis haga clic con el botón derecho del ratón sobre el mapa `TJAN1`. Seleccione la opción `Raster Operations, Attribute Map`.
- La ventana del mapa de atributos se abrirá. Seleccione la tabla `Trisk` y el atributo `Risk Value`. Escriba `TJAN2` en el nombre del mapa. Haga clic en `Show`.
- La ventana de `Display options` se abrirá. De clic en `OK`.
- Evalúe el contenido del mapa `TJAN2` y cierre el mapa cuando haya terminado.

Cree un script para elaborar los mapas de riesgo para el factor temperatura del resto de los meses.



- Utilice los conocimientos aprendidos para crear un nuevo un script. Use las siguientes fórmulas:

Rem ILWIS script for calculating a temperature risk map

```
TFeb1.mpr{dom=Trisk.dom} = clfy(TFEB,Trisk)
TMar1.mpr{dom=Trisk.dom} = clfy(TMAR,Trisk)
TApr1.mpr{dom=Trisk.dom} = clfy(TAPR,Trisk)
TMay1.mpr{dom=Trisk.dom} = clfy(TMAY,Trisk)
TJun1.mpr{dom=Trisk.dom} = clfy(TJUN,Trisk)
TJul1.mpr{dom=Trisk.dom} = clfy(TJUL,Trisk)
TAug1.mpr{dom=Trisk.dom} = clfy(TAUG,Trisk)
TSep1.mpr{dom=Trisk.dom} = clfy(TSEP,Trisk)
TOct1.mpr{dom=Trisk.dom} = clfy(TOCT,Trisk)
TNov1.mpr{dom=Trisk.dom} = clfy(TNOV,Trisk)
TDec1.mpr{dom=Trisk.dom} = clfy(TDEC,Trisk)
```

```
Tfeb2.mpr{dom=value;vr=-1000000:1000000} = MapAttribute(TFEB1,Trisk.tbt.'Risk value')
Tmar2.mpr{dom=value;vr=-1000000:1000000} = MapAttribute(TMAR1,Trisk.tbt.'Risk value')
Tapr2.mpr{dom=value;vr=-1000000:1000000} = MapAttribute(TAPR1,Trisk.tbt.'Risk value')
Tmay2.mpr{dom=value;vr=-1000000:1000000} = MapAttribute(TMAY1,Trisk.tbt.'Risk value')
Tjun2.mpr{dom=value;vr=-1000000:1000000} = MapAttribute(TJUN1,Trisk.tbt.'Risk value')
Tjul2.mpr{dom=value;vr=-1000000:1000000} = MapAttribute(TJUL1,Trisk.tbt.'Risk value')
Taug2.mpr{dom=value;vr=-1000000:1000000} = MapAttribute(TAUG1,Trisk.tbt.'Risk value')
Tsep2.mpr{dom=value;vr=-1000000:1000000} = MapAttribute(TSEP1,Trisk.tbt.'Risk value')
Toct2.mpr{dom=value;vr=-1000000:1000000} = MapAttribute(TOCT1,Trisk.tbt.'Risk value')
Tnov2.mpr{dom=value;vr=-1000000:1000000} = MapAttribute(TNOV1,Trisk.tbt.'Risk value')
Tdec2.mpr{dom=value;vr=-1000000:1000000} = MapAttribute(TDEC1,Trisk.tbt.'Risk value')
```

- Guarde el script y nombre lo `Trisk`.
- Córralo y revise el contenido de los mapas.

9.6. Mapa índice de riesgo para el factor precipitación

Para clasificar los mapas de precipitación, se creara un nuevo dominio.



- En la lista de operaciones de Ilwis, seleccione New Domain. La ventana de New Domain se abrirá.
- Nombre al nuevo dominio PPrisk y seleccione la opción Group. Haga clic en OK.
- Una nueva ventana se abrirá. Teclee las siguientes clases y sus límites superiores:

| Class name | Upper value |
|------------|-------------|
| 10 | 24.44 |
| 9 | 71.56 |
| 8 | 118.68 |
| 7 | 165.79 |
| 6 | 212.91 |
| 5 | 260.03 |
| 4 | 307.15 |
| 3 | 354.26 |
| 2 | 401.38 |
| 1 | 450 |

- Cierre la ventana cuando haya terminado.

Use el nuevo dominio para clasificar los mapas de precipitación. Después, reclasifique el mapa de precipitación en un mapa de índice de riesgo por precipitación.



- Haga doble clic en Map calculation de la lista de operaciones de Ilwis y teclee la siguiente expresión en la caja de texto:

clfy(PPJAN,PPrisk)

(Esto significa clasifica el mapa PPJAN con el dominio PPrisk)

- Nombre al nuevo mapa PPJAN1. Seleccione el dominio PPrisk y de clic en Show.
- Acepte todos los valores predefinidos de la ventana Display Options.
- Revise el nuevo mapa.

Para continuar con el ejercicio transforme el dominio recién creado en un dominio Value. Repita los pasos que llevó a cabo para el índice de riesgo del factor temperatura.



- Use los conocimientos que tiene y cree una nueva tabla llamada `PPrisk` usando el dominio `PPrisk`.
- Agregue una nueva columna llamada `Risk value` y seleccione el dominio `value`. Cambie la precisión a 1.0
- Teclee los valores de riesgo que aparecen a continuación:

| Class name | Risk value |
|-------------------|--------------------|
| Class name | Upper value |
| 10 | 10 |
| 9 | 9 |
| 8 | 8 |
| 7 | 7 |
| 6 | 6 |
| 5 | 5 |
| 4 | 4 |
| 3 | 3 |
| 2 | 2 |
| 1 | 1 |

- Cuando haya terminado cierre la tabla.

El siguiente paso será crear un mapa de atributos, en donde las clases de riesgo recibirán sus valores numéricos correspondientes.



- En el catálogo de Ilwis haga clic con el botón derecho del ratón sobre el mapa raster `PPJAN1` y seleccione la opción `Raster Operations, Attribute Map`.
- La ventana del mapa de atributos se abrirá. Seleccione la tabla `PPrisk`, el atributo `Risk Value` y acepte el dominio `Value`. Nombre al nuevo mapa raster `PPJAN2`.
- Acepte todos los valores predefinidos y haga clic en `Show`.
- El nuevo mapa raster se abrirá. Revise su contenido y ciérrelo con haya terminado.

A continuación cree un script para los siguientes once meses del año.



- Utilice los conocimientos aprendidos para crear un nuevo un script. Use las siguientes fórmulas:

Rem ILWIS script for calculating a precipitation risk map

```
PPFeb1.mpr{dom=PPrisk.dom} = clfy(PPFEB,PPrisk)
PPMar1.mpr{dom=PPrisk.dom} = clfy(PPMAR,PPrisk)
PPApr1.mpr{dom=PPrisk.dom} = clfy(PPAPR,PPrisk)
PPMay1.mpr{dom=PPrisk.dom} = clfy(PPMAY,PPrisk)
PPJun1.mpr{dom=PPrisk.dom} = clfy(PPJUN,PPrisk)
PPJul1.mpr{dom=PPrisk.dom} = clfy(PPJUL,PPrisk)
PPAug1.mpr{dom=PPrisk.dom} = clfy(PPAUG,PPrisk)
PPSep1.mpr{dom=PPrisk.dom} = clfy(PPSEP,PPrisk)
PPOct1.mpr{dom=PPrisk.dom} = clfy(PPOCT,PPrisk)
PPNov1.mpr{dom=PPrisk.dom} = clfy(PPNOV,PPrisk)
PPDec1.mpr{dom=PPrisk.dom} = clfy(PPDEC,PPrisk)
```

```
PPFeb2.mpr{dom=value;vr=-10000000:10000000} = MapAttribute(PPFeb1,PPrisk.tbt.'Risk value')
PPMar2.mpr{dom=value;vr=-10000000:10000000} = MapAttribute(PPMar1,PPrisk.tbt.'Risk value')
PPApr2.mpr{dom=value;vr=-10000000:10000000} = MapAttribute(PPApr1,PPrisk.tbt.'Risk value')
PPMay2.mpr{dom=value;vr=-10000000:10000000} = MapAttribute(PPMay1,PPrisk.tbt.'Risk value')
PPJun2.mpr{dom=value;vr=-10000000:10000000} = MapAttribute(PPJun1,PPrisk.tbt.'Risk value')
PPJul2.mpr{dom=value;vr=-10000000:10000000} = MapAttribute(PPJul1,PPrisk.tbt.'Risk value')
PPAug2.mpr{dom=value;vr=-10000000:10000000} = MapAttribute(PPAug1,PPrisk.tbt.'Risk value')
PPSep2.mpr{dom=value;vr=-10000000:10000000} = MapAttribute(PPSep1,PPrisk.tbt.'Risk value')
PPOct2.mpr{dom=value;vr=-10000000:10000000} = MapAttribute(PPOct1,PPrisk.tbt.'Risk value')
PPNov2.mpr{dom=value;vr=-10000000:10000000} = MapAttribute(PPNov1,PPrisk.tbt.'Risk value')
PPDec2.mpr{dom=value;vr=-10000000:10000000} = MapAttribute(PPDec1,PPrisk.tbt.'Risk value')
```

- Guarde el script y nombre lo PPrisk.
- Córralo y revise el contenido de los mapas.

9.7. Mapa índice de riesgo climatológico de incendio

Para obtener el mapa índice de riesgo climatológico incendio sume los mapas de índice de riesgo para los factores de temperatura y precipitación.



- Utilice los conocimientos aprendidos para crear un nuevo un script. Use las siguientes fórmulas.

Rem ILWIS script for calculating a weather risk map

$WJan = TJan2 + PPJan2$
 $WFeb = TFeb2 + PPFeb2$
 $WMar = TMar2 + PPMar2$
 $WApr = TApr2 + PPApr2$
 $WMay = TMay2 + PPMay2$
 $WJun = TJun2 + PPJun2$
 $WJul = TJul2 + PPJul2$
 $WAug = TAug2 + PPAug2$
 $WSep = TSep2 + PPSep2$
 $WOct = TOct2 + PPOct2$
 $WNov = TNov2 + PPNov2$
 $WDec = TDec2 + PPDec2$

- Guarde el script y nómbrelo `Wrisk`.
- Corra el script y revise el contenido de los mapas.

Usted ha creado los mapas de índice de riesgo climatológico de incendio para los 12 meses del año.

9.8. Modelo climatológico de riesgo de incendio

El paso final para crear el modelo de riesgo climatológico de incendio es sumar el mapa de índice de riesgo climatológico de cada mes con el mapa de riesgo estático. De esta forma el modelo incluirá los factores más importantes relacionados con los incendios forestales. Estos factores son la topografía (pendiente, orientación y elevación), el combustible (tipos de vegetación), el ser humano (factores y ignición) y el clima (temperatura y precipitación).

Debido a que los mapas de precipitación y temperatura usaron un tamaño de pixel mayor (500 m) que el resto de los submodelos (15 m). Para sumar ambos modelos, será necesario establecer la misma resolución. Para no perder la información generada en los submodelos con mayor resolución, escoja la georreferencia FinalA.



- Haga doble clic en Resample de la lista operaciones. La ventana de Resample se abrirá.
- Seleccione el mapa WJAN y la georeferencia FinalA. Asegúrese de que la opción Nearest Neighbour este seleccionada.
- Nombre al mapa WIJAN y haga clic en Show.
- El mapa WIJAN ahora tendrá el mismo tamaño de píxel y número de filas y columna que el mapa raster del modelo digital elevación Demok.

A continuación cree un script llamado Wrisk para cambiar el tamaño de píxel los mapas de los once meses restantes.



- Utilice los conocimientos aprendidos para crear un nuevo un script. Use las siguientes fórmulas:

Rem ILWIS script for resampling map

```
W1Feb.mpr{dom=value.dom;vr=10:12} = MapResample(Wfeb,finala.grf,nearest)
W1Mar.mpr{dom=value.dom;vr=10:12} = MapResample(Wmar,finala.grf,nearest)
W1Apr.mpr{dom=value.dom;vr=10:12} = MapResample(Wapr,finala.grf,nearest)
W1May.mpr{dom=value.dom;vr=10:12} = MapResample(Wmay,finala.grf,nearest)
W1Jun.mpr{dom=value.dom;vr=10:12} = MapResample(Wjun,finala.grf,nearest)
W1Jul.mpr{dom=value.dom;vr=10:12} = MapResample(Wjul,finala.grf,nearest)
W1Aug.mpr{dom=value.dom;vr=10:12} = MapResample(Waug,finala.grf,nearest)
W1Sep.mpr{dom=value.dom;vr=10:12} = MapResample(Wsep,finala.grf,nearest)
W1Oct.mpr{dom=value.dom;vr=10:12} = MapResample(Woct,finala.grf,nearest)
W1Nov.mpr{dom=value.dom;vr=10:12} = MapResample(Wnov,finala.grf,nearest)
W1Dec.mpr{dom=value.dom;vr=10:12} = MapResample(Wdec,finala.grf,nearest)
```

- Guarde el script y nómbrelo Wrisk2.
- Córralo y revise el contenido de los mapas.

Ahora que los modelos estático y climático de riesgo de incendio tienen la misma resolución y pueden sumarse. Cree un nuevo script.



- Utilice los conocimientos aprendidos para crear un nuevo un script. Use las siguientes fórmulas:

Rem ILWIS script for calculating a weather risk map

$$W2Jan = Cstatic + (2 * W1Jan)$$

$$W2Feb = Cstatic + (2 * W1Feb)$$

$$W2Mar = Cstatic + (2 * W1Mar)$$

$$W2Apr = Cstatic + (2 * W1Apr)$$

$$W2May = Cstatic + (2 * W1May)$$

$$W2Jun = Cstatic + (2 * W1Jun)$$

$$W2Jul = Cstatic + (2 * W1Jul)$$

$$W2Aug = Cstatic + (2 * W1Aug)$$

$$W2Sep = Cstatic + (2 * W1Sep)$$

$$W2Oct = Cstatic + (2 * W1Oct)$$

$$W2Nov = Cstatic + (2 * W1Nov)$$

$$W2Dec = Cstatic + (2 * W1Dec)$$

- Guarde el script y nómbrelo `Wrisk3`.
- Córralo y revise el contenido de los mapas.

Reclasifique los mapas en ocho categorías de riesgo de mínimo a máximo.



- Cree un nuevo dominio llamado `CStWe` (**Class group**) con la información mostrada en la tabla 6. Después cree una representación apropiada, seleccionando Edit, Representation.
- Reclasifique los mapas raster `WJan2`, `WFeb2...WDec2` utilizando el dominio `CStWe`. Nombre a los nuevos mapas `WJan3`, `WFeb3...WDec3`.
- Cree un script si lo cree necesario.

Tabla 6. Categorías del modelo climático de riesgo de incendio

| Intervalo de valores | Categoría de riesgo |
|----------------------|---------------------|
| 0 – 34 | Mínimo |
| 34 – 42 | Bajo |
| 42 – 46 | Moderado |
| 46 – 49 | Medio |
| 49 – 54 | Medio alto |
| 54 – 59 | Alto |
| 59 – 62 | Muy alto |
| 62 – 70 | Máximo |

¡Felicidades! Usted acaba de crear un modelo multitemporal de riesgo incendio para el área de estudio. Sin embargo ahora necesita saber si su clasificación es correcta. Piense cómo podría validar los resultados de estos modelos.

10. Validación

En esta sección aprenderá como validar los modelos. Para ello, cruce del mapa de áreas quemadas con el mapa estático de riesgo de incendio. De esta forma, sabrá si las escamas de incendio coinciden con las categorías de alto riesgo del submodelo. Esta es una forma de saber si su modelo está funcionando bien. Sin embargo, existen otras técnicas que puede usar para soportar sus resultados (p.e. Análisis ROC).



- Sobrelape los mapas `BurntA` y `Cstatic2` y compárelos.
- Haga clic en la opción Raster Operations de la lista de operaciones de Ilwis y seleccione la operación Cross. Una nueva ventana se abrirá.
- Seleccione el mapa `BurntA` y el mapa `Cstatic 2`.
- Nombre a la tabla `Statval` y de clic en Show.
- Revise los contenidos de la tabla.



- Si desea convertir estos resultados en gráficos, haga clic con el botón derecho del ratón sobre la tabla `Valstat` del el catálogo de Ilwis y seleccione Create a Graph.
- Una nueva ventana se abrirá. Seleccione en el eje de las x a la columna `Cstatic2` y en el eje de las y a la columna Área. Haga Clic en OK.

Evalúe las tablas y gráficas que creó. ¿En que categorías de riesgo se encuentran mayormente distribuidas las áreas quemadas? ¿Se puede usar este modelo para ayudar a realizar planes de prevención de incendios?

11. Lo que usted ha aprendido

Usted ha finalizado el ejercicio modelando el riesgo de incendio forestal para una zona crítica en Michoacán, México. A lo largo de este ejercicio usted ha aprendido:

- A identificar y a mapear las áreas quemadas, combinando las bandas espectrales de una imagen ASTER.
 - A evaluar los factores que influyen los incendios forestales, utilizando un mapa de escamas de incendio.
 - A desarrollar un submodelo de ignición.
 - A desarrollar un modelo de riesgo de incendio estático.
 - A desarrollar un modelo climatológico de riesgo de incendio.
 - A identificar apropiadamente las áreas de alto, medio y bajo riesgo en los modelos estático y climático de riesgo incendio forestal.
-

- A reconocer los cambios en la distribución del riesgo incendio forestal a lo largo del año.
- A validar el modelo de riesgo y
- A utilizar y Ilwis para desarrollar éste modelo

Finalmente, cabe mencionar que este tipo de modelos siempre puede ser mejorado. ¿Tienen en mente que otros factores pueden ser incluidos en el modelo de riesgo incendio? Escriba y justifique cuáles son esos factores. Después escriba un párrafo corto describiendo como las autoridades locales pueden usar estos mapas para prevenir incendios y mejorar las acciones en contra de éstos.

References

- 1 Pyne, S., Andrews, P. L., & Laven, R. D. (1996). *Introduction to wildland fire*. New York: John Wiley & Sons.
 - 2 Bachmann, A., & Allgöwer, B. (2000). *The need for a consistent wildfire risk terminology*. Paper presented at the Proceedings of the Joint Fire Science Conference and Workshop: "Crossing the Millennium: Integrating Spatial Technologies and Ecological Principles for a New Age in Fire Management", Boise, ID.
 - 3 Grimm, E. C. (1984). Fire and other factors controlling the big woods vegetation of Minnesota in the mid-nineteenth century. *Ecological Monographs*, **54**: 291-311.
 - 4 Whelan, R. J. (1995). *The ecology of fire*. Cambridge: Cambridge University Press.
 - 5 Catchpole, W. (2002). Fire properties and burn patterns in heterogeneous landscapes. In R. A. Bradstock, J. E. Williams & A. M. Gill (Eds.), *Flammable Australia. The fire regimes and biodiversity of a continent* (pp. 46-75). Cambridge: Cambridge University Press.
 - 6 DeBano, L. F., D. G. Neary, & Ffolliott, P. F. (1998). *Fire's effects on ecosystems*. New York: John y Wiley y Sons.
 - 7 Uhl, C., & Kaffman, J. B. (1990). Deforestation, fire susceptibility and potencial tree responses to fire in the eastern Amazon. *Ecology*, **71**: 437-449
 - 8 Alexander, M. E. (1982). Calculating and interpreting forest fire intensities. *Canadian Journal of Botany* **60**: 349-357.
 - 9 Böhme, G., & Böhme, H. (1996). *Fuego, agua, tierra y aire: Una historia cultural de los elementos* (ed. Herder). Barcelona.
 - 10 Martínez, J., & Martín, P. (2004). El factor humano en los incendios forestales: Análisis de factores socio-económicos relacionados con la incidencia de incendios forestales en España. In E. Chuvieco & M. Martín (Eds.), *Nuevas Tecnologías para la estimación del riesgo de incendios forestales* (pp. 101-141). Madrid: Consejo Superior de Investigaciones Científicas.
 - 11 CONAFOR. (2007). Retrieved 12/06/2007, from www.conafor.gob.mx
 - 12 FAO. (2007). *Fire management- Global assessment 2006. FAO forestry paper No. 151*. Rome.
 - 13 González-Jácome, A., & del_Amo, S. (1999). *Agricultura y Sociedad en México: Diversidad, enfoques, estudios de caso*. Mexico city: Universidad Iberoamericana and Plaza y Valdés S. A. de C. V.
 - 14 COFOM. (2006). *Incendios forestales. Guia práctica para comunicadores*. Zapopan, Mexico.
 - 15 Bond, W. J., & Wilgen, B. W. V. (1996). *Fire and Plants* (Population and community biology series 14). London: Chapman & Hall.
 - 16 Jhonson, E. (1996). *Fire and Vegetation Dynamics: Studies from the North American Boreal Forest*: Cambridge University Press.
 - 17 COFOM. (2007). Incendios Forestales: Gobierno_del_estado_de_Michoacan.
 - 18 Shay, J., Kunec, D., & Dyck, B. (2001). Short term effects of fire frequency on vegetation composition and biomass in mixed prairie in south western Manitoba. *Plant Ecology*, **155**: 157-167.
 - 19 Ellingson, L. J., Kauffman, J. B., Cummings, D. L., Sanford, R. L., & Jaramillo, V. J. (2000). Soil N dynamics associated with deforestation, biomass burning and pasture conversion in a Mexican tropical dry forest. *Forest Ecology and Management*, **197**: 41-51.
 - 20 Wright, H. A., & Bailey, A. W. (1982.). *Fire ecology: United States and Southern Canada*. New York Wiley-Interscience.
 - 21 Mallik, A. U. (1986). Near-ground micro-climate of burned and unburned Calluna heathland. *Journal of Environmental Management*, **23**: 157-171.
-

- 22 Schwilk, D. W., Keeley, J. E., & Bond, W. J. (1997). The intermediate disturbance hypothesis
does not explain fire and diversity pattern in fynbos. *Plant Ecology*, **132**: 77-84.
- 23 Collins, S. L. (1992). Fire frequency and community heterogeneity in tallgrass prairie
vegetation. *Ecology* **73**: 2001-2006.
- 24 Roy, P. S. (2004). Forest fire and degradation assessment using satellite remote sensing and
geographic information system. In M. V. K. Sivakumar, P. S. Roy, K. Harmesen & S. K. Saha
(Eds.), *Satellite Remote Sensing and GIS applications in Agricultural Meteorology* (pp. 361-
400). Geneva, Switzerland: World Meteorological Organization.
- 25 Hardy, C. (2005). Wildland fire hazard and risk: Problems, definitions, and context. *Forest
Ecology and Management*, **211**: 73-82.
- 26 van_Westen, C. J. (1997). Hazard, vulnerability and risk analysis. In C. J. van_Westen, A.
Saldaña, P. Uría & G. Chávez (Eds.), *ILWIS 2.1 Applications Guide* (pp. 1-18). Enschede, The
Netherlands: ITC.
- 27 FAO. (2006). *Fire management: voluntary guidelines. Principles and strategic actions*.
Rome, Italy.
- 28 Lentile, L. B., Holden, Z. A., Smith, A. M. S., Falkowski, M. J., Hudak, A. T., Morgan, P.,
Lewis, S. L., Gessler, P. E., & Benson, N. C. (2006). Remote sensing techniques to assess
active fire characteristics and post-fire effects. *International Journal of Wildland Fire*, **15**:
319-345.
- 29 Chuvieco, E., & Congalton, R. G. (1989). A simple method for fire growth mapping using
AVHRR channel 3 data. *Remote Sensing of Environment*, **29**(2): 147-159.
- 30 Sunar, F., & Özkan, C. (2001). Forest fire analysis with remote sensing data. *International
Journal of Remote Sensing*, **22**(12): 2265-2277.
- 31 Chuvieco, E., & Salas, J. (1996). Mapping the spatial distribution of forest fire danger using
GIS. *International Journal of Geographical Information Science*, **10**(3): 333-345.
- 32 Justice, C. O., & Korontzi, S. (2001). A review of the status of satellite fire monitoring and
the requirements for global environmental change research. In F. J. Ahern, J. G. Goldammer
& C. O. Justice (Eds.), *Prospective sensors for space-borne fire observation*. The Hague, The
Netherlands: Kugler Publications.
- 33 Oertel, D., Briess, D., Roeser, H. P., Jahn, H., Zhukov, B., Lanzl, F., Haschberger, P.,
Gonzalo, J., Tourne, I. F., & Gutman, G. (2001). Prospective sensors for space-borne fire
observation. In F. J. Ahern, J. G. Goldammer & C. O. Justice (Eds.), *Global and Regional
Vegetation Fire Monitoring from Space*: (pp. 171-198). The Hague, The Netherlands: Kugler
Publications.
- 34 Zhukov, B., Lorenz, E., Oertel, D., Wooster, M., & Roberts, G. (2006). Spaceborne detection
and characterization of fires during the bi-spectral infrared detection (BIRD) experimental
small satellite mission (2001-2004). *Remote Sensing of Environment*, **100**: 29-51.
- 35 Roy, D. P., Jin, Y., Lewis, P. E., & Justice, C. O. (2005). Prototyping a global algorithm for
systematic fire affected area mapping using MODIS time series data. *Remote Sensing of
Environment*, **97**: 137-162.
- 36 Li, Z., NADON, S., CIHLAR, J., & STOCKS, B. (2000). Satellite-based mapping of
Canadian boreal forest fires: evaluation and comparison of algorithms. *International Journal
of Remote Sensing*, **21**(16): 3071-3082.
- 37 Murthy, M. S. R., Badarinath, K. V. S., Gharai, B., & Rajashekar, G. (2006). *Perspectives of
Geoinformatics in Forest Fire Management. Indian forest fire response and assessment
system*: National Remote Sensing Agency.
- 38 Fraser, R. H., Li, Z., & Cihlar, J. (2000). Hotspot and NDVI differencing synergy (HANDS):
A new technique for burned area mapping over boreal forest. *Remote Sensing of Environment*
74: 362-376.
- 39 Tracy, B. F., & McNaughton, S. J. (1997). Elk grazing and vegetation responses following a
late season fire in Yellowstone National Park. *Plant Ecology*, **130**: 111-119.
-

- 40 Sunuprpto, H. (2000). *Forest fire monitoring and damage assessment using remotely sensed data and geographical information systems (A case study in South Sumatra Indonesia)*. ITC, Enschede.
- 41 Domenikiotis, C., Dalezios, N. R., Loukas, A., & Karteris, M. (2002). Agreement assessment of NOAA/AVHRR NDVI with Landsat TM NDVI form mapping burned forested areas. *International Journal of Remote Sensing*, **23**(20): 4235-4246.
- 42 Chuvieco, E., Martin, M. P., & Palacios, A. (2002). Assessment fo different spectral indices in the red-near-infrared spectral domain for burned land discrimination. *International Journal of Remote Sensing*, **23**(23): 5103-5110.
- 43 Holben, B. N. (1986). Characteristics of maximum/value composite images from temporal AVHRR data. *International Journal of Remote Sensing*, **7**: 1417-1434.
- 44 Sunee, S., Hussin, Y. A., & de Gier, A. (2001, 5-9 November). *Assessment of forest recovery after fire using Landsat TM images and GIS techniques : a case study of Mae Wong national park, Thailand*. Paper presented at the ACRS Proceedings of the 22nd Asian Conference on Remote Sensing ACRS, Singapore.
- 45 Barbosa, P., Cardoso-Pereira, J. M., & Grégoire, J. M. (1998). Compositing Criteria for Burned Area Assessment Using Multitemporal Low Resolution Satellite Data. *Remote Sensing of Environment*, **65**(1): 38-49.
- 46 Chuvieco, E., Ventura, G., Martín, M. P., & Gómez, I. (2005). Assessment of multipemporal compositing techniques of MODIS and AVHRR images for burned land mapping. *Remote Sensing of Environment*, **94**: 450-462.
- 47 Salas, F. J., & Chuvieco, E. (1994). G.I.S. applications to forest fire risk mapping. *Wildfire*, **3**: 7-13.
- 48 Rathaur, S., Kushwaha, S. P. S., & Hussin, Y. A. (2006). *Fire risk assessment for tiger preybase in Chilla range and vicinity, Rajaji national park, India using remote sensing and GIS*. Paper presented at the ACRS Proceedings of the 27th Asian conference on remote sensing ACRS, 9-13 October, 2006 Ulanbaatar, Mongolia. Bangkok : Asian Association of Remote Sensing (AARS).
- 49 Neeraj, S., & Hussin, Y. A. (1996). Spatial modelling for forest fire hazard prediction, management and control in Corbett national park, India. In J. Saramaki, B. Koch & H. G.Lund (Eds.), *Remote sensing and computer technology for natural resources assessment* (pp. 185-192). University of Joensuu.
- 50 Maselli, F., Rodolfi, A., Bottai, L., Romanelli, S., & Conese, C. (2000). Classification of Mediterranean vegetation by TM and ancillary data for the evaluation of fire risk. *International Journal of Remote Sensing*, **21**(17): 3303-3313.
- 51 Chen, K., Blong, R., & Jacobson, C. (2001). MCE-RISK: integrating multicriteria evaluation and GIS for risk decision-making in natural hazards. *Environmental Modelling & Software*, **16**: 387-397.
- 52 Chuvieco, E., & Salas, J. (2004). Métodos para la integración de variables de riesgo: el papel de los sistemas de información geográfica. In E. Chuvieco & M. Martín (Eds.), *Nuevas tecnologías para la estimación del reisco de incendios forestales*. Madrid: Consejo Superior de Investigaciones científicas.
- 53 Hernandez-Leal, P. A., Arbelo, M., & Gonzalez-Calvo, A. (2006). Fire risk assessment using satellite data. *Advances in Space Research*, **37**: 741-746.
- 54 Lozano, F. J., Suarez-Seoane, S., & de Luis, E. (2007). Assessment of several spectral indices derived from multi-temporal Landsat data for fire occurrence probability modelling. *Remote Sensing of Environment*, **107**: 533-544.
- 55 Rowell, A., & Moore, P. F. (2000). *Global review of forest fires*. Gland, Switzerland: WWF and IUCN.
- 56 Jiménez, R., I. Cruz, M. Schmidt, R. Ressler, & López, G. (2004). Detección temprana de incendios. *Biodiversitas*, **52**: 1-15.
- 57 COFOM. (2007). Retrieved 12/06/2007, 2007, from <http://cofom.michoacan.gob.mx/mision.htm>
-

- 58 SEMARNAT-CONAFOR. (2007). *Prioridades en 2007 del Programa Nacional de Protección contra Incendios Forestales: fortalecer las acciones de prevención, detectar con oportunidad la presencia de incendios, disminuir la superficie afectada y garantizar la seguridad de combatientes y pobladores de zonas forestales*. Paper presented at the Primera reunión de trabajo el Grupo Intersecretarial para la Protección contra Incendios Forestales, Zapopan, México.
- 59 Sánchez, O. C. (1999). Incendios Forestales en México. In H. S. Fragoso, M. S. Massieu, H. C. Rodarte-Ramon & F. J. Garfias_y_Ayala (Eds.), *Incendios forestales y agropecuarios: prevención e impacto y restauración de los ecosistemas*: Universidad Nacional Autónoma de México, Secretaría de Medio Ambiente, Recursos Naturales y Pesca, Instituto Politécnico Nacional.
- 60 Manzo-Delgado, L., Aguirre-Gómez, R., & Álvarez, R. (2004). Multitemporal analysis of land surface temperature using NOAA-AVHRR: preliminary relationships between climatic anomalies and forest fires. *International Journal of Remote Sensing*, **25**(20): 4417-4423.
- 61 Rodríguez-Trejo, D. A. (1996). *Incendios forestales*. Mexico: Universidad Autónoma de Chapingo, Mundi Pesa.
- 62 CDI. (2007). Campaña Nacional de Control de Incendios Forestales. Retrieved 2007, from http://cdi.gob.mx/index.php?id_seccion=685
- 63 CONAFOR. (2007). México y Estados Unidos firman un memorandum de entendimiento para fortalecer la cooperación en materia forestal [Electronic Version]. *México Forestal* from <http://www.mexicoforestal.gob.mx/nota.php?id=173>.
- 64 COFOM. (2007). *Reporte del Departamento de Combate de Incendios Forestales*. Morelia: COFOM.
- 65 Salas, J., & Cocero, D. (2004). El concepto de peligro de incendio. Sistemas actuales de estimación del peligro. In E. Chuvieco & P. Martín (Eds.), *Nuevas tecnologías para la estimación del riesgo de incendios forestales*. Madrid: Consejo Superior de Investigaciones Científicas.
- 66 Galindo, I., & Barrón, J. (2003). *Índice de riesgos forestales de la República Mexicana*. Retrieved from.
- 67 Villers-Ruiz, L., & Lopez-Blanco, J. (2004). Comportamiento del fuego y evaluación del riesgo por incendios en las áreas forestales de México: un estudio en el volcán La Malinche. In L. Villers-Ruiz & J. Lopez-Blanco (Eds.), *Incendios forestales de México: Métodos de evaluación* (1 ed., pp. 61-78). Mexico city: UNAM.
- 68 Miranda-Salazar, R. (2004). Determinación de las áreas de riesgos a incendios forestales del parque ecológico Chipinque, Nuevo León. In L. Villers-Ruiz & J. Lopez-Blanco (Eds.), *Incendios forestales de México: Métodos de evaluación* (pp. 99-106). Mexico city: UNAM.
- 69 Ceballos, G., Rodríguez, P., & Medellín, R. A. (1998). Assessing Conservation Priorities in Megadiverse Mexico: Mammalian Diversity, Endemicity, and Endangerment. *Ecological Applications*, **8**(1): 8-17.
- 70 Villaseñor, J., Ibarra-Manríquez, G., Meave, J., & Ortíz, E. (2005). Higher Taxa as Surrogates of Plant Biodiversity in a Megadiverse Country. *Conservation Biology*, **19**(1): 232-238.
- 71 Gobierno_de_Michoacán. (2007). from www.michoacan.gob.mx
- 72 CONABIO. (1998). *La diversidad biológica de México: estudio de país*. Mexico: Comisión Nacional para el Conocimiento y Uso de la Biodiversidad.
- 73 INEGI. (2005). *II Censo de Población y Vivienda*. Mexico.
- 74 Lemaresquier, T., & Santizo, R. (2005). Desarrollo humano y desarrollo local. In Programa_de_las_Naciones_Unidas_para_el_Desarrollo (Ed.), *Informe sobre Desarrollo Humano, México 2004* (pp. 17-47). Mexico city: Grupo Mundi-Prensa.
- 75 (1999). Enciclopedia de los Municipios de México Centro Nacional de Desarrollo Municipal, Gobierno del Estado de Michoacán.
- 76 Bocco, G., Mendoza, M., & Masera, O. R. (2001). La dinámica del cambio del uso del suelo en Michoacan. Una propuesta metodológica para el estudio de los procesos de deforestación. *Boletín del Instituto de Geografía, UNAM*(44): 18-30.
-

- 77 Sáenz-Romero, C., Guzmán-Reyna, R. R., & Rehfeldt, G. E. (2006). Altitudinal genetic variation among *Pinus oocarpa* populations in Michoacán, Mexico Implications for seed zoning, conservation, tree breeding and global warming. *Forest Ecology and Management*, **229**: 340-350.
- 78 Martínez-Elorreaga, E. (2005, 29/03/2005). El 80% de la pérdida de los bosques se debe al cambio del uso de suelo. *La Jornada Michoacán*, p. 11.
- 79 Asociación Agrícola Local de Productores de Aguacate de Uruapan Michoacán (AALPAUM). (2008). Producción de aguacate [Electronic Version] from <http://www.aproam.com/CULTIVO/produccion.htm>
- 80 Koolhoven, W., Hendrikse, J., Nieuwenhuis, W., Retsios, B., Schouwenburg, M., Wang, L., Budde, P., & Nijmeijer, R. (2007). ILWIS Help (Version 3.31). Enschede: ITC.
- 81 Budde, P., Broekema, L., Dost, R., van Duren, I., Eelderink, L., & Verplak, N. (1997). *Ilwis 2.1 for Windows Reference Guide*. Enschede: Ilwis Department, International Institute for Aerospace Survey & Earth Sciences.
- 82 Martínez-Elorreaga, E. (2005, 29/03/2005). El 80% de la pérdida de los bosques se debe al cambio de uso de suelo. *La Jornada Michoacán*.
- 83 Juárez-Navarro, A. (2007, 12/02/2007). Ha desaparecido 80% de bosques *Cambio de Michoacán*.
- 84 Couturier, S. (2006). *Evaluation des erreurs de cartes de végétation avec une approche par ensembles flous et avec la simulation d'images satellite*. UPS-UNAM, Toulouse.
- 85 (1994-1996). Statgraphics Plus for Windows (Version 2.0). Rockville, MD, USA: Statistical graphics Corp.
- 86 Brown, A. A., & Davis, K. P. (1973). *Forest fire: control and use*. New York: McGraw-Hill.
- 87 CONABIO. (2007). Suceptibilidad a los incendios de la vegetación natural. from <http://www.conabio.gob.mx/mapaservidor/incendios/modis/tablas2007/tablas2007/vegetacion.html>
- 88 Labat, J. N. (1995). Végétation du Nord-Ouest du Michoacán Mexique. In J. Rzedowski & G. C. Rzedowski (Eds.), *Flora del Bajío y de regiones adyacentes* (Vol. Fascículo complementario VIII). Patzcuaro, Michoacán, México Instituto de Ecología A. C.
- 89 Maas, J. M., Martínez-Yrizar, A., Patiño, C., & Sahrukhan, J. (2002). Distribution and annual net accumulation of above-ground dead phytomass and its influence on throughfall quality in a Mexican tropical deciduous forest ecosystem. *Journal of tropical ecology*, **18**: 821-834.
- 90 Rothermel, R. C. (1972). *A Mathematical Model for Predicting Fire Spread in Wildland Fuels*. Ogden, UT.
- 91 McArthur, A. G. (1973). *Forest fire danger meter, Mark V*. (Forest Research Institute, Forest and Timber Bureau of Australia). Canberra.
- 92 Andrews, P. L. (1986). *Behave: Fire Behavior Prediction and Fuel Modeling System*. Ogden, UT.
- 93 Finney, M. A. (1998). *FARSITE: Fire Area Simulator-model development and evaluation*. Ogden, UT: Department of Agriculture, Forest Service, Rocky Mountain Research Station.
- 94 García-Aguirre, M. C., Ortiz, M. A., Zamorano, J. J., & Reyes, Y. (2007). Vegetation and landform relationships at Ajusco volcano Mexico, using a geographic information system (GIS). *Forest Ecology and Management* **239**: 1-12.
- 95 Pianka, E. R. (1978). *Evolutionary Ecology*. New York, USA: Harper and Row Publishers.
- 96 Sánchez-González, A., & López-Mata, L. (2003). Clasificación y ordenación de la vegetación del norte de la Sierra Nevada a lo largo de un gradiente altitudinal. *Anales del Instituto de Biología, Universidad Nacional Autónoma de México, Ser. Bot.* , **74**(1): 47-71.
- 97 González-Hidalgo, J. C., Sánchez-Montahud, J. R., & Bellot-Abad, J. (1996-97). Efecto de la vegetación y orientación de la ladera en perfiles de humedad en el suelo de un ambiente semiárido del interior de España. In *Cuadernos I. Geografica* (Vol. 22-23, pp. 81-96): Logroño.
-

- 98 Delgado, J. D., Arroyo, N. L., Arévalo, J. R., & Fernández-Palacios, J. M. (2007). Edge effects of roads on temperature, light, canopy cover and height in laurel and pine forest (Tenerife, Canary Islands). *Landscape and Urban Planning*, **81**: 328-340.
- 99 (1999-2006). ArcToolbox Help- How Viewshed (3D Analyst) works (Version 9.2): ESRI, Inc.
- 100 Ormsby, T., & Alvi, J. (1999). *Extend the power of ArcView GIS* (ed. M. Karman, L. Godin & S. Boden). California: Environmental Systems Research Institute, Inc.
- 101 Chuvieco, E., Cocero, D., Riaño, D., Martín, P., Martínez-Vega, J., Riva, J. d. I., & Pérez, F. (2004). Combining NDVI and surface temperature for the estimation of live fuel moisture content in forest fire danger rating. *Remote Sensing of Environment*, **92**: 322-331.
- 102 Dilley, A. C., Millie, S., O'Brien, D. M., & Edwards, M. (2004). The relation between Normalized Difference Vegetation Index and vegetation moisture content at three grassland locations in Victoria, Australia. *International Journal of Remote Sensing*, **25**(19): 3913-3928.
- 103 Verbesselt, J., Fleck, S., & Coppin, P. (2002). *Estimation of fuel moisture content towards Fire Risk Assessment: A review*. Paper presented at the Forest fire research and wildland fire safety: Proceedings of IV International Conference on Forest Fire Research 2002 Wildland Fire Safety Summit, Rotterdam.
- 104 Tveito, O. E. (2007). Chapter 6. The Developments in Spatialization of Meteorological and Climatological Elements. In H. Dobesch, P. Dumolard & I. Dyras (Eds.), *Spatial Interpolation for climate data* (pp. 282). London: ISTE Ltd.
- 105 García-Soto, E. (1973). *Modificaciones al sistema de clasificación climática de Köppen*. México. UNAM, Mexico city.
- 106 Hengl, T. (2007). *A Practical Guide to Geostatistical, Mapping of Environmental Variables* (JRC Scientific and Technological Reports). Italy: European Commission and Institution for Environment and Sustainability.
- 107 Eastman, J. R. (1987-2006). Idrisi Andes (Version 15). Worcester MA USA Clark Labs, Clark University.
- 108 Mas, J. F., Puig, H., Palacio, J. L., & Sosa-López, A. (2004). Modelling deforestation using GIS and artificial neural networks. *Environmental Modelling & Software*, **19**: 461-471.
- 109 Pontius, R. G., & Schneider, L. C. (2001). Land-cover change model validation by an ROC method for the Ipswich watershed, Massachusetts, USA. *Agriculture, Ecosystems and Environment* **85**: 239-248.
- 110 Southgate, R., Paltridge, R., Masters, P., & Carthew, S. (2007). Bilby distribution and fire: a test of alternative models of habitat suitability in the Tanami Desert, Australia. *Ecography*, **30**: 759-776.
- 111 Justice, C. O., Giglio, L., Korontzi, S., Owens, J., Morisette, J. T., Roy, D., Descloitres, J., Alleaume, S., Petitcolin, F., & Kaufman, Y. (2002). The MODIS fire products. *Remote Sensing of Environment*, **83**: 244-262.
- 112 Justice, C. O., Vermote, J. R. G. Townshend, R. DeFries, D. P. Roy, D. P. Hall, V. V. Salomonson, J. L. Privette, G. Riggs, A. Strahler, W. Lucht, R. Myneni, Y. Knyazikhin, S. W. Running, R. R. Nemani, Z. Wan, A. Huete, W. van Leeuwen, R. E. Wolfe, L. Giglio, J.-P. Muller, P. Lewis, & Barnsley, M. J. (1998). The moderate resolution imaging spectroradiometer (MODIS): land remote sensing for global change research. *IEEE Transactions on Geoscience and Remote Sensing*, **36**: 1228–1249.
- 113 Parkinson, C. L., & Greenstone, R. (Eds.). (2000). *EOS Data Products Handbook* (Vol. 2). Maryland: NASA.
- 114 Gibson, D. J., Hartnett, D. C., & Merrill, G. L. S. (1990). Fire Temperature Heterogeneity in Contrasting Fire Prone Habitats: Kansas Tallgrass Prairie and Florida Sandhill. *Bulletin of the Torrey Botanical Club*, **117**(4): 349-356.
- 115 Center_for_Earth_Observation. (2007). ASTER [Electronic Version] from <http://www.yale.edu/ceo>.
- 116 Yamaguchi, Y., Kahle, A. B., Tsu, H., Kawakami, T., & Pniel, M. (1998). Overview of Advanced Spaceborne Thermal Emission and Reflection Radiometer (ASTER). *IEEE Transactions on Geoscience and Remote Sensing*, **46**: 1062-1071.
-

- 117 Morisette, J. T., Giglio, L., Csiszar, I., & Justice, C. O. (2005). Validation of the MODIS active fire product over Southern Africa with ASTER data. *International Journal of Remote Sensing*, **26**(19): 4239 - 4264.
- 118 Manual de organización de la Comisión Forestal del Estado, CXXXIV Segunda Sección (2004).
- 119 Rzedowski, J. (1978). *La vegetación de México* (ed. E. Limusa). México city.
- 120 Aguado, I., & Rodríguez, F. (2004). El factor meteorológico en los incendios forestales. In E. Chuvieco & M. P. Martin (Eds.), *Nuevas tecnologías para la estimación del riesgo de incendios forestales* (pp. 62-99). Madrid: Consejo Superior de Investigaciones Científicas.
- 121 Manzo-Delgado, L., Sánchez-Colón, S., & Álvarez, R. (2008). Assessment of seasonal forest fire risk using NOAA-AVHRR: a case study in central Mexico. *International Journal of Remote Sensing*, **In press**.
- 122 Burgan, R. E., & Rothermel, R. C. (1984). *Behave: Fire Behavior Prediction and Fuel Modeling System - FUEL Subsystem* (No. General Technical Report INT-167). Ogden, UT.: USDA Forest Service.
-